PHYSICAL REVIEW LETTERS

VOLUME 6 JUNE 15, 1961 NUMBER 12

ELECTROSTATIC SOUND WAVE MODES IN A PLASMA*

F. W. Crawford

Microwave Laboratory, W. W. Hansen Laboratories of Physics, Stanford University, Stanford, California

(Received April 17, 1961; revised manuscript received May 31, 1961)

The dispersion relation for ion waves in an infinite plasma is[1,2]

$$\omega^2 = \frac{\omega_{pi}^2}{1 + (\omega_{pi}^2 m_p/\beta^2 \gamma k T_e)}, \qquad (1)$$

where m_p is the positive-ion mass, β is the phase constant, T_e is the electron temperature, zero ion temperature is assumed, and k is Boltzmann's constant. The constant γ depends on the assumptions made concerning collisions and will lie between 1 and 3.[2] The ion plasma frequency is given by

$$\omega_{pi} = (n_p e^2/\epsilon_0 m_p)^{1/2}, \qquad (2)$$

where n_p is the ion density, e is the electronic charge, and ϵ_0 is the permittivity of free space.

In the long-wavelength limit $\omega/\beta \to (\gamma k T_e/m_p)^{1/2}$, giving rise to the so-called electrostatic sound wave mode of propagation[1] with velocity independent of n_p. A low-frequency cutoff dependent on tube dimensions might be expected.

Ion waves have often been suggested as a source of low-frequency fluctuations occurring in the parameters of dc discharges.[3] To test this hypothesis, dc mercury-vapor discharges at a pressure of ~1μ have been studied in tubes of the type shown in Fig. 1. Each contained an oxide-coated spiral cathode, mounted transversely in a molybdenum cup. One tube of uniform diameter was available, and eight others of various column diameters, but roughly similar construction in the enlarged section containing the cathode assembly. The dimensions were comparable to the electron-neutral mean free path. Spectra of anode voltage fluctuations were observed to contain peaks varying slowly with current, and typical results are shown in Fig. 1. Similar spectra were picked up on a ring sliding along the outside of the glass. Attempts to

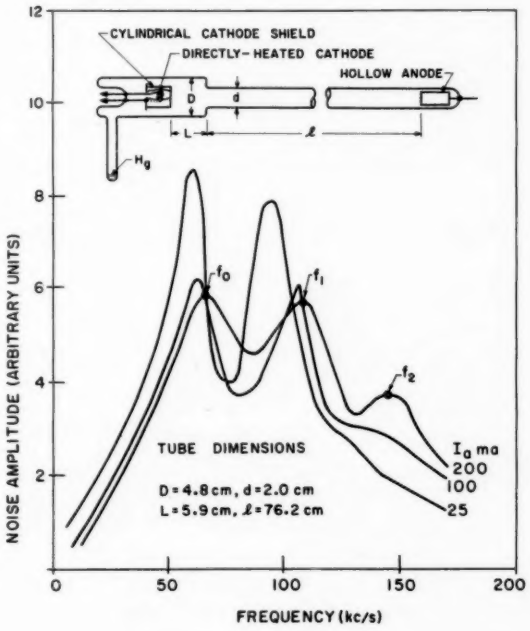

FIG. 1. Experimental discharge tube, and typical spectra of low-frequency fluctuations.

measure phase shift have indicated that the fluctuations must travel along the column at velocities $>10^9$ cm/sec over most of its length, but that over the first few centimeters the phase velocity is of the order of 10^7 cm/sec.[4]

Although it is doubtful whether longitudinal ion wave modes have ever been observed, it is possible that radial modes, generated near the cathode, and near cutoff within the column, could explain these results. Their theory may be derived from the cylindrical-polar form of the wave equation, and if such solutions are valid the frequencies of higher order modes should bear fixed numerical relations to the frequency of the lowest mode. For a mode in which the potential varies as $\cos n\phi$, and is assumed to have a node at the wall, β will be determined by the zeros of $J_n(\beta d/2)$.

Data on the relations between the frequencies of peaks observed in Tubes I-IX are shown on Fig. 2(a) over a wide range of current and number density ($\sim 10^8 - 10^{10}$ ions/cc). Most of the frequency ratios are distributed about the average values 1.68 and 2.34 which are close to the ratios suggested by our simple theoretical considerations. The occasional second harmonics observed could easily arise through nonlinearities.

Assuming that radial electrostatic sound waves are involved, we may substitute for the constants in the expression for the frequency,

$$f_0 = (2.405/\pi d)(\gamma k T_e/m_p)^{1/2},$$

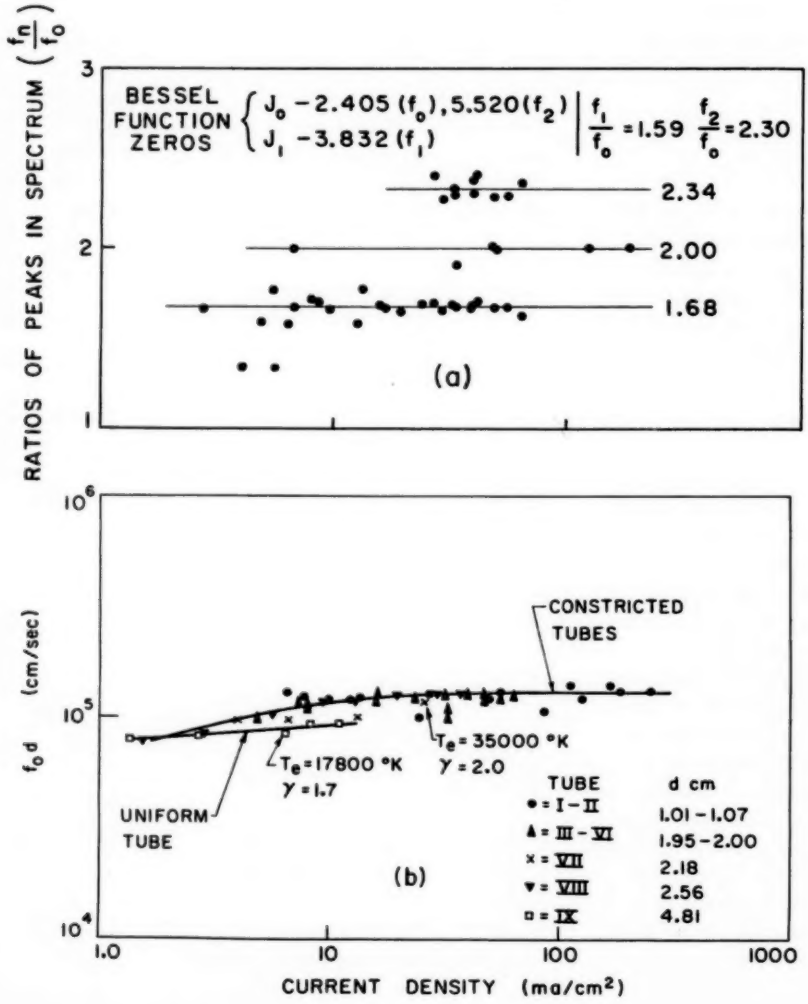

FIG. 2. (a) Frequency ratios of peaks in fluctuation spectra. (b) ($f_0 d$) variation with column current density.

to obtain the result

$$f_0 d = 490(\gamma T_e)^{1/2} \text{ cm/sec}, \quad (3)$$

where f_0 is in cps, d is in cm, and T_e is in °K.

Figure 2(b) shows $(f_0 d)$ plotted against column current density. It has been assumed that the plasma column fills the tube and no correction has been attempted for sheath thickness. Langmuir probe measurements of T_e were made at the points marked. Substitution of these values in Eq. (3) gives values of γ in the range expected. The temperatures were measured nearer to the anode than the cathode so that the values may not be appropriate to the actual generation region.

The results suggest that an electrostatic sound wave mechanism may be operating, and that it is enhanced by the presence of a constriction. The Bessel function relations are appropriate to the first and second radially varying modes, and the first azimuthally varying mode, though it is difficult to see why an azimuthally varying mode should be excited so strongly and detected so easily. To determine the ratios more accurately, modification of Eq. (1) is required to include the axial and radial drift velocities of the ions and electrons.

It is a pleasure to acknowledge many discussions of the problems involved in this work with Dr. G. S. Kino, and private communications from Dr. R. L. Moore and Dr. I. Alexeff on the radial ion wave mechanism.

---

*This work was sponsored by the U. S. Atomic Energy Commission.

[1]L. Tonks and I. Langmuir, Phys. Rev. 33, 195 (1929).

[2]L. Spitzer, Physics of Fully-Ionized Gasses (Interscience Publishers, Inc., New York, 1956).

[3]K. G. Emeléus, Nuovo cimento 3, 490 (1956).

[4]F. W. Crawford and J. D. Lawson, J. Nuclear Energy, Part C (to be published); F. W. Crawford, Microwave Laboratory Report No. 762, Stanford University, Stanford, California, 1960 (unpublished).

ENHANCED DIFFUSION AND OSCILLATIONS IN WEAKLY IONIZED PLASMAS

Jean-François Bonnal, Georges Briffod, and Claude Manus
Section d' Ionique Générale, Service de Physique Appliquée, Centre d' Etudes Nucléaires de Saclay, Gif-sur-Yvette (Seine-et-Oise), France

(Received May 8, 1961)

The present study deals with observations on enhanced diffusion performed on a weakly ionized plasma.

Experiments have been performed with a Reflex-type discharge in H_2, N_2, and Ar, the pressure, density, and magnetic field conditions of which are variable. The discharge works in continuous mode. The diffusion is measured by means of the escape flux of the ions transversally to the magnetic field B_0. The measurement is made with a probe external to the plasma, negatively polarized with regard to the plasma potential. The variation of the escape flux as a function of the magnetic field for different values of the pressure parameter is shown in Figs. 1 and 2.

All curves show three separate regions:

1. $B < B_C$: The escape flux decreases with the magnetic field and increases with the pressure according to the classical laws of diffusion confirmed experimentally by several researchers[1-3] (Fig. 1).

2. $B_C < B < B_M$: A new diffusion mode appears in which the escape flux increases with the mag-

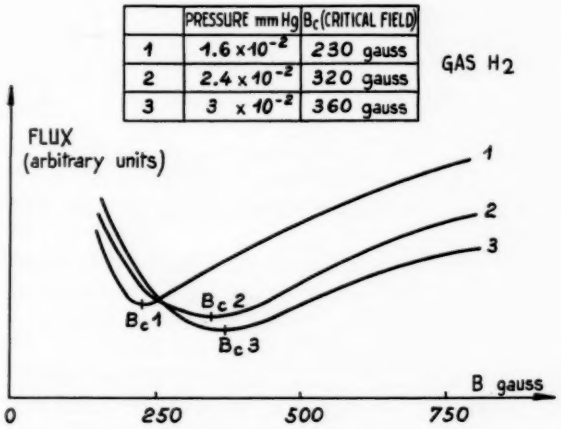

FIG. 1. Escape flux of ions transversally to the magnetic field; $0 < B < 1000$ gauss. These results have been obtained with a cold-cathode P.I.G. discharge, working with hydrogen, of length 110 mm, diameter 30 mm, voltage between anode and cathode 400 volts, current 200 ma.

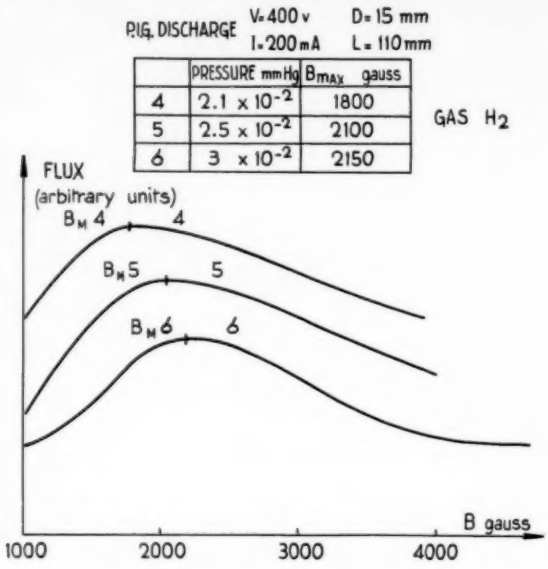

FIG. 2. Escape flux of ions transversally to the magnetic field; $1000 < B < 4000$ gauss.

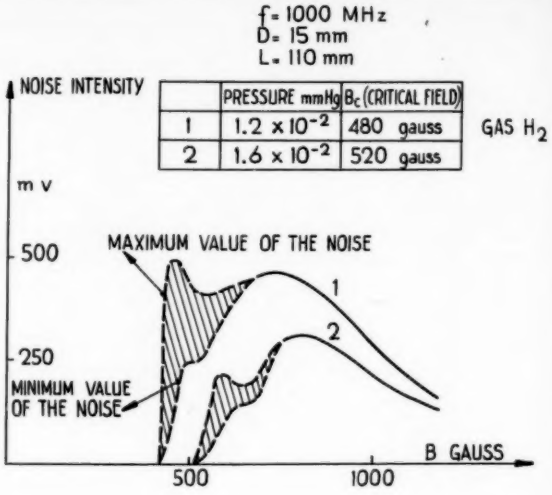

FIG. 3. High-frequency noise level.

netic field. This has to be connected with the Lehnert experiments. The influence of the pressure on the position of the curves is just opposite to that of the previous mode: The escape flux grows as the pressure decreases. (This mode is accompanied by a considerable noise emission.)

On each curve, the maximum value of the flux is reached for $B = B_M$. As the pressure decreases, both this maximum and the critical magnetic field are shifted toward lower field values.

3. $B > B_M$: The escape flux decreases again along with the noise level. But the order of the curves with respect to the pressure is maintained (Fig. 2).

Regarding the dependence of the critical field on the discharge radius and the atomic mass of the gas (H_2, N_2, Ar), the laws are similar to those pointed out by Lehnert and Hoh.[4-6]

Finally, the critical magnetic field is independent of the density of the charged particles.

The intense emission of noise by the discharge above the critical field is detected by an external antenna for the high-frequency component and is observed on the oscillogram of the anode-cathode voltage for the low-frequency components. The high-frequency spectrum is particularly wide and reaches values higher than the plasma frequency.

The relative variation of the noise level with the magnetic field at 1000 Mc/sec is shown in Fig. 3. The general trend of these curves and their dependence on the pressure are similar to those of Fig. 2.

To sum up: (1) The noise appears only in the case of $B > B_c$; (2) its amplitude increases as the pressure decreases; and (3) its maximum value shifts toward weak magnetic field as the pressure decreases.

The amplitude of the low-frequency noise spectrum follows roughly a variation identical to the variation shown in Fig. 3.

The following remarks can be made:

(a) Even though the length of the discharge and the pressure range are entirely different from the conditions corresponding to the experiments carried out by Lehnert, there appears a critical magnetic field and an enhanced escape flux.[7]

(b) The high-frequency noise spectrum is very important and is connected with the value of the escape flux. These different observations, mainly the existence in the spectrum of high-frequency noise of components corresponding to frequency higher than the plasma frequency, has suggested a theoretical treatment based on a microscopic approach. The instabilities are related to the existence of anisotropies in the velocity distribution function, anisotropies due mainly to the existence of an electrical field inside the plasma. This treatment is quite different from that developed by Hoh[8] and Kadomtsev

and Nedospasov,[9] and will be published in the near future.

[1]A. Simon, Phys. Rev. 98, 317 (1955).
[2]A. Simon, Proceedings of the Second United Nations International Conference on Peaceful Uses of Atomic Energy, 1958 (United Nations, Geneva, 1958), Vol. 32, p. 343.
[3]R. J. Bickerton, Proc. Phys. Soc. (London) B70, 305 (1957).
[4]B. Lehnert, reference 2, p. 349.
[5]F. C. Hoh and B. Lehnert, Proceedings of the Fourth International Conference on Ionization Phenomena in Gases, Uppsala, 1959 (North-Holland Publishing Company, Amsterdam, 1959), Vol. II, p. 604.
[6]F. C. Hoh and B. Lehnert, Phys. Fluids 3, 600 (1960).
[7]J. F. Bonnal, G. Briffod, and C. Manus, Compt. rend. 250, 2859 (1960).
[8]F. C. Hoh, Phys. Rev. Letters 4, 559 (1960).
[9]B. B. Kadomtsev and A. V. Nedospasov, J. Nuclear Energy, Part C, 1, 230 (1960). See also T. K. Allen, G. A. Paulikas, and R. V. Pyle, Phys. Rev. Letters 5, 409 (1960).

OBSERVATIONS OF de HAAS–van ALPHEN OSCILLATIONS IN p-TYPE PbTe†

P. J. Stiles,* E. Burstein, and D. N. Langenberg
University of Pennsylvania, Philadelphia, Pennsylvania
(Received May 3, 1961)

We should like to report the results of a study of de Haas–van Alphen (dH-vA) oscillations in the magnetic susceptibility of p-type PbTe by pulsed magnetic field techniques. Although extensive studies of the dH-vA effect in metals have been made, as far as we know this is the first time that susceptibility oscillations have been observed in a semiconductor. Oscillations in transport properties such as magnetoresistance and Hall effect have, of course, been observed in semiconductors as well as in metals. Because studies of magnetoresistance and Hall effect oscillations require electrical contacts and involve the current as an additional parameter, the measurement of susceptibility oscillations by the impulse method[1] has the advantage of greater simplicity. We feel that such measurements will have wide application in the study of the band structure of semiconductors.

In each of the four p-type PbTe samples studied, more than 30 oscillations were observed. Three of the PbTe samples were cut from a single boule as close to each other as possible. Hall effect measurements made by Allgaier[2] yielded a hole density of $3\times10^{18}/\text{cm}^3$ for this boule. The fourth PbTe sample had a hole density of about $1\times10^{18}/\text{cm}^3$. These samples were circular cylinders with the cylinder axis parallel to one of the three principal symmetry directions. The magnetic field was applied along the axis of the cylinder. A typical photograph of the oscillations in dm/dt, where m is the total magnetic moment of the sample, is shown in Fig. 1 and the successive maxima and minima are plotted versus B^{-1} in Fig. 2 for two different orientations. Table I lists the periods measured in the three symmetry directions.

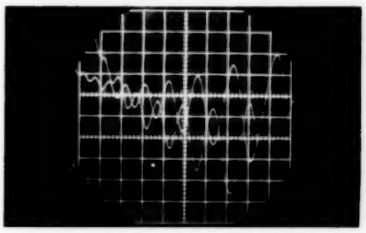

FIG. 1. dH-vA oscillations in p-type PbTe. The double trace shows the oscillations for increasing and decreasing magnetic field. The magnetic field varies from 7.3 kgauss at the left to 16.4 kgauss at the right.

It has been suggested by earlier workers that the energy surfaces at the edge of the valence band in PbTe are ellipsoids of revolution oriented along the $\langle 111\rangle$ directions.[3] Allgaier has recently suggested on the basis of his magnetoresistance and Hall effect studies at 77°K and room temperature that an additional valence band maximum appears to be involved. Our data indicate a band maximum at $\vec{k}=0$ and band maxima at the centers of the $\{111\}$ faces of the Brillouin zone, although it is not clear that the additional valence band maximum we see is the one suggested by Allgaier. The extremal cross sections associated with the $\vec{k}=0$ maximum vary

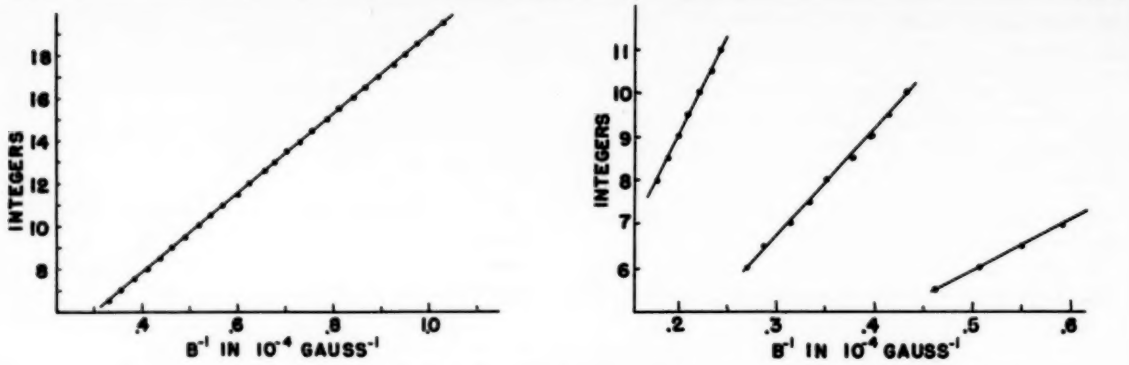

FIG. 2. Successive maxima and minima in dm/dt are plotted as integers and half integers vs B^{-1}, with $n = 3.9 \times 10^{18}$ holes/cm^3 and $T = 4.2$°K. (a) The plot for the longer period observed with $\vec{B} \| \langle 100 \rangle$. (b) The plots for all three periods observed with $\vec{B} \| \langle 111 \rangle$. Twenty-four more maxima and minima observed in the series with the smallest slope are not shown here.

with orientation by about 25%. Assuming parabolic bands, the energy surfaces at the {111} zone faces are ellipsoids of revolution with a longitudinal to transverse mass ratio of 6.4 ± 0.3. From the dependence of the oscillation amplitude on magnetic field and on temperature, we derive a transverse effective mass for the ellipsoids of $(0.042 \pm 0.006) m_0$ (m_0 = free electron mass) and an equivalent broadening temperature, T_b, of about 7°K to 10°K. T_b includes the apparent broadening due to hole density variations in the sample as well as collision broadening. We feel that the large value of T_b is primarily due to variations in hole density. On this basis the value of T_b observed in these experiments corresponds to a 10% variation in hole density, a reasonable value for such materials.

If the complete geometry of the Fermi surface is known, one can determine the total number of holes from the total volume enclosed by the surface in $\vec{k}$ space. We estimate the number of holes in the three crystals cut from a single boule to be 3.9×10^{18}/cm^3, assuming four ellipsoids and a sphere at $\vec{k} = 0$ of cross section equal to the average of the three measured cross sections. This is reasonably close to the density of 3×10^{18}/cm^3 obtained from Hall effect measurements. At this concentration the Fermi level is 0.035 ± 0.005 ev below the top of the ellipsoidal band. By comparing the results from the two samples with different hole densities, and assuming parabolic bands and our value of the ellipsoid transverse effective mass, we obtain an estimate of the effective mass of the central section, $m^* = (0.12 \pm 0.02) m_0$. We also estimate that the band edge at $\vec{k} = 0$ is higher in electron energy than the band edge at the Brillouin zone face by 0.002 ± 0.002 ev.

It is of interest to consider the factors determining the sensitivity of the impulse method for observing the dH-vA effect in semiconductors and to compare this sensitivity with that achieved

Table I. Experimental dH-vA periods.

Orientation of the magnetic field	Period[a] (gauss$^{-1} \times 10^6$) Ellipsoids	Period[a] (gauss$^{-1} \times 10^6$) $\vec{k} = 0$ section	Measured hole density[b] (cm^{-3})
⟨100⟩	13.3	6.07	9.5×10^{17}
⟨100⟩	5.37	2.63	3.9×10^{18}
⟨110⟩	7.50	2.42	
	3.70		
⟨111⟩	8.39	2.15	
	4.18		

[a] There is an error of 2% associated with each period, primarily due to the calibration of the magnetic field.
[b] Calculated from dH-vA periods.

in observations of the effect in metals. The experimentally observed signal is proportional to $dm/dt = V(dm/dH)(dH/dt)$, where V is the sample volume and M is the magnetization. In semiconductors the carrier density is orders of magnitude less than it is in metals, the oscillation period is much longer, and dM/dH may be smaller by a factor of 10^5. On the other hand, because of the longer period in semiconductors, larger field inhomogeneities due to eddy current shielding can be tolerated. Furthermore, the eddy currents are reduced by higher resistivities. Both V and dH/dt may therefore be larger for a semiconductor than for a metal and the smaller sensitivity due to the small dM/dH can be partially compensated. The signals observed in the present experiments are 10-100 times smaller than typical signals observed in experiments on metals. Nevertheless the sensitivity is quite adequate. In fact, the sensitivity of the method is such that the only limitation to observing the effect in semiconductors is the theoretical one that the materials must have $E_F > k(T + T_b)$, where E_F is the Fermi energy measured relative to the edge of the band in question. Thus, in addition to the requirement that the sample be degenerate ($E_F > kT$), one needs uniform carrier densities and long collision times ($E_F > kT_b$). The requirements of a long collision time ($E_F > \hbar/\tau$) can be expressed in terms of the density and mobility of the carrier as $n^{2/3}\mu > 10^{15}$ volt sec for the case of a single spherical energy band. There are a number of semiconductors which readily satisfy these conditions, such as the lead salt series PbS, PbSe, and PbTe,[4] which we are now investigating.

The authors wish to express their thanks to R. S. Allgaier, W. W. Scanlon, and B. B. Houston for many enlightening discussions and for supplying the crystals investigated. We would also like to thank L. Indyk and B. N. Taylor for their valuable assistance in setting up the experiment. We also wish to express our appreciation to Dr. D. N. Stevens for his interest and encouragement in supporting this work.

---

†This work was supported in part by the U. S. Atomic Energy Commission and is a contribution from the Laboratory for Research on the Structure of Matter.

*Philco Fellow.

[1]D. Shoenberg, in Progress in Low-Temperature Physics, edited by J. C. Gorter (North-Holland Publishing Company, Amsterdam, 1957), Vol. 2, p. 226.

[2]R. S. Allgaier (private communication).

[3]R. S. Allgaier, Phys. Rev. 119, 555 (1960); K. Shogenji and S. Uchiyama, J. Phys. Soc. Japan 12, 1164 (1957).

[4]C. D. Kuglin, M. R. Ellett, and K. F. Cuff, Phys. Rev. Letters 6, 177 (1961), have reported magnetoresistance oscillations in n-type PbTe.

GROUND STATE OF AN ISING FACE-CENTERED CUBIC LATTICE

A. Danielian
Wheatstone Physics Laboratory, King's College, London, England
(Received May 4, 1961)

Many antiferromagnetic compounds have a face-centered cubic (fcc) magnetic structure. Although in the case of nearest neighbor interactions the ground state of such systems is clearly degenerate, no exact information has been available regarding either the magnitude of its degeneracy or any of its thermodynamic properties. In the case of an antiferromagnetic Ising triangular lattice, it has been shown that the entropy per spin is finite[1] and the zero-field susceptibility infinite[2] at $T = 0°K$. In this Letter we show that, assuming nearest neighbor Ising interactions, simple topological and energy arguments lead to a complete classification of the ground-state configurations. Hence, a precise enumeration of the states is possible and exact thermodynamic results are deduced at $T = 0°K$.

We consider an antiferromagnetic system consisting of N spin moments on an fcc lattice. Each spin is capable of existing in one of two possible states denoted +, -, and interacts with its nearest neighbors (n.n.) only. The interaction energy is $+J$ for a pair of like spins (++ or --) and $-J$ for a pair of unlike spins (+- or -+).

First, the energy of the ground state of the system is determined. An fcc lattice of N sites can be subdivided into N tetrahedra, such that each n.n. interaction bond is found on one and only one tetrahedron; hence there are a total of $6N$ such bonds. In the ground state, each one of these tetrahedra must be in its own ground state, i.e., two of its spins in the state + and two in the state -. This ground state of the tetrahedron is denoted by the symbol ω, and the corresponding energy is $-2J$. Hence the energy of the ground state of the fcc system is $-2NJ$. It then also follows that every tetrahedron in the lattice is in state ω.

We next consider the fcc lattice built up of layers of triangular lattices. In Fig. 1 such a layer (1) is shown—the circles at the centers of the triangles denote sites on layer (2) which is immediately under layer (1), and points at the centers of the remaining triangles denote sites on layer (3) which is immediately above layer (1). Each triangle of (1) is the base of a tetrahedron, the vertex of which is a site either on (2) or (3). Also, each site on a given layer is the vertex of a tetrahedron, the base of which is a triangle on an adjacent layer.

Since in the ground state of the fcc system each tetrahedron is in the state ω, it follows that each triangle of spins in a given layer should be in one of the states (++-) or (--+). Therefore any triangular layer should also be in one of its ground states. The number of such states is of the order $2^{0.47n}$, where n is the number of spins (or sites) on a triangular lattice.[1]

Thirdly, we note that if the configuration of the ground state of layer (1) is determined, then the configurations of both layers (2) and (3) are also determined. This obtains because each triangle has one of the configurations (++-) or (--+), and since it is also required that each tetrahedron be in the state ω, the state of the spin at the vertex of the tetrahedron is determined, and this vertex is in the adjacent layer. It follows that the ground configurational state of the whole fcc system is determined by the ground configurational state of any one of its triangular layers; hence we can deduce that its degeneracy is $\leq 2^{0.47n}$, $n \sim N^{2/3}$. We now proceed to show that the strict inequality holds.

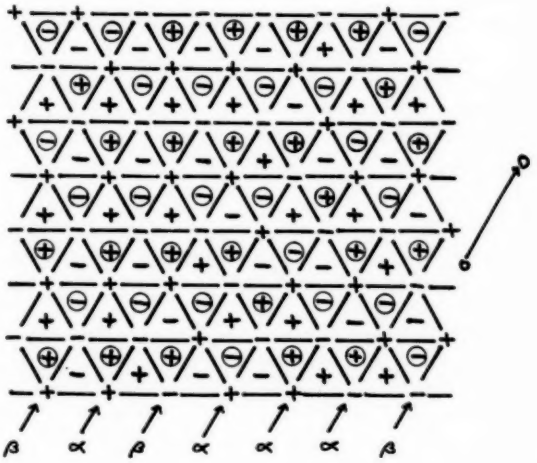

FIG. 1. Three successive layers of a face-centered cubic lattice: layer (1) denoted by triangles; sites on layer (2) denoted by circles; and sites on layer (3) are at the centers of the remaining triangles.

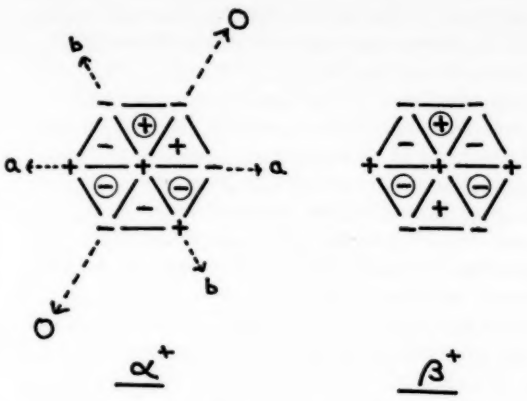

FIG. 2. The α^+ and β^+ clusters. Notation as for Fig. 1.

Figure 2 shows two clusters, each having a central spin with its 12 nearest neighbors. Such clusters contain 8 tetrahedra: 6 having the triangles of (1) as bases, the remaining two having the central spin for their vertices and their bases on layers (2) and (3), respectively. The condition that each tetrahedron must be in the state ω reduces the number of basic types of such clusters to four. Two of them, α^+ and β^+, are shown in Fig. 2; the other two, α^- and β^-, are obtained simply by reversing all the spins.

It follows that in the ground state, each + spin is at the center of an α^+ or β^+ cluster and each - spin is at the center of an α^- or β^- cluster. The possible ground states of a triangular layer can therefore be obtained by grouping these four clusters. The number of possibilities is restricted by a property of the α cluster. If a particular site—chosen as origin—is the center of an α cluster, then the adjacent clusters along the 00 axis must also be α clusters. Hence all clusters along the 00 axis must be α clusters. On the other hand, adjacent clusters along aa or bb axes may be either α or β. If one therefore looks at the triangular layer along the 00 direction, one can have a row (parallel to 00) of α clusters followed by another row of either α clusters or β clusters. Thus the triangular layer will consist of rows, each consisting entirely of α or β clusters (e.g., Fig. 1). The number of arrangements is clearly 2^R, where R is the number of rows.

The degeneracy of the ground state of the fcc system is therefore $\exp(AN^{1/3}\ln 2)$, and it follows that in the limit $N=\infty$ the entropy per spin tends to zero as $T\to 0°K$.

In the above scheme all triangular layers have identical configurations and since all possible configurations have zero moment, it follows that the susceptibility is zero at $T=0°K$.

I am grateful to Dr. M. F. Sykes for drawing my attention to this problem and for valuable discussions.

[1]G. H. Wannier, Phys. Rev. 79, 357 (1950).
[2]M. F. Sykes (to be published), based on the theory developed by M. E. Fisher, Phys. Rev. 113, 969 (1959).

SUPERCONDUCTIVITY AT HIGH MAGNETIC FIELDS AND CURRENT DENSITIES IN SOME Nb-Zr ALLOYS*

T. G. Berlincourt, R. R. Hake, and D. H. Leslie
Atomics International, Division of North American Aviation, Canoga Park, California
(Received May 24, 1961)

Zero electrical resistance at unusually high magnetic fields and current densities has recently been reported in the compound Nb_3Sn,[1,2] and in the alloy Mo—25 at.% (atomic percent) Re.[3] The present results on Nb-Zr alloys were obtained during the course of a systematic investigation of resistive superconducting transitions in certain Ti, Zr, Nb, Hf, and Ta-rich binary alloys in magnetic fields up to 30 kgauss. The data show that cold-worked Nb-rich Nb-Zr alloys display zero electrical resistance at current densities as high as 10^5 amp/cm^2 at 30 kgauss and at 4.2°K.[4,5] As far as we are aware, only the specially prepared Nb-clad "Nb_3Sn" cores of Kunzler et al.[1] have exhibited greater zero-resistance current-carrying capacities above 10 kgauss. The present measurements also reveal some interesting high-field superconducting effects in cold-rolled Nb-Zr alloys: (a) a marked dependence of the magnitude of

the maximum zero-resistance current upon the direction of the externally applied transverse magnetic field relative to the rolled surface of the specimen, and (b) an anomalous increase of the maximum zero-resistance current with increase of magnetic field strength over certain field regions in certain alloy specimens.[6]

Figures 1 and 2 show curves of critical current density, J_c, vs magnetic field strength, H, for some Nb−25 at.% Zr and Nb−12 at.% Zr specimens for different temperatures and transverse field orientations. Preliminary data for Nb−38 at.% Zr and Nb−88 at.% Zr specimens have also been obtained and will be reported at a later date. The source materials, method of fabrication, and cross-sectional dimensions of the specimens are indicated in Table I. For each alloy specimen the data were normally taken by slowly increasing the current through the sample at constant field strength until the least detectable resistive voltage, V_γ, was observed. For the data of Figs. 1 and 2, $V_\gamma \approx 0.25$ μv. Separate tests using higher sensitivity apparatus indicated that J_c vs H curves are virtually the same for $0.005\ \mu v \leq V_\gamma \leq 0.25\ \mu v$. The current required to produce V_γ divided by the cross-sectional area of the specimen was defined to be the "critical current density," J_c. (In cases where $J_c \geq 2\times10^4$ amp/cm^2, the onset of resistance was accompanied by the almost simultaneous burnout of the specimen.) The specimens were copper-

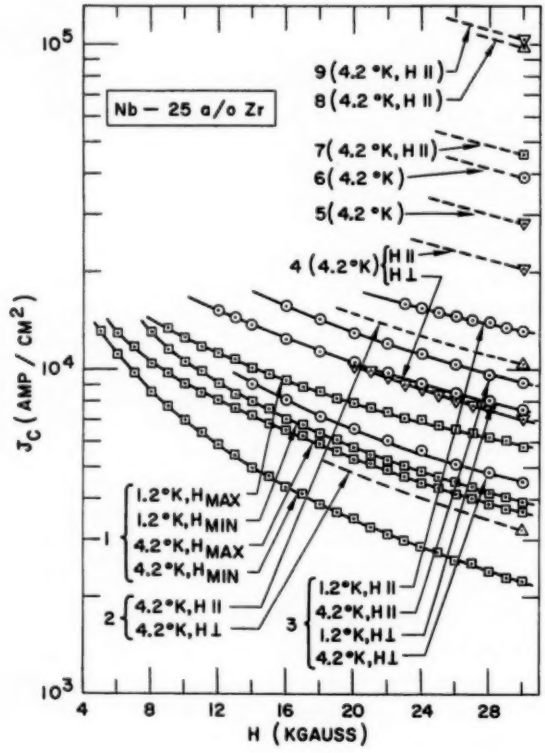
Nb − 25 a/o Zr
9 (4.2 °K, H ||)
8 (4.2 °K, H ||)
7 (4.2 °K, H ||)
6 (4.2 °K)
5 (4.2 °K)
4 (4.2°K) {H ||, H ⊥}
1 {1.2°K, H_MAX; 1.2°K, H_MIN; 4.2°K, H_MAX; 4.2°K, H_MIN}
2 {4.2°K, H ||; 4.2°K, H ⊥}
3 {1.2°K, H ||; 4.2°K, H ||; 1.2°K, H ⊥; 4.2°K, H ⊥}
J_C (AMP / CM^2)
H (KGAUSS)

FIG. 1. Critical current density, J_c, for restoration of the first observable resistance vs applied transverse magnetic field, H, for Nb−25 at.% Zr alloy specimens 1 to 9 at different temperatures and field orientations parallel ($H\parallel$) and perpendicular ($H\perp$) to the rolled faces of the specimens. For specimen 1, which was ground to thickness, H_{max} and H_{min} designate field directions such that J_c is, respectively, a maximum and a minimum at 30 kgauss and 4.2°K. For source material, fabrication method, and cross-sectional dimensions of the specimens see Table I.

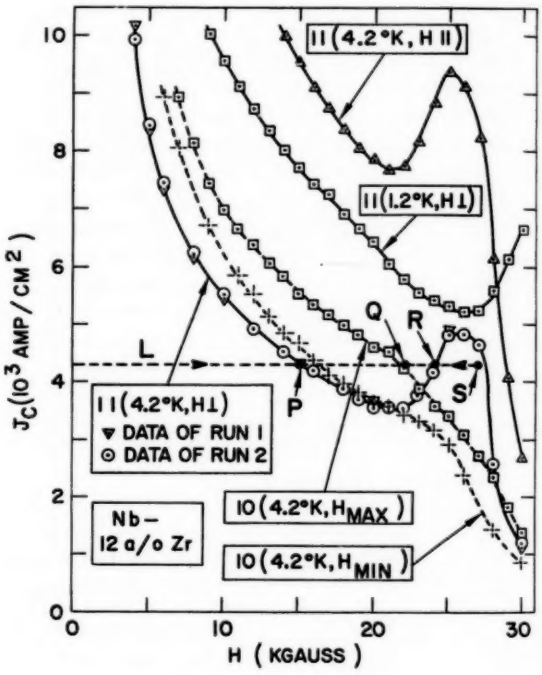

FIG. 2. Critical current density, J_c, for restoration of the first observable resistance vs applied transverse magnetic field, H, for Nb−12 at.% Zr alloy specimens 10 and 11 at different temperatures and field orientations parallel ($H\parallel$) and perpendicular ($H\perp$) to the rolled face of the specimen. For specimen 10, which was ground to thickness, H_{max} and H_{min} designate field directions such that J_c is, respectively, a maximum and a minimum at 30 kgauss and 4.2°K. For source material, fabrication method, and cross-sectional dimensions of the specimens see Table I. The line L and points P, Q, R, S are explained in the text.

plated over 0.6 cm at their ends and were then soft-soldered between copper current lugs. The copper potential leads (spaced about 0.7 cm apart) were clamped against the specimens with beryllium-copper spring clips.

Aside from the large high-field current densities observed for some Nb-Zr specimens, the wide range of J_c values ($\approx 2\times10^3$ - 10^5 amp/cm^2) shown in Fig. 1 for specimens of the same nominal alloy composition is surprising. Further investigation will be required to isolate the important variables affecting the high-field superconducting resistive characteristics. Micrographic examination of the various source materials (see Table I) under polarized light indicated that all the samples were predominantly bcc as might be expected from an inspection of the phase diagram,[7] considering that the source material alloys were all arc-quenched. A small amount of second phase material (probably hcp) was apparent under the microscope in all the source materials. Comparison of the J_c vs H curves for specimens fabricated from the same source material, but with different amounts of cold-work (see Figs. 1, 2, and Table I) suggests that the more intensive the cold-working, the higher the value of J_c. Cold-working has previously been observed to increase the "critical fields"[8] and the high-field critical currents[6,9,10] in pure Nb.

The data of Figs. 1 and 2 also show that J_c values for cold-rolled specimens depend markedly upon the direction of the transverse magnetic field relative to the rolled face of the specimen. Polar plots of J_c vs transverse field orientation for the cold-rolled specimens of Figs. 1 and 2 are roughly elliptical in shape with maxima and minima at field directions, respectively, parallel ($H\parallel$) and perpendicular ($H\perp$) to the rolled faces of the specimens, regardless of (a) the position in which the specimens were soldered into the current lugs, or (b) the cross-sectional geometry of the specimens. J_c vs H data for these two extremal field directions are shown for several cold-rolled specimens in Figs. 1 and 2. The ratio $J_c(H\parallel)/J_c(H\perp)$ at 30 kgauss and 4.2°K varies between 2 and 3 for the cold-rolled specimens. A less prominent orientation effect is also observed in specimens No. 1 (Fig. 1) and No. 10 (Fig. 2)

Table I. Source, fabrication method, and cross-sectional dimensions of Nb-Zr alloy specimens.

Specimen number	Source material	Atomic percent Zr[a]	Fabrication[b]	Cross-sectional dimensions (cm)
1	a.m.[c] button $L1$	25	ground to 0.019 cm	0.019 ×0.022
2	a.m. button $L1$	25	c.r.[d] from 0.100 to 0.025 cm	0.023 ×0.025
3	a.m. casting $M2$	25	c.r. from 0.033 to 0.015 cm	0.015 ×0.023
4	a.m. casting $M2$	25	c.r. from 0.091 to 0.030 cm	0.018 ×0.030
5	CBC wire[e]	25	None	0.025 diam
6	CBC wire	25	None	0.025 diam
7	CBC wire	25	c.r. to ≈0.007-cm strip	0.0074×0.066
8	CBC wire	25	c.r. to ≈0.007-cm strip	0.0069×0.037
9	CBC wire	25	c.r. to ≈0.007-cm strip	0.0069×0.038
10	a.m. button $L2$	12	ground to 0.025 cm	0.025 ×0.025
11	a.m. button $L2$	12	c.r. from 0.100 to 0.025	0.023 ×0.025
12	a.m. button $L2$	12	c.r. from 0.100 to 0.025	0.022 ×0.023

[a] Calculated from weights of starting materials.
[b] The method of producing the desired strip thickness is given. Specimens of small width were sheared from the strips so produced.
[c] a.m. means arc-melted.
[d] c.r. means cold-rolled with no intermediate or final anneal.
[e] Wire produced by the Chase Brass and Copper Company. An arc-melted ingot of diameter 0.89 cm was cold-drawn to 0.025-cm diameter wire with no intermediate or final anneal.

which have not been cold-rolled. The orientation dependence may be associated with preferred crystalline orientation and/or the configuration of the dislocation network. The orientation dependence observed here, in fields where flux penetration of the specimen is doubtless nearly complete, is not to be confused with the well-known field orientation dependence of the bulk specimen superconducting transition, which is determined strictly by the specimen geometry. Indeed, for most of the present specimens the nearly square cross sections (see Table I) insure that the field sees nearly identical specimen geometry whether set parallel or perpendicular to the rolled face of the specimen.

The J_c vs H curves for Nb–12 at.% Zr specimens at 4.2°K (Fig. 2) show anomalous peaks at fields of about 25 kgauss. At 1.2°K the J_c values increase and the peak apparently moves to a higher field value. The "peak effect" can be observed in a rather striking way by increasing the magnetic field at a constant current such as to pass through the anomalous J_c-H region, e.g., along line L of Fig. 2. As the field is increased a resistive voltage first appears at point P, reaches a maximum of 125 μv at point Q, and then disappears at point R. The appearance and disappearance of resistive voltage is also observed upon lowering the field from point S. A peak very similar to that shown in Fig. 2, and occurring at the same field value, was observed in another Nb–12 at.% Zr specimen (No. 12, Table I) in two different runs, in between which the specimen was resoldered to the current lugs. Anomalous positive slope in J_c vs H curves has also been observed in cold-rolled Ti–29 at.% Ta[11] and cold-rolled Nb.[6] An unusual decrease in the resistance with increasing magnetic field over narrow field regions has been previously observed in superconducting transitions of Nb[9] and of Ti–29 at.% V,[11] and is probably related in origin to the "peak effect" in the J_c vs H curves of Fig. 2.

The observation of large high-field critical currents in flexible Nb–25 at.% Zr wire suggests the use of such wire for superconducting solenoids generating fields possibly well in excess of 30 kgauss. Investigation of this prospect and further studies of high-field superconducting phenomena are in progress in this laboratory.

We wish to thank D. M. Sellman and P. Q. Sauers for valuable assistance in the electrical measurements, H. Conrad for metallurgical advice, and C. G. Rhodes for micrographic examinations. We are also grateful to J. Port and A. Springmeyer of the Chase Brass and Copper Company for their expert fabrication of Nb-Zr wire, and to H. Reiss for his enthusiastic encouragement of this work.

---

*This research was supported by the U. S. Atomic Energy Commission.

[1]J. E. Kunzler, E. Buehler, F. S. L. Hsu, and J. H. Wernick, Phys. Rev. Letters 6, 89 (1961).

[2]V. D. Arp, R. H. Kropschot, J. H. Wilson, W. F. Love, and R. Phelan, Phys. Rev. Letters 6, 452 (1961).

[3]J. E. Kunzler, E. Buehler, F. S. L. Hsu, B. T. Matthias, and C. Wahl, J. Appl. Phys. 32, 325 (1961).

[4]J. E. Kunzler and co-workers have independently studied the resistive superconducting properties of Nb-Zr alloys at high magnetic fields. Kunzler [Bull. Am. Phys. Soc. 6, 298 (1961)] has reported a critical current density of 10^4 amp/cm^2 for Nb–33 at.% Zr at 80 kgauss and 1.5°K.

[5]Recent work of J. K. Hulm and R. D. Blaugher (to be published) shows that the superconducting transition temperatures of Nb-Zr alloys with between 10 and 30 at.% Zr are about 11°K.

[6]Both these effects have been recently observed below 8 kgauss in pure cold-rolled Nb by M. A. R. Le Blanc and W. A. Little, Proceedings of the Seventh International Conference on Low-Temperature Physics, 1960 (University of Toronto Press, Toronto, 1960), p. 198.

[7]M. Hansen, Constitution of Binary Alloys (McGraw-Hill Book Company, Inc., New York, 1958), p. 1023.

[8]J. J. Hauser, Bull. Am. Phys. Soc. 6, 123 (1961).

[9]T. G. Berlincourt, Phys. Rev. 114, 969 (1959).

[10]S. H. Autler and L. J. Donadieu, Bull. Am. Phys. Soc. 6, 64 (1961).

[11]T. G. Berlincourt, D. H. Leslie, and R. R. Hake (unpublished).

ASPHERICAL 3d ELECTRON DISTRIBUTION IN BODY-CENTERED CUBIC METALS

Frank Stern
U. S. Naval Ordnance Laboratory, White Oak, Silver Spring, Maryland
(Received March 15, 1961)

We have estimated the asphericity of the $3d$ electron atomic scattering factor for x-ray and polarized neutron diffraction in body-centered cubic metals on the basis of a simple energy-band model. The results agree with the neutron observations on iron,[1] which indicate a departure of the $3d$ charge distribution from spherical symmetry.

At a lattice site having cubic symmetry, atomic d levels are split into a doubly degenerate set called e_g and a triply degenerate set called t_{2g}.[2] Electrons in these states have an aspherical charge distribution and an atomic scattering factor which is not a smooth function of the Bragg angle.[3] In metals the overlap of wave functions of neighboring atoms leads to energy bands which have no degeneracy in general except for wave vectors in directions of high symmetry. The charge density will still have cubic symmetry, and can be expanded in the form

$$\rho(\vec{r}) = \sum \rho_l(r) Y_l(\theta, \phi), \qquad (1)$$

where r, θ, and ϕ are spherical polar coordinates and the $Y_l(\theta, \phi)$ are cubically symmetric combinations of spherical harmonics of order l, normalized to 4π on the unit sphere.[4] If the total charge density in the crystal can be written as a sum of charge densities centered on the individual lattice points,[5] the atomic scattering factor will be

$$f(\mu, \beta, \gamma) = \sum i^l Y_l(\beta, \gamma) \int \rho_l(r) j_l(\mu r) 4\pi r^2 dr, \qquad (2)$$

where μ, β, and γ are the spherical polar coordinates of the change in the wave vector upon diffraction, i.e., $\mu = 4\pi \sin\theta_{\text{Bragg}}/\lambda$, and $j_l(\mu r)$ is the spherical Bessel function of order l. For cubically symmetric combinations of d states of pure e_g symmetry, for example, the charge density has the form $\rho(\vec{r}) = \rho_0(r)[1 + (9/21)^{1/2} Y_4(\beta, \gamma)]$, and Eq. (2) reduces to the corresponding expression given by Weiss and Freeman.[3]

Determination of the $3d$ charge density in a metal requires a summation of charge densities of all the occupied states in the $3d$ band. A rough estimate, but one which probably displays the essential features of the asphericity, is to use the charge density near the peak of the radial wave function, since this will give the dominant contribution to the atomic scattering factor. We have in that way estimated the asphericity for metallic iron, using the results of a cohesive energy calculation[6] in which energy values and wave functions were found for each of the five $3d$ bands for 13 inequivalent points of high symmetry in the Brillouin zone. The total volume of the Brillouin zone was divided among the 13 points, and the weighted sum of the charge density peak heights of the occupied states was calculated. The ferromagnetism of iron was taken into account by displacing the spin-up and spin-down bands with respect to each other ("up" here is the direction opposite to that of the magnetization). If we assume that the charge density in iron is contributed by seven $3d$ electrons and one $4s$ electron per atom,[6] and that the observed moment of 2.2 Bohr magnetons per atom is entirely contributed by an excess of $3d$ electrons with spin up, we find that there are 4.6 $3d$ electrons with spin up, and 2.4 $3d$ electrons with spin down. Under these assumptions, the total charge density near the peak at 0.4 Bohr radii is found to have 44% e_g symmetry and 56% t_{2g} symmetry. A spherically symmetric charge distribution would be 40% e_g. The net spin-up charge density near the peak is 52% e_g, which we will compare with the experimental value, 50%.[1,3]

Two corrections, neither of which has a large effect on the results for iron, must be made to the calculated asphericity. Exchange polarization contracts the wave functions of spin-up electrons relative to those of spin down. As an upper limit to this effect, we take the result of Wood and Pratt[7] that the ratio of spin-up to spin-down charge density is 1.14 near the peak in the $3d$ radial wave function. The result is to change the fraction of the net spin-up peak having e_g symmetry from 52% to 51%. The exchange polarization effect is small in all cases studied.

A second correction is the explicit crystal field shift. Callaway and Edwards[2] find that the e_g states are raised relative to the t_{2g} states by $0.094Z$-$0.128Z$ ev, depending on the choice of wave functions, where Z is the net charge near each nucleus. We estimate an upper limit to Z to be 2.7, of which 1.0 comes from the uniformly distributed $4s$ electron, and 1.7 is an estimate of

the $3d$ charge density which is spread out.[8] Thus an upper limit to the amount by which the e_g states are raised is 0.35 ev, which is about 4% of the $3d$ bandwidth. If we take this shift into account for iron, the net spin-up charge density peak is 56% e_g. If both the exchange and crystal field corrections are made, the charge density peak is 54% e_g.

For comparison with experiment we use the average of the corrected and uncorrected values described above. Thus the calculated net spin-up charge density peak in iron has 53% e_g symmetry, and the calculated total charge density peak has 43% e_g symmetry. The former value is to be compared with the estimate[3] from polarized neutron diffraction measurements[1] that the net spin-up charge distribution in iron is 50% e_g. Pickart and Nathans[9] find in ordered Fe_3Al that the net spin-up charge, for those iron atoms which have only iron atoms as nearest neighbors, is about 60% e_g. The x-ray form factor measurements of Batterman, Chipman, and DeMarco[10] do not appear to allow an estimate of the asphericity of the total $3d$ electron charge distribution to be made.

It is tempting to try to extend the calculation made for iron to other body-centered cubic metals, and in particular to disordered ferromagnetic alloys.[11] Our calculation can be so extended if the relative order of energy levels is determined primarily by the bcc structure, and only secondarily by the particular transition elements occupying the lattice sites. Results based on this assumption are shown in Table I. The minimum asphericity of the net spin-up charge peak occurs near the alloy having the highest moment, while the maximum occurs for an atomic number slightly less than that of iron.

The asphericities calculated using charge-density peak heights differ only slightly from those that would be found from density-of-states considerations. That makes possible a simple description of the results. In nonmagnetic material the lowest states of both spins are filled until all valence electrons are used up. This fixes the position of the nonmagnetic Fermi level. In magnetic material the asphericity of the net spin-up charge density is determined by the symmetry character of the states in the neighborhood of the nonmagnetic Fermi level. In iron these states have predominantly e_g symmetry,[6] which accounts for our results. This qualitative method can be extended to face-centered cubic metals. Recent band structure calculations for nickel and fcc iron[12] suggest that the nonmagnetic Fermi level corresponding to the ten valence electrons of nickel lies in a portion of the band having states of predominantly t_{2g} symmetry, while the nonmagnetic Fermi level for the nine valence electrons of cobalt lies in a region of more nearly e_g character. These estimates are consistent with the results of polarized neutron diffraction experiments for nickel and cobalt.[1,3,13]

Table I. Calculated asphericity of the $3d$ charge density peak. The columns represent body-centered cubic transition metals and alloys.[a] The numbers of $3d$ electrons per atom having spin up and spin down are given by N_+ and N_-, respectively. The third row gives the percentage of the total charge density peak with e_g symmetry. The fourth row gives the corresponding percentage for the net spin-up peak height. The first number of each pair is calculated directly from the band structure,[b] while the second number includes corrections for exchange polarization and crystal field effects. The best value to use in comparing with experiment is the average of the two percentages.

$N_+ - N_-$	1.5	1.8	2.1	2.2	2.5	2.2
$N_+ + N_-$	6.3	6.6	6.9	7.0	7.5	7.8
X ray	44, 37	42, 41	45, 43	44, 43	40, 39	39, 39
Neutron	58, 42	49, 48	55, 56	52, 54	44, 46	48, 47

[a] See reference 11.
[b] See reference 6.

The author thanks Dr. E. Callen and Dr. R. A. Ferrell for helpful comments on the manuscript.

[1] R. Nathans, C. G. Shull, G. Shirane, and A. Andresen, J. Phys. Chem. Solids 10, 138 (1959).

[2] J. Callaway and D. M. Edwards, Phys. Rev. 118, 923 (1960).

[3] R. J. Weiss and A. J. Freeman, J. Phys. Chem. Solids 10, 147 (1959).

[4] The first four nonvanishing Y_l are: $Y_0 = 1$, $Y_4 = (21/4)^{1/2}(1-5s)$, $Y_6 = (13/32)^{1/2}(2-21s+231t)$, $Y_8 = (561/64)^{1/2}(1-18s-52t+65s^2)$, where $s = (x^2y^2+y^2z^2+z^2x^2)r^{-4}$ and $t = x^2y^2z^2r^{-6}$. Our $Y_l = (4\pi)^{1/2}K_{l,1}$ in the notation of reference 2.

[5] In a general case the coefficients of $Y_l(\beta,\gamma)$ in Eq. (2) will be modified by terms which arise because the atomic cell does not have spherical symmetry.

[6] F. Stern, Phys. Rev. 116, 1399 (1959).

[7] J. H. Wood and G. W. Pratt, Jr., Phys. Rev. 107, 995 (1957).

[8] This value is obtained from the results of reference 6, which show that at the surface of the atomic sphere the charge density contributed by seven $3d$ electrons is the same as that of 1.7 electrons uniformly distributed. However, this is likely to be a substantial

overestimate, because the wave functions of reference 6 were calculated without exchange, and are too spread out.

[9]S. J. Pickart and R. Nathans (unpublished).

[10]B. W. Batterman, D. R. Chipman, and J. J. DeMarco, Phys. Rev. 122, 68 (1961).

[11]R. M. Bozorth, Ferromagnetism (D. Van Nostrand Company, Inc., Princeton, New Jersey, 1951), p. 441.

[12]J. Hanus, Massachusetts Institute of Technology Solid State and Molecular Theory Group Quarterly Progress Report, October 15, 1960 (unpublished); J. H. Wood, ibid., April 15, 1958 (unpublished).

[13]R. Nathans and A. Paoletti, Phys. Rev. Letters 2, 254 (1959).

VARIATION OF THE ELASTIC MODULI AT THE SUPERCONDUCTING TRANSITION

G. A. Alers and D. L. Waldorf

Scientific Laboratory, Ford Motor Company, Dearborn, Michigan

(Received May 22, 1961)

Very recently there has been considerable interest in the changes in the Debye θ_0[1] and the zero-point energy[2] associated with the transition from the normal to the superconducting state. Of much longer standing is the problem of observing the discontinuity in the bulk modulus associated with the zero-field superconducting transition and relating it to measurements of the pressure dependence of the critical field.[3] A calculation of all these quantities can be made if the changes in all the elastic moduli of a given superconductor are known. This Letter presents measurements of the change in all three elastic moduli of the cubic superconductors Pb, V, and Nb. Tantalum was also studied but will not be discussed because it showed impurity-sensitive anomalous behavior in both the normal and superconducting states.

The measurements were made using 10-Mc/sec sound pulses in a modified "sing-around" apparatus designed and built by Forgacs[4] to have a sensitivity of one part in 10^7. Changes in the three elastic moduli $C_L = \frac{1}{2}(C_{11} + C_{12} + 2C_{44})$, $C = C_{44}$, and $C' = \frac{1}{2}(C_{11} - C_{12})$ were directly determined. The Ta and Nb single crystals were purchased from the Linde Company and were nominally 99.9% pure. The vanadium sample was prepared in this laboratory to a purity of 99.98%. The lead crystal was grown from high-purity lead to which 0.02% Bi was added in order to keep the electron mean free path at helium temperatures much less than the wavelength of the sound waves used. With these purities, no difficulty with attenuation changes at the superconducting transition was encountered. Corrections for dimensional changes at the transition are too small to be considered in all cases.[5] No correction for a deviation from adiabatic sound wave propagation conditions within the samples was necessary for V and Nb, but for Pb a correction of at most two parts per million near 4°K might be necessary for the longitudinal mode and the bulk modulus.

The actual measurements of the difference in the elastic moduli between the normal and superconducting states are shown in Figs. 1, 2, and 3. It is to be noted that the moduli in the superconducting state are always less than in the normal state. The dip in the C modulus difference for niobium near 2°K is probably associated with impurities since vacuum outgassing decreases its depth. The sag in $\Delta C_L/C_L$ for Pb around 4°K can be eliminated by a reasonable correction for the deviation from adiabatic conditions for the sound wave. But the drop in $\Delta C_L/C_L$ below 2°K would remain.

The method of measurement also yielded the

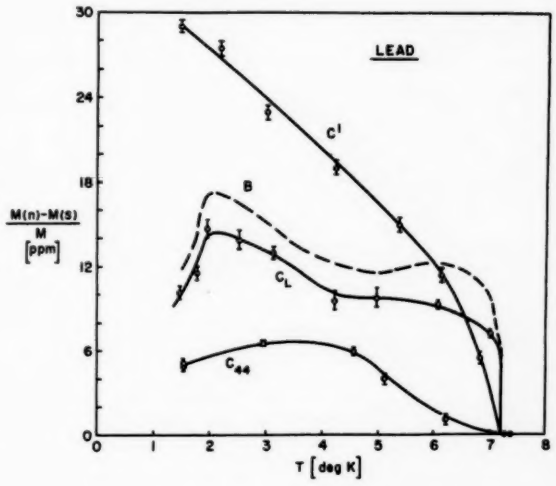

FIG. 1. The difference in the elastic moduli of lead between the normal and the superconducting states as a function of temperature.

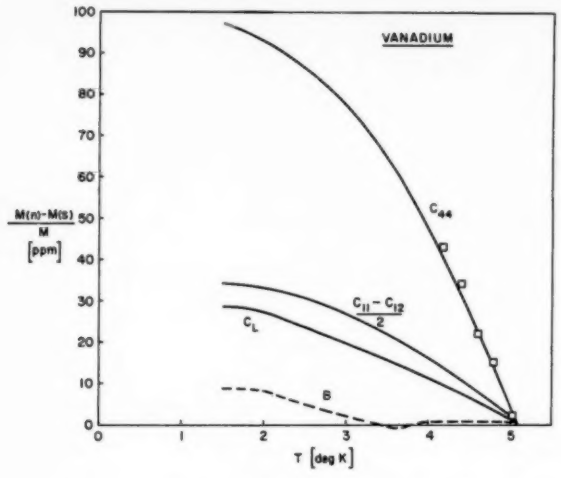

FIG. 2. The difference in the elastic moduli of vanadium between the normal and superconducting states as a function of temperature.

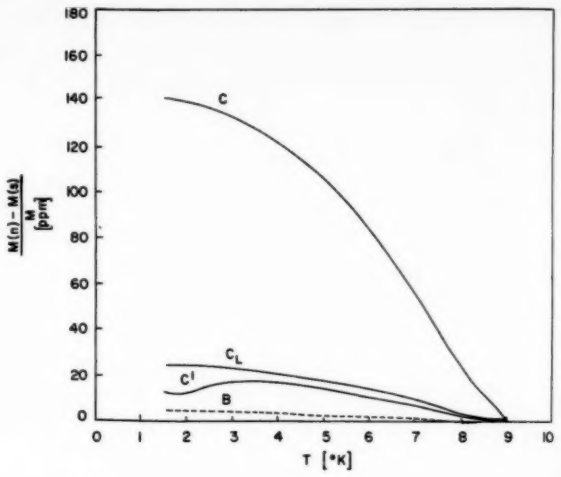

FIG. 3. The difference in the elastic moduli of niobium between the normal and superconducting states as a function of temperature.

temperature dependence of the elastic moduli in both the normal and superconducting states. In the normal state the moduli varied according to the relationship

$$M = M_0(1 - \alpha T^2), \tag{1}$$

as T approached zero. The values of α are given in column 3 of Table I. Since the elastic moduli are second derivatives with respect to a strain of the total energy of the solid, it seems reasonable that this T^2 dependence can be attributed to the conduction electrons which have an internal energy proportional to T^2.

Temperature-dependent elastic moduli may be expected to make the Debye θ temperature-dependent. Daunt and Olsen[2] have shown that a temperature-dependent θ can produce a large contribution to the specific heat from the zero-point

Table I. The adiabatic elastic moduli at 4.2°K and the Debye temperature θ_0 computed from them for the superconductors Pb, V, and Nb. The other columns are quantities derived from the present measurements as is described in the text.

Element	Modulus [10^{11} dyne cm^{-2}]	α [10^{-7} deg K^{-2}]	θ_0 [°K]	$\theta_{(n)} - \theta_{(s)}$ [°K]	$\frac{3}{4}K\Delta\theta$ [10^{-7} ev/atom]	$H_0^2/8\pi$ [10^{-7} ev/atom]	$\Delta B/B$ [ppm]	$(B/4\pi)(\partial H_C/\partial p)^2$ [ppm]
Pb	C_L = 6.99	34	105	4.6×10^{-4}	0.45	4.7	4.0	3.2
	C = 1.94	57.5						3.6
	C' = 0.506	69.2						4.6
								4.7
V	C_L = 22.18	3.3	400	1.5×10^{-2}	15	6.2	$<\frac{1}{2}$	2.1
	C = 4.60	10.3						
	C' = 5.65	4.6						
Nb	C_L = 22.50	2.7	277	1.6×10^{-2}	15	17	0.7	2.7
	C = 3.09	12.8						
	C' = 6.01	2.3						

lattice vibrations. They have used this contribution to explain the anomalously low specific heat observed in superconductors.[6] Unfortunately, their argument neglects other energy terms which necessarily compensate for the zero-point energy variations. If the specific heat is derived from the entropy, which is more easily specified than the total energy, it is easily shown that a temperature-dependent θ simply introduces a correction factor of the form $(1 - 2\,d\ln\theta/d\ln T)$ to the usual T^3 lattice specific heat. Using the present measurements to estimate this correction factor, it follows that the contribution to the specific heat from a temperature-dependent θ is too small and of the wrong sign to explain the observed specific heat of superconductors.[6]

Even though the zero-point energy does not appreciably affect the specific heat, it is an important part of the total lattice kinetic energy. Chester[7] has shown that the difference in the lattice kinetic energy between the normal and superconducting states should be comparable to the total free-energy difference between the two states. If one assumes that the relative changes in sound velocity observed at 10 Mc/sec are the same at all frequencies, then the change in zero-point energy between the normal and superconducting states can be calculated. Column 6 of Table I gives this calculated change in zero-point energy, while column 7 shows the total free-energy change at 0°K as determined from the critical magnetic field. The two energy changes are indeed quite comparable. Thus, if all the frequencies are changed by a fractional amount equal to the changes observed at 10 Mc/sec, then the zero-point energy contribution to the lattice kinetic energy must not be neglected.

It is interesting to note that the modulus most affected by the transition to superconductivity is the smallest shear modulus (C for Nb and V and C' for Pb and Ta). Since the change in modulus is related thermodynamically to the change in the critical field with stress,[8] the present results would indicate that a shear stress would be most effective in changing the critical field. Pippard[9] has shown that the critical field in cubic superconductors must depend upon a higher power of the shear stress than the first. Thus measurements of the variation of the critical field with shear stress should not only be large but also nonlinear. This effect has been observed recently by Seraphim and Marcus.[10]

Column 8 of Table I gives the discontinuous change in the bulk modulus observed at the superconducting transition in zero magnetic field. It is related to the pressure derivative of the critical field by

$$\Delta B/B = (B/4\pi)[dH_c/dP]^2 \text{ at } T = T_c. \qquad (2)$$

Column 9 gives the right side of Eq. (2) as computed from the dH/dP data of several authors.[2,11] The agreement is excellent for the soft superconductor Pb but very poor for vanadium and niobium. The failure in the case of the hard superconductors is probably associated with impurity effects and demands further study.

The authors wish to thank Dr. A. W. Overhauser for his encouragement to make the measurements and for his important contributions to the interpretation of the final data. Mr. R. L. Forgacs of this laboratory also deserves special recognition for his design of the electronic apparatus which has far outperformed its original specifications.

[1]B. S. Chandrasekhar and J. A. Rayne, Phys. Rev. Letters 6, 3 (1961).

[2]J. G. Daunt and J. L. Olsen, Phys. Rev. Letters 6, 267 (1961).

[3]D. Shoenberg, Superconductivity (Cambridge University Press, New York, 1952), p. 75.

[4]R. L. Forgacs, IRE Trans. on Instrumentation I-9, 359 (1960).

[5]J. L. Olsen and H. Rohrer, Helv. Phys. Acta 33, 675 (1960).

[6]C. A. Bryant and P. H. Keesom, Phys. Rev. Letters 4, 460 (1960); H. A. Boorse, A. T. Hirshfeld, and H. Leupold, Phys. Rev. Letters 5, 246 (1960).

[7]G. V. Chester, Phys. Rev. 103, 1693 (1956).

[8]W. P. Mason, Physical Acoustics and the Properties of Solids (D. Van Nostrand Company, Inc., Princeton, New Jersey, 1958), p. 341.

[9]A. B. Pippard, Phil. Mag. 46, 1115 (1955).

[10]D. P. Seraphim, Bull. Am. Phys. Soc. 6, 129 (1955); P. Marcus and D. P. Seraphim (to be published).

[11]See review by J. L. Olsen and H. Rohrer, Helv. Phys. Acta 33, 872 (1960).

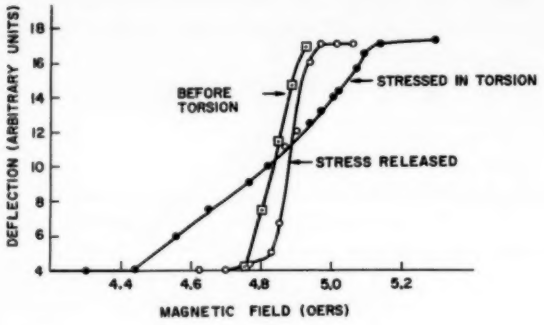

FIG. 2. Effect of twist on the magnetic transition curve of a single-crystal rod of Sn oriented with tetrad axis nearly at 45° to the crystal axis.

hence the transition curve is broadened but its mean position is not displaced. This behavior is observed in a reversible way, as shown by Fig. 2.

We wish to thank A. Burgess and P. Roland for assistance with the measurements, and Y. Budo for assistance in the design and construction of the apparatus.

[1]C. Grenier, Compt. rend. 240, 2302 (1955).

[2]Milan D. Fiske, J. Phys. Chem. Solids 2, 191 (1957).

[3]L. D. Jennings and C. A. Swenson, Phys. Rev. 112, 31 (1958).

[4]C. A. Swenson and C. H. Hinrichs, Proceedings of the Seventh International Conference on Low-Temperature Physics, 1960 (University of Toronto Press, Toronto, 1961), p. 345.

[5]M. Garfinkel and D. E. Mapother, Phys. Rev. 122, 459 (1961).

[6]J. L. Olsen and H. Rohrer, Helv. Phys. Acta 30, 49 (1957).

[7]G. D. Cody, Phys. Rev. 111, 1078 (1958).

[8]G. A. Alers and D. L. Waldorf, preceding Letter [Phys. Rev. Letters 6, 677 (1961)].

[9]D. F. Gibbons and C. A. Renton, Phys. Rev. 114, 1257 (1959).

[10]D. P. Seraphim, J. I. Budnick, and W. B. Ittner, III, Trans. Am. Inst. Mining, Met., Petrol. Engrs. 218, 527 (1960).

[11]See (1); the general relation between β_{ij} and the $(\partial^2 H_c/\partial\sigma_i\partial\sigma_j)$ has a factor 2 when either i or j (but not both) is 4, 5, 6, and a factor 4, when both are.

[12]See reference 2, pp. 195, 197.

[13]G. A. Alers (private communication); consistent results for the elastic constant discontinuities of Ta like those[8] for Pb, Nb, V are not yet available. The value of $\Delta C_{44}/C_{44}$ seemed the most reliable of the measured values kindly sent us by Dr. Alers (it changed much less on annealing the specimen and had a more reasonable temperature dependence), but the value of β_{44} is less certain than the other two second order results, i.e., the terms in (3) and (4).

[14]$\beta_{11}+2\beta_{12}$ is of order 10^{-10} gauss/atm^2; Jennings and Swenson[3] measured $(\partial^2 T/\partial p^2)_{T_c}$, but even if it vanishes, the evaluation of $(\partial^2 H_c/\partial p^2)_{T_c}$ from it brings in additional terms of order 10^{-10}.

[15]The general relation is $\Delta S_{ij}=-(1/4\pi)(\beta_i\beta_j)$, where the S_{ij} are the elastic compliance coefficients. See for example reference 9.

[16]The magnitude of the second order effect at 200 atm appears to be only a few percent of the first order effect assuming that second order shear effects are not much greater in magnitude than second order volume effects; it may be estimated from the measured value of $(\partial^2 T_c/\partial p^2)_{T_c}=7.8\times10^{-10}$ deg/atm^2, which gives $(\partial^2 H/\partial p^2)_{T_c}\cong 2\times10^{-8}$ gauss/atm^2. If the observed small values of ΔH_c are in fact second order effects, the first order coefficient β_1 would be even smaller.

[17]Grenier's measurements[1] have been extrapolated to T_c, and account has been taken of the angle of the stress with the tetrad axis [see (6)].

[18]Two perpendicular directions define the shear, the stresses being tangential to the planes perpendicular to these directions.

VALENCE SPIN-ORBIT SPLITTING AND CONDUCTION g TENSOR IN Si†

L. Liu

Institute for the Study of Metals and Department of Physics, University of Chicago, Chicago, Illinois

(Received May 15, 1961)

Roth et al. have calculated conduction g tensors in semiconductors, and have obtained excellent agreement with experiment for Ge[1,2] and InSb.[3] In the absence of crystal wave functions the calculations for these crystals and Bi[4] were based on a two-level approximation to the effective-mass sum rule. Then the g tensor could be estimated from observed spin-orbit splittings and effective masses. Roth also analyzed Si in the two-band approximation, but her original estimate of the isotropic g shift was too large by a factor of 3. Elliott pointed out[5] that because of the proximity of the conduction band edge along Δ to the point X, the crystal spin-orbit splitting should be small (at X it is zero by symmetry). Our calculations show that the valence spin-orbit splitting at Δ is actually too small by a factor of 3 to explain the experimental g shift. Yafet realized[6] that in Si the term considered by Roth might give the wrong sign for the isotropic g shift; our calculations have verified his conjecture. Finally, recent spin resonance experiments by Feher and Wilson[7] on strained Si samples have shown that $\delta g_{\perp}$, which is negligible in the two-band model, is actually greater than $\delta g_{\parallel}$. Therefore the two-band approximation is inadequate for Si, and a detailed calculation using crystal wave functions is required.

Several quantum-mechanical calculations of the g factor of electrons in crystals have been reported using cellular methods.[8,9] Here we use the orthogonalized plane wave (OPW) method, which is well suited to Si. We begin with the spin-orbit splitting of the valence band; the spin-orbit splitting was first calculated from OPW wave functions by Cohen and Falicov.[10]

OPW crystal wave functions are divided into a "smooth" plane wave part and a core part:

$$\psi_{\vec{k}}^{\alpha}=\sum_{\vec{K}}a^{\alpha}(\vec{k}+\vec{K})\,|(\vec{k}+\vec{K})^{\alpha}\rangle+\sum_{t}b_{\vec{k}}^{\alpha}\,|\phi_{t,\vec{k}}{}^{\alpha}\rangle, \tag{1}$$

where α labels irreducible representations, $(\vec{k}+\vec{K})^{\alpha}$ is a symmetrized combination of plane waves, and $b_{\vec{k}}^{\alpha}$ is determined from the requirement that $\psi_{\vec{k}}^{\alpha}$ be orthogonal to the core orbital ϕ_t. In computing $\langle\psi_{\vec{k}}^{\alpha}|H_{\text{s.o.}}|\psi_{\vec{k}}^{\beta}\rangle$, where $H_{\text{s.o.}}$ is the spin-orbit operator, we find that 96% of the matrix element comes from core-core terms. The spin-orbit splitting of the p valence bands along $\vec{k}=(\Delta 00)$ is therefore conveniently expressed in terms of the $2p$ core orbitals. For instance, at $\vec{k}=0$,

$$\Delta_{\text{s.o.}}(\Gamma_{25'})=3\,|A_{\Gamma_{25'}}|^{2}\,|\langle 2p_y|H_{\text{s.o.}}^{x}|2p_z\rangle|, \tag{2}$$

where

$$A_{\Gamma_{25'}}=(2/\sqrt{3})a(111)b_{2p}(111)+\sqrt{2}\,a(002)b_{2p}(002)+\cdots \tag{3}$$

The parameters a and b are taken from the band calculation of Kleinman and Phillips.[11] Sixty-five plane waves were used in the expansion (3).

Consider first the $2p$ spin-orbit splitting $3\,|\langle 2p_y|H_{\text{s.o.}}^{x}|2p_z\rangle|$. Tomboulian and Cady[12] completed the identification of the x-ray emission lines $2p^{3/2}\rightarrow 2s$ and $2p^{1/2}\rightarrow 2s$ for the second row of the periodic table. Their values for the $2p$ spin-orbit splitting for Mg and Si are listed in the first line of Table I. By invoking Slater's rule that the missing electron gives an extra screening charge $0.3e$, we can use Tomboulian and Cady's values for the spin-orbit splittings to estimate the $2p$ splitting in neutral Mg and Si (second line of Table I). Calculated values for Mg[13] and Si are listed in the third line. It will be seen that the discrepancies are quite similar for Mg and Si. These discrepancies are not understood; in the calculations quoted below, the corrected experimental value for the $2p$ spin-orbit splitting is used.

From (2) and (3) we now find $\Delta_{\text{s.o.}}(\Gamma_{25'})=0.042$ ev, in good agreement with the infrared value 0.0441 ± 0.0004 ev of Zwerdling et al.[14] A plot of $\Delta_{\text{s.o.}}(\Delta_5)$ is given in Fig. 1.

Starting from the effective-mass $(\vec{k}\cdot\vec{p})$ Hamiltonian and treating $H_{\text{s.o.}}$ as a perturbation, Roth[1] has derived the following formulas for the g tensor in Si:

$$\delta g_{\parallel}=\delta g_{x}=\text{Re}\frac{4}{mi}\sum_{\mu,\nu}\frac{1}{E_{0\mu}E_{0\nu}}\langle\Delta_1|p_y|\Delta_5{}^{\mu y}\rangle\langle\Delta_5{}^{\mu y}|H_{\text{s.o.}}^{x}|\Delta_5{}^{\nu z}\rangle\langle\Delta_5{}^{\nu z}|p_z|\Delta_1\rangle$$

$$+\text{Re}\frac{8}{mi}\sum_{\mu,\nu}\frac{1}{E_{0\mu}E_{0\nu}}\langle\Delta_1|H_{\text{s.o.}}^{x}|\Delta_1{}',{}^{\mu}\rangle\langle\Delta_1{}',{}^{\mu}|p_y|\Delta_5{}^{\nu z}\rangle\langle\Delta_5{}^{\nu z}|p_z|\Delta_1\rangle, \tag{4}$$

$$\delta g_{\perp} = \delta g_{y,z} = \mathrm{Re}\frac{4}{mi}\sum_{\mu,\nu}\frac{1}{E_{0\mu}E_{0\nu}}\langle\Delta_1|p_z|\Delta_5{}^{\mu z}\rangle\langle\Delta_5{}^{\mu z}|H_{\mathrm{s.o.}}{}^{y}|\Delta_1{}^{\nu}\rangle\langle\Delta_1{}^{\nu}|p_x|\Delta_1\rangle$$

$$+\mathrm{Re}\frac{4}{mi}\sum_{\mu,\nu}\frac{1}{E_{0\mu}E_{0\nu}}\langle\Delta_1|H_{\mathrm{s.o.}}{}^{y}|\Delta_5{}^{\mu z}\rangle\langle\Delta_5{}^{\mu z}|p_z|\Delta_1{}^{\nu}\rangle\langle\Delta_1{}^{\nu}|p_x|\Delta_1\rangle$$

$$+\mathrm{Re}\frac{4}{mi}\sum_{\mu,\nu}\frac{1}{E_{0\mu}E_{0\nu}}\langle\Delta_1|p_z|\Delta_5{}^{\mu z}\rangle\langle\Delta_5{}^{\mu z}|p_x|\Delta_5{}^{\nu z}\rangle\langle\Delta_5{}^{\nu z}|H_{\mathrm{s.o.}}{}^{y}|\Delta_1\rangle. \quad (5)$$

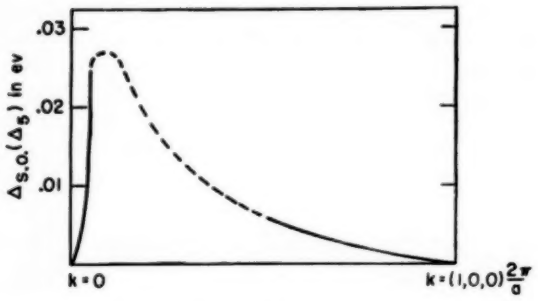

FIG. 1. Sketch of the spin-orbit splitting of the Δ_5 valence band of silicon. The dashed curve represents interpolation from the calculated results. Note that although there is a spin-orbit splitting for the valence state $\Gamma_{25'}$ at $\vec{k}=0$, the lower split level is associated with $\Delta_{2'}$. So as far as Δ_5 band is concerned, the splitting is equal to zero at the zone center.

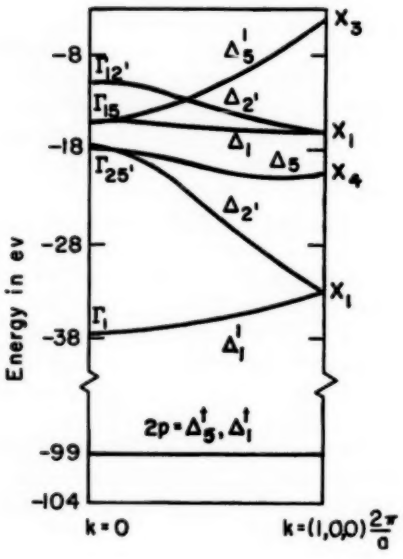

FIG. 2. Sketch of the energy bands of silicon along [100] axis of the Brillouin zone, after Kleinman and Phillips. Superscript t is used to denote the $2p$ core states.

Figure 2 shows the relevant energy levels. The conduction band edge is believed[15] to be at $\Delta = 0.85(2\pi a^{-1})$. Note the $2p$ core levels.

Because of the selection rule $\langle X_4{}^{n}|H_{\mathrm{s.o.}}|X_4{}^{n}\rangle = 0$, the most important matrix elements of $H_{\mathrm{s.o.}}$ are $\langle\Delta_5{}^{n}|H_{\mathrm{s.o.}}|\Delta_5{}^{n'}\rangle \simeq \langle X_4{}^{n}|H_{\mathrm{s.o.}}|X_4{}^{n'}\rangle \neq 0$. From Table II we see that terms of this form, in which one of the levels is a $2p$ core state, make the largest contribution to δg. Comparison with Feher and Wilson's values is made in Table III; the agreement is excellent.

According to Roth[16] the "one-valley" interband term H_2 is responsible for donor spin-lattice relaxation for $H \| (100)$. Roth's expression for H_2 is

$$H_2 = \tfrac{1}{2}A\beta\{\epsilon_{xy}(\sigma_x H_y + \sigma_y H_x) + \text{cyclic term}\}, \quad (6)$$

where A is given in terms of the deformation potential E_{yz} by

$$A = \frac{4i}{3m}\frac{\langle\Delta_{2'}|p_x|\Delta_{2'}\rangle\langle\Delta_{2'}|E_{yz}|\Delta_1\rangle}{E_{12'}{}^{2}E_{15}}$$

$$\times\{\langle\Delta_1|p_y|\Delta_5{}^{y}\rangle\langle\Delta_5{}^{y}|H_{\mathrm{s.o.}}{}^{y}|\Delta_{2'}\rangle$$

$$+\langle\Delta_1|H_{\mathrm{s.o.}}{}^{y}|\Delta_5{}^{z}\rangle\langle\Delta_5{}^{z}|p_y|\Delta_{2'}\rangle\}. \quad (7)$$

We have calculated all the matrix elements in A except that of the deformation potential. From Feher and Wilson's measured value[7] of A (0.44 $\pm$ 0.04), we find that $\langle\Delta_{2'}|E_{yz}|\Delta_1\rangle = 23$ ev. For comparison, the intraband shear deformation

Table I. Spin-orbit splitting of $2p$ core state.

	Mg	Si
Exp. (ev)	0.27	0.72
Corr. exp. (ev)	0.22	0.60
Calc. (ev)	0.17	0.49

Table II. Relative magnitude of contributions to g tensor. The first term in $\delta g_{\parallel}$ is the only one contributing in the two-band approximation.

	Term in Eqs. (4) and (5) involving:			Relative magnitude with respect to first term in Eq. (4)
$\delta g_{\parallel}$	$\langle\Delta_1\|p_y\|\Delta_5^{y}\rangle$,	$\langle\Delta_5^{y}\|H_{s.o.}^{x}\|\Delta_5^{z}\rangle$,	$\langle\Delta_5^{z}\|p_z\|\Delta_1\rangle$	1
	$\langle\Delta_1\|p_y\|\Delta_5^{1y}\rangle$,	$\langle\Delta_5^{1y}\|H_{s.o.}^{x}\|\Delta_5^{z}\rangle$,	$\langle\Delta_5^{z}\|p_z\|\Delta_1\rangle$	0.7
	$\langle\Delta_1\|p_y\|\Delta_5^{y}\rangle$,	$\langle\Delta_5^{y}\|H_{s.o.}^{x}\|\Delta_5^{1z}\rangle$,	$\langle\Delta_5^{1z}\|p_z\|\Delta_1\rangle$	0.7
	$\langle\Delta_1\|p_y\|\Delta_5^{ty}\rangle$,	$\langle\Delta_5^{ty}\|H_{s.o.}^{x}\|\Delta_5^{z}\rangle$,	$\langle\Delta_5^{z}\|p_z\|\Delta_1\rangle$	-2.6
	$\langle\Delta_1\|p_y\|\Delta_5^{y}\rangle$,	$\langle\Delta_5^{y}\|H_{s.o.}^{x}\|\Delta_5^{tz}\rangle$,	$\langle\Delta_5^{tz}\|p_z\|\Delta_1\rangle$	-2.6
$\delta g_{\perp}$	$\langle\Delta_1\|p_z\|\Delta_5^{z}\rangle$,	$\langle\Delta_5^{z}\|p_x\|\Delta_5^{z}\rangle$,	$\langle\Delta_5^{z}\|H_{s.o.}^{y}\|\Delta_1\rangle$	-0.5
	$\langle\Delta_1\|p_z\|\Delta_5^{z}\rangle$,	$\langle\Delta_5^{z}\|H_{s.o.}^{y}\|\Delta_1^{1}\rangle$,	$\langle\Delta_1^{1}\|p_x\|\Delta_1\rangle$	0.3
	$\langle\Delta_1\|p_z\|\Delta_5^{tz}\rangle$,	$\langle\Delta_5^{tz}\|H_{s.o.}^{y}\|\Delta_1^{1}\rangle$,	$\langle\Delta_1^{1}\|p_x\|\Delta_1\rangle$	-0.2
	$\langle\Delta_1\|p_z\|\Delta_5^{z}\rangle$,	$\langle\Delta_5^{z}\|H_{s.o.}^{y}\|\Delta_1^{t}\rangle$,	$\langle\Delta_1^{t}\|p_x\|\Delta_1\rangle$	-3.1
	$\langle\Delta_1\|p_z\|\Delta_5^{tz}\rangle$,	$\langle\Delta_5^{tz}\|H_{s.o.}^{y}\|\Delta_1^{t}\rangle$,	$\langle\Delta_1^{t}\|p_x\|\Delta_1\rangle$	-0.3

Table III. g tensor for Si.

	$\delta g_{\parallel}$	$\delta g_{\perp}$
Calc.	-0.0027	-0.0036
Exp.	-0.0028	-0.0040

potential matrix element is $E_2 = \langle\Delta_1|E_{yy}|\Delta_1\rangle = 7$ ev.[17] Evaluation of this discrepancy requires a detailed theory of deformation potentials.

The author wishes to express his gratitude to Professor J. C. Phillips for suggesting the problem and for many helpful comments, to Professor M. H. Cohen and Dr. L. M. Falicov for interesting discussions, and to Dr. L. Kleinman for showing him the Si wave functions.

†Work supported in part by the Office of Naval Research.

[1]L. M. Roth, Phys. Rev. 118, 1534 (1960).

[2]L. M. Roth and B. Lax, Phys. Rev. Letters 3, 217 (1959).

[3]L. M. Roth, B. Lax, and S. Zwerdling, Phys. Rev. 114, 90 (1959).

[4]M. H. Cohen and E. I. Blount, Phil. Mag. 5, 115 (1960).

[5]R. J. Elliott, Phys. Rev. 96, 280 (1954), and private communication.

[6]Y. Yafet (private communication).

[7]G. Feher and D. K. Wilson, 1960 Prague Conference [Czech. J. Phys. (to be published)], and private communication.

[8]Y. Yafet, Phys. Rev. 85, 478 (1952).

[9]H. Brooks (unpublished).

[10]M. H. Cohen and L. M. Falicov, Phys. Rev. Letters 5, 544 (1960).

[11]L. Kleinman and J. C. Phillips, Phys. Rev. 118, 1153 (1960).

[12]D. H. Tomboulian and W. M. Cady, Phys. Rev. 59, 422 (1941).

[13]We are grateful to Dr. L. M. Falicov for the Mg value.

[14]S. Zwerdling, K. J. Button, B. Lax, and L. M. Roth, Phys. Rev. Letters 4, 173 (1960).

[15]J. C. Phillips, Phys. Rev. 112, 685 (1958).

[16]L. M. Roth, Lincoln Laboratory, Solid State Research Quarterly Progress Report, April 15, 1960 (unpublished), p. 38, and Prague Conference on Semiconductors, 1960 [Czech. J. Phys. (to be published)].

[17]R. W. Keyes, in Solid State Physics, edited by F. Seitz and D. Turnbull (Academic Press, New York, 1960), Vol. 11.

SUPERCONDUCTING CHARACTERISTICS OF SUPERIMPOSED METAL FILMS

Paul H. Smith, Sidney Shapiro, John L. Miles, and James Nicol
Advanced Research Division, Arthur D. Little, Inc., Cambridge, Massachusetts
(Received May 31, 1961)

The electrical properties of superimposed films of superconductors and normal metals have been examined in a series of experiments employing the techniques of resistance measurement, persistent currents, and electron tunneling. The results indicate that the normal metal, e.g., Ag in a Ag-Pb pair, does in fact go superconducting and that the system behaves as does a superconductor with a transition temperature determined both by the constituent materials and by their relative thicknesses. It is argued that the observations are not due to alloying, diffusion, or similar effects. The experiments are compared with those of Meissner[1] on the contact resistance between crossed plated wires of normal and superconducting metals.

Measurements of resistance, critical temperature, critical current, and critical field vs temperature were made on long thin films prepared by vacuum deposition on glass substrates at pressures lower than 2×10^{-5} mm Hg. Typically these samples were made by superimposing along the length of an Ag film, 1 cm long and 0.3 mm wide, a longer Pb film, 0.15 mm wide, to the ends of which potential and current connections were soldered. Several such samples were deposited simultaneously on the same substrate with, if desired, different thicknesses of either metal. There was a negligible delay and no exposure to the atmosphere between successive depositions. Table I shows the thicknesses of two typical sets of films of "open-faced" and "closed" sandwich construction, illustrated in Fig. 1(b). In general, the longitudinal resistance of the samples was 1 or 2 ohms at room temperature and lower by a factor of 4 at a temperature just above T_c.

Table I. Total thickness in angstroms.

Sample No.	Lead	Silver
1A-1	484 ±30	110 ±30
1A-2	490 ±30	362 ±30
1A-3	518 ±30	886 ±30
1A-4	598 ±30	1840 ±30
35-1	508 ±30	···
35-2	417 ±30	7100 ±30
35-3	487 ±30	7140 ±30

Resistance was measured by passing a low-frequency current through the sample and displaying its voltage-current characteristic on an oscilloscope. Critical temperatures were determined to within a few millidegrees by the first appearance of zero slope, corresponding to zero resistance, at the origin of the trace. Isothermal critical fields were determined similarly by applying an external magnetic field,

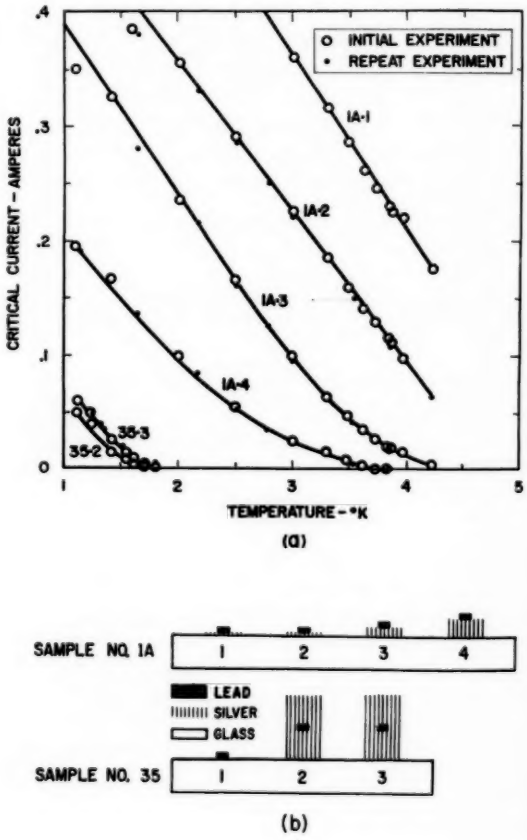

FIG. 1. (a) Critical current vs temperature for Ag-Pb samples of different geometry and silver thickness. The repeat data were obtained one week after the initial experiment. (b) Schematic cross section of the samples showing geometry and relative thickness. The critical current for sample 35-1 (pure lead) was 0.35 ampere, and was virtually independent of temperature.

tangential to the films and normal to the direction of current flow. Critical currents were obtained by noting the value of the instantaneous current at which the characteristic deviated from zero slope. Near the critical temperature critical currents as small as 25 microamperes were measured.

Figure 1(a) shows the variation with temperature of the critical currents of the samples described in Fig. 1(b) and Table I. The progressive depression of the transition temperature ($I_c = 0$) with increasing thickness of Ag for virtually constant thickness of Pb is to be noted; in particular the low transition temperature, 1.87°K, of samples 35-2 and 35-3. A progressive reduction in the critical currents, at a given temperature, also occurs with increasing thickness of Ag, but variation in total thickness complicates comparison between samples. All the curves show a linear relationship between I_c and T, except for the gradual approach to the T axis at small values of I_c. The latter may be indicative of intermediate-state effects. The reproducibility of the observations may be judged from the two sets of data points shown in Fig. 1. One set was obtained after cooling the specimens to 80°K within 10 minutes of deposition; the second set, in one case, was obtained one week later after storage at room temperature. No obvious change occurred in the properties of the films. So far, only preliminary data on the critical fields have been obtained but, as might be expected, the critical fields for the superimposed films are lower than for pure Pb films at the same temperature.

The systematic change of the transition temperature with increasing Ag on a constant thickness of Pb, the reproducibility, and the very low transition temperatures (e.g., the transition temperatures of samples 35-2 and 35-3 were approximately one-fourth that of pure Pb) make it unlikely that the effects are secondary in nature and the result of impurities, strains, diffusion, or alloying. All metals used were 99.999% pure. The nature of the effects was unchanged by the type of construction ("open-faced" or "closed" sandwiches) or by the sequence of deposition. The data did not change with the passage of time. Finally, the Pb-Ag phase diagram is well known[2] and the superconducting properties of the alloy system have been studied.[3] The solid solubility of Ag in Pb is extremely small (a maximum of 0.2 at.% at 300°C) and that of Pb in Ag is modest (a maximum of 2.8 at.% at 600°C, dropping to 0.8 at.% at 300°C). Further, any solid alloy of Pb and Ag is a mixture of the two solid solutions. Allen has shown that the transition temperature of Pb is substantially unaltered by the addition of Ag up to a Ag concentration of about 80% whereupon the mixture ceases to be superconducting. His results suggest that the superconductivity of the alloy is due to the presence of a continuous phase of Pb containing some Ag in solution; when this phase is not present in sufficient amount to form a continuous path through the specimen the alloy remains normal. It follows, therefore, that the maximum amount of Ag in Pb has a negligible effect on the transition temperature of Pb, whereas Ag containing the maximum amount of Pb remains normal.

The results reported in the preceding paragraphs indicate that a pure "normal" metal film in immediate contact with a film of a superconductor will depress the transition temperature of the superconductor, the depression being greater for increasing thickness of the normal metal. To determine if the "normal" metal actually becomes superconducting, two additional sets of experiments were performed.

In the first, Ag films of various thicknesses were sandwiched between Pb films in a persistent current loop, arranged so that the current flowed through the Ag. Since Sn was present elsewhere in the loop, persistent currents were observed only below 3.7°K. In one loop containing about 2800 A of Ag between two Pb films, each about 2000 A thick, a persistent current of 2.9 amperes at 3.64°K was observed. Although a change in current of a few percent would be easily detected, no change was observed in a period of $1\frac{1}{2}$ hours. From prior experience in the use of the persistent current loop and the associated measuring techniques,[4] the inductance of the loop is known to be less than 10^{-10} henry. Accordingly, the upper limit to the loop resistance can be set at 10^{-15} ohm, whereas the computed resistance of the Ag (using known area, thickness, and bulk resistivity) is greater than 10^{-12} ohm. Thus unquestionably a substantial reduction in the resistance of the Ag was observed. In a further experiment, a Au film was sandwiched between a Pb film and a Sn film. In this case, a persistent current could not be generated above 3.57°K, well below the transition temperatures of both Sn and Pb; thereafter the critical current increased smoothly to more than 2 amperes at 3°K.

In the final set of experiments, electron tunneling[5-7] from Pb and Sn films through a Formvar dielectric layer into the Ag side of a Pb-Ag sample was observed. These preliminary experiments have demonstrated the presence of an electron energy gap in the Ag, with a low-temperature limiting value of 0.00016 ev in a sample consisting of 5700 A Ag superimposed on 1500 A Pb and having a transition temperature above 4.2°K.

Following measurements of the contact resistance between crossed plated wires, Meissner[1] has reported the depression of the transition temperature of a superconductor by an adjacent normal metal and the possibility of passing a supercurrent through a thin normal metal film between bulk superconducting metals, but the conditions under which these effects occurred did not preclude the possibility of oxide barrier layer formation or physical penetration of the metal films. He therefore found difficulty in drawing clear-cut conclusions regarding the relationship between the various observations or their fundamental importance. On the other hand, the experiments reported in this Letter demonstrate that when a film of a normal conductor is placed in direct contact with a film of a superconductor, the combination exhibits the attributes of a superconductor, including the ability to pass a supercurrent through the otherwise "normal" metal, the presence of an energy gap throughout the sample,[8] and a transition temperature which depends upon the film thicknesses and the materials involved.

This work has been greatly helped by the advice of R. S. Davis and A. E. Slade and the assistance of R. M. Sawdo to whom grateful acknowledgements are made.

---

[1]H. Meissner, Phys. Rev. 117, 672 (1960). This paper contains references to earlier work.

[2]M. Hansen, Constitution of Binary Alloys, (McGraw-Hill Book Company, New York, 1958), 2nd ed., p. 40.

[3]J. F. Allen, Phil. Mag. 16, 1005 (1933).

[4]Arthur D. Little, Inc., Progress Report, October, 1960 (unpublished), p. 12.

[5]J. Nicol, S. Shapiro, and P. H. Smith, Phys. Rev. Letters 5, 461 (1960).

[6]S. Shapiro and P. F. Strong, Bull. Am. Phys. Soc. 6, 121 (1961); P. H. Smith, S. Shapiro, and J. L. Miles, Bull. Am. Phys. Soc. 6, 121 (1961).

[7]I. Giaever, Phys. Rev. Letters 5, 147, 464 (1960); I. Giaever and K. Megerle, Phys. Rev. 122, 1101 (1961).

[8]Tunneling experiments are being continued to obtain simultaneous measurements of the energy gap on opposite sides of a Ag-Pb sample, this information being pertinent to the question of a position-dependent energy gap, proposed by R. H. Parmenter [Phys. Rev. 118, 1173 (1960)].

SUPERCONDUCTIVITY IN THE NEIGHBORHOOD OF METALLIC CONTACTS*

Leon N. Cooper†
Brown University, Providence, Rhode Island

(Received May 26, 1961)

In the previous Letter, Smith, Shapiro, Miles, and Nicol[1] confirm earlier reports by Meissner[2] and others of a change in the superconducting properties of thin metallic films in contact with thin films of other metals. Parmenter[3] has constructed a theory of such contacts, but a boundary condition he employs is yet to be justified from more fundamental considerations. In this note we should like to present a simple microscopic theory of superconductivity in such contact neighborhoods based on a modification of the parameter $[N(0)V]$ which occurs in the BCS[4] expression for the energy gap:

$$\epsilon_0 = 2(\hbar\omega)_{av} e^{-1/N(0)V}. \tag{1}$$

If two metallic samples—one a superconductor, the other not—are placed in contact, the properties of the entire material change from that of a superconductor in one material to that of a normal metal in the other. The range of the interaction between electrons that produces the superconducting state—the interaction due to phonon exchange and that due to the screened Coulomb repulsion—has been estimated to be about 10^{-8} cm.[5] This might suggest that at a contact surface the change from superconducting to normal properties would occur in this very short distance. However, due to the large coherence distance between zero-momentum pairs, the superconducting correlation can extend deep into a volume where the interaction between the electrons is in fact zero. In this respect the situation is similar to that of the deuteron whose wave function extends large distances beyond the range of the nuclear potential. This creates the possibility that thin films of differing metals deposited on one another profoundly influence each other's superconducting properties.

To be specific, we consider two thin metallic films in contact over the plane $x = 0$. The left-hand film (called 1) has a thickness t_1, while the right-hand film (called 2) has a thickness t_2. In this situation the electron-electron interaction is a function not only of momenta and the relative coordinate r, but also depends upon the absolute position of the two electrons in the x direction, x_1 and x_2:

$$V(r,k,\ldots) = v \text{ if } x_1 \text{ and } x_2 < 0$$
$$= 0 \text{ if } x_1 \text{ or } x_2 \text{ are larger than zero.} \tag{2}$$

Due to this electron-electron interaction there is a nonzero matrix element $V_{k'k}$ for scattering from a two-electron state labelled by k to one labelled by k'. This matrix element, summed over all k' and averaged over k in the interaction region, yields $[N(0)V]_{av}$ in (1), which determines the energy gap and the transition temperature. In a detailed treatment, of course, the energy gap might be a function of direction as well as position.

The essential observation made here is that this average will be decreased if the electron normalization volume is increased while the electron-electron interaction acts over only a part of the volume. This should result in a decrease of the transition temperature of a superconductor in contact with a normal metal. At the same time under the proper circumstances, the same argument implies that a normal film in contact with a superconductor can itself become a superconductor.

To illustrate, consider the extremely simple case of two metals in perfect contact (no oxide barrier between them) with the same Fermi energy and the same effective mass. In this case, if the film to the right is normal usually,

$$[N(0)V]_{1+2} = \frac{t_1}{t_1 + t_2}[N(0)V]_1, \tag{3}$$

where $[N(0)V]_1$ is the interaction constant for a pure specimen of metal 1 while $[N(0)V]_{1+2}$ is that for films 1 and 2 in contact. Due to the exponential dependence of the energy gap on $N(0)V$, under the above conditions even the thinnest films of normal material would produce drastic alterations of the energy gap in a thin superconducting film.

However, matters are not quite this simple. The differing Fermi momenta in two metals produce refraction and, for some angles of incidence, total internal reflection. More important,

under usual experimental conditions a chemisorbed oxygen layer is almost certain to form between the two metals. This will create a potential barrier of the order of several tenths of an electron volt for a distance of several angstroms. Such a barrier will tend to separate the two materials, as will any mechanical barrier or separation.

We therefore expect that the factor $t_1/(t_1+t_2)$ gives the greatest reduction of the effective interaction and that the actual reduction factor should have the form, crudely,

$$t_1/(t_1+\beta t_2), \qquad 0 \leq \beta \leq 1 \quad (4)$$

where β is determined by the barrier between films, the difference in effective mass and well depth—all of the effects which prevent electrons from freely moving from one film to the other. Preliminary calculations indicate that a reasonable value of β will at least crudely reproduce the data of Smith et al.[1]

The arguments presented above have as a necessary converse the implication that the contact region of nonsuperconducting materials should become superconducting when in contact with superconductors. The effective penetration of electrons from one region to another is limited among other things by the electron mean free path; the further superconducting electrons penetrate into the "normal area" the smaller the energy gap should be. However, as there should be only one transition temperature for an entire sample, one might expect in a lead-silver contact that the energy gap would vary spatially, reaching its minimum at the outer silver surface, in spite of the fact that the transition temperature remains high.

The ideas discussed here have many experimental consequences. It would be of great interest to measure the critical temperature as a function of film thickness when specimens have been placed on one another in a high vacuum to reduce the surface layer. The influence of different effective masses and Fermi momenta in the two neighboring specimens as well as of the purity of the nonsuperconducting film on T_c is of interest. Also the variation of T_c with surface layer would be interesting, especially in the light of recent tunneling experiments. More detailed theoretical investigations of these and related questions are being pursued at present.

The author wishes to thank Dr. P. H. Smith, Dr. S. Shapiro, Dr. J. L. Miles, and Dr. J. Nicol for communication of their results prior to publication. He also wishes to thank Professor J. Dillon for a very helpful conversation.

---

*This work was supported in part by the U. S. Atomic Energy Commission.

†Alfred P. Sloan Research Fellow.

[1]P. H. Smith, S. Shapiro, J. L. Miles, and J. Nicol, preceding Letter [Phys. Rev. Letters 6, 686 (1961)].

[2]H. Meissner, Phys. Rev. 117, 672 (1960) (see for further references).

[3]R. H. Parmenter, Phys. Rev. 118, 1173 (1960).

[4]J. Bardeen, L. N. Cooper, and J. R. Schrieffer, Phys. Rev. 108, 1175 (1957).

[5]D. Pines, Phys. Rev. 109, 280 (1958).

CORE RECONSTITUTION IN HEAVY DEFORMED NUCLEI*

Raymond K. Sheline
Florida State University, Tallahassee, Florida
(Received May 8, 1961)

It has generally been assumed that in those regions of the nuclear periodic table where there is a considerable prolate deformation, a smooth systematics of rotational and vibrational characteristics would be obtained as protons and neutrons are added. Recently considerable evidence has been collecting to show that the smooth trends in these systematics are not always obtained. It is the purpose of this paper to enumerate these deviations in the systematics, to classify them according to their position in the nuclear periodic table, and finally to give a tentative explanation involving structural changes expected on the basis of the Nilsson level systematics.

In the case of octupole vibrations (that is, bands with $K=0$ and $I=1-, 3-, 5-, \ldots$) experimental evidence at first seemed[1] to indicate a random relationship between the energy of the octupole vibration and the neutron or proton number. Recent experimental evidence supplied by multiple Coulomb excitation[2] and exceedingly careful decay scheme work[3] together with the earlier work[4] determines the scheme of octupole vibrational energies versus neutron number for the different isotopes shown in Fig. 1(a).

It is immediately obvious that a sharp discontinuity or singularity in octupole vibrational energies occurs at 142 neutrons. Figure 1(b) shows a similar discontinuity in the hindrance factor observed in the α decay from the ground state of even nuclei to octupole vibrations of nuclei in the vicinity of 142 neutrons.[5] A second effect involving β and γ vibrations has recently been pointed out by Durham, Rester, and Class.[6] They have demonstrated a discrepancy in the nuclear strength parameter, ρ, between Th^{232} and U^{238} and a similar discrepancy in the ratio of $E0$ to $E2$ transition probabilities from β vibrational states between these two nuclei. It should again be noted that Th^{232} has 142 neutrons.

If one considers systematics of the ground-

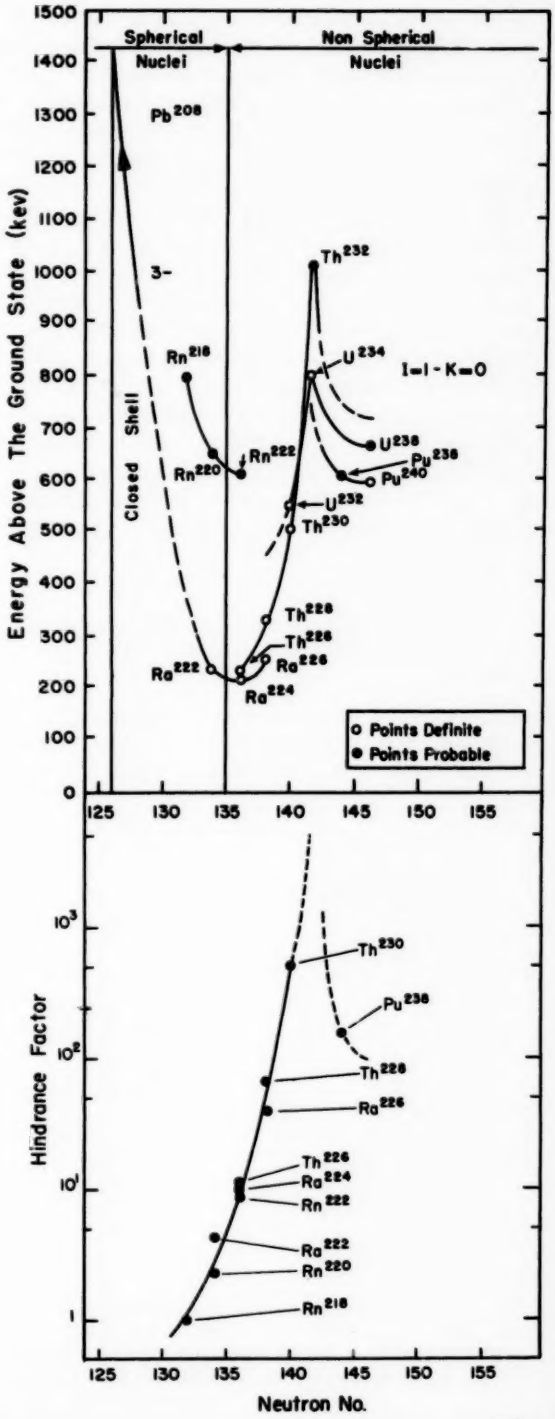

FIG. 1. (a) Energy of the octupole vibrations in the actinide region as a function of neutron number. (b) The hindrance factor in α decay from the ground state of even-even nuclei to the octupole vibrational state in the daughter nucleus. The neutron number is that of the daughter nucleus.

state rotational band instead of vibrational states, the effects are much smaller. But, as was first pointed out by Hollander,[7] the energy of the first rotational state goes through a minimum at 142 neutrons in U and at 146 neutrons in Pu. Furthermore, a kink in the ground-state to ground-state alpha-decay systematics to nuclei of 144 neutrons has been observed by Chetham-Strode.[8]

One is tempted to propose that the discontinuity in octupole vibrations at 142 neutrons is the result of a change from permanent to metastable pear shape just at this number of neutrons. This proposal has been seriously considered, but must be rejected for a number of reasons. For example, the expected increase in moment of inertia, $\hbar^2/2\mathcal{I}$, of the rotational band superimposed on the octupole vibration as one goes to an unstable pear shape does not occur. Perhaps the most significant reason is the need for a more general structural change which can explain the deviations in the systematics not only for vibrational bands, but also for the ground state and other nuclear parameters. It seems possible that such an explanation may result from the reconstitution of the core of the nucleus in the region of neutron number 142.

In Fig. 2(a) the Nilsson levels indicate that the $i_{13/2}[606]$ level, which was emptied in the process of achieving a deformation, may again be expected to fill at about 142 neutrons. These structural changes (both the emptying and the refilling of the $i_{13/2}$ level) are shown schematically in Fig. 2(a) as a dotted line. Such a reconstitution of the core might be expected to change the deformation of the nucleus but should not change its general prolate shape. Consequently, for most nuclear properties one would expect a small discontinuous effect. However, for nuclear vibrations determined by a collection of intrinsic states which are suddenly drastically altered, the effect might be large.

Indeed, an attempt[9] to calculate the energy of the octupole vibration does suggest a "knee" in the curve at 142 neutrons. It remains to be seen if more sophisticated calculations can reproduce the major discontinuity indicated in Fig. 1(a).

Perhaps most interesting is the fact that such a structural change makes two predictions which

Table I. Level assignments for odd neutrons with neutron number ≥ 139. Energies of the levels in kev above the ground state are listed in the body of the table. For energies and level assignments see, e.g., Mottelson and Nilsson.[a]

Neutron number	3/2+ [631]	5/2- [752]	5/2+ [633]	7/2- [743]	1/2+ [631]	5/2+ [622]	7/2+ [624]	9/2- [734]	Isotope
139			0						Th^{229}
		185	0	390					Th^{231}
141	(313)		0	(295)	((400))				U^{233}
			0						Pu^{235}
143				0	0.08				U^{235}
				0	145				Pu^{237}
					0	(145)			U^{237}
145			(512)	392	0	286			Pu^{239}
					0				Cm^{241}
						(0)			U^{239}
147						0	172		Pu^{241}
						0			Cm^{243}
							(0)		Pu^{243}
					((631))	255	0	394	Cm^{245}

[a]B. R. Mottelson and S. G. Nilsson, Kgl. Danske Videnskab. Selskab, Mat.-fys. Skrifter 1, No. 8 (1959).

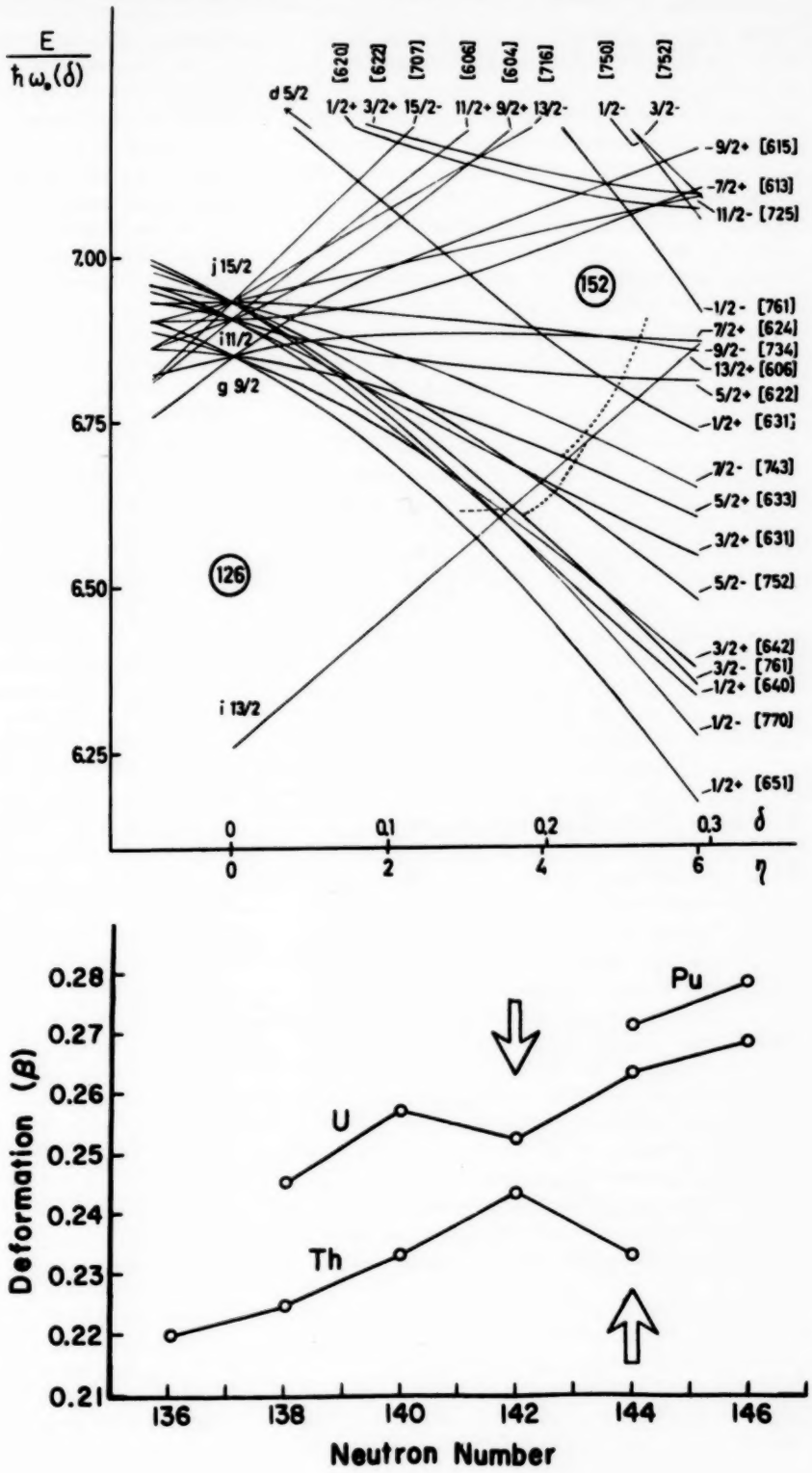

FIG. 2. (a) Nilsson neutron levels for the actinide region. The dotted line represents the emptying of the $i_{13/2}$[606] level as additional neutrons are added with the consequent decrease in deformation. (b) The measured deformation as a function of neutron number in this vicinity.[10]

are amenable to test. In the first place, the refilling of the $i_{13/2}[606]$ level should produce a small but definite decrease in the deformation. This may have recently been observed by Bell, Bjørnholm, and Severiens[10] and is reproduced in Fig. 2(b). A more direct test of the structural change is shown by the dotted line in Fig. 2(a). If the refilling of the $i_{13/2}$ level comes with the addition of two neutrons in going from 139 to 141 neutrons, then, as indicated in Fig. 2(a), one expects to see the $\frac{5}{2}+[633]$ ground state repeated both for 139- and 141-neutron nuclei. Table I gives the assignments for odd-neutron levels in the actinides.[11] The only exception to regular filling (see arrow in Table I) is when one goes from 139 to 141 neutrons. In both cases the ground state is the $\frac{5}{2}+[633]$ state. Table I shows that the energy differences in neutron levels for various nuclei differ and therefore that no single Nilsson level diagram is adequate to explain all nuclei in this region. Consequently one might expect that this refilling of the $i_{13/2}$ level in another set of nuclei might occur at a slightly different neutron number, e.g., in going from 141 to 143 neutrons.

There are, then, a large number of structural changes which occur as one successively adds neutrons and protons to a nucleus. There is the sudden drastic change from a spherical to a deformed nucleus. This occurs as one goes from 88 to 90 neutrons[12] and from 86 to 88 protons.[13] There is the more gradual return from a deformed prolate nuclear shape to the spherical shape in the vicinity of the Os and Ir isotopes.[14] Finally, it seems probable that even within the region of prolate deformation, there are fairly drastic structural changes brought about both by neutrons and by protons in both the partial breakup and reconstitution of the core of the nucleus. Whereas the evidence here has been presented exclusively for the refilling of neutron levels in the actinides, there is some evidence for a similar effect in the rare earths. Each of these structural changes ought to result in forbidden transitions between nuclei with different structures. Experimental observation of such a nuclear Franck-Condon principle in the region of 142 neutrons would represent additional evidence for this proposal.

The suggestion presented here uses the older model in which two particles are placed in each of the Nilsson levels until all are used. Levels are therefore either full or empty. The diffuseness of the Fermi surface and the consequent partial occupation of many levels in the vicinity of the Fermi surface, as suggested by the more recent model, should smear out to some extent the effect of core reconstitution.

---

*This research has been supported by the U. S. Atomic Energy Commission and by the U. S. Army Research Office.

[1]See, e.g., B. Elbek, in Proceedings of the International Conference on Nuclear Structure, Kingston, Canada, edited by D. A. Bromley and E. W. Vogt (University of Toronto Press, Toronto, 1960).

[2]R. Diamond, B. Elbek, and F. Stevens (private communication).

[3]S. Bjørnholm and O. B. Nielsen (to be published); E. Arbman and O. B. Nielsen (to be published); E. Arbman, S. Bjørnholm, and O. B. Nielsen (to be published); S. Bjørnholm, A. Knutsen, and O. B. Nielsen (preliminary results).

[4]See, e.g., F. Asaro, F. S. Stephens, Jr., and I. Perlman, Phys. Rev. 92, 1495 (1953); F. S. Stephens, Jr., F. Asaro, and I. Perlman, Phys. Rev. 96, 1568 (1954); F. S. Stephens, Jr., F. Asaro, and I. Perlman, Phys. Rev. 100, 1543 (1955); F. S. Stephens, Jr., F. Asaro, and I. Perlman, Phys. Rev. 107, 1091 (1957).

[5]See, e.g., I. Perlman and J. O. Rasmussen, in Handbuch der Physik, edited by S. Flügge (Springer-Verlag, Berlin, 1957), Vol. 42, p. 142.

[6]F. E. Durham, D. H. Rester, and C. M. Class, Phys. Rev. Letters 5, 202 (1960).

[7]J. M. Hollander, Phys. Rev. 103, 1590 (1956).

[8]A. Chetham-Strode, Jr., Ph.D. thesis, University of California, 1956 (unpublished).

[9]S. A. E. Johansson, Nuclear Phys. 22, 529 (1961).

[10]R. E. Bell, S. Bjørnholm, and J. C. Severiens, Kgl. Danske Videnskab. Selskab, Mat.-fys. Medd. 32, No. 12 (1960).

[11]B. R. Mottelson and S. G. Nilsson, Kgl. Danske Videnskab. Selskab, Mat.-fys. Skrifter 1, No. 8 (1959).

[12]B. R. Mottelson and S. G. Nilsson, Phys. Rev. 99, 1615 (1955).

[13]G. Scharff-Goldhaber, Phys. Rev. 103, 837 (1956).

[14]R. K. Sheline, Revs. Modern Phys. 32, 1 (1960).

INTERFERENCE IN THE RADIATIVE CAPTURE OF NEUTRONS*

R. E. Coté and L. M. Bollinger
Argonne National Laboratory, Argonne, Illinois

(Received May 8, 1961)

The interest in the shapes of resonances in the cross sections of nuclides for interactions with s-wave neutrons has now extended over a period of twenty years. In spite of the long and rather intense study of this problem in which the shapes of resonances attributed to scattering, fission, and radiative capture have been investigated extensively, the shapes associated with some processes have not been observed. One of these is the resonance capture which results in a single mode of radiative decay of the compound nucleus, i.e., decay by emission of the gamma ray to a particular energy level of this nucleus. If this can be considered to be a single-channel process in the compound nucleus model, the theory says definitely that the partial radiation widths which correspond to each mode of de-excitation should belong to a statistical population drawn from a χ^2 distribution with 1 degree of freedom, and the wave amplitudes associated with each mode should add coherently to give the cross sections of the particular process.[1] In other words, the process should be similar to the elastic scattering of neutrons in these particulars. Data already presented[2] indicate that the observed partial widths are consistent with the χ^2 distribution with 1 degree of freedom.

Here we are concerned with the second point. Coherent addition of the wave amplitudes is usually made apparent through interference effects. However, in contrast to the situation for scattering resonances, resonances which are caused predominantly by capture have shown none of the asymmetries associated with interference effects, the explanation being that the interference effects cancel because of the addition of very many interference terms of random signs. It is therefore apparent that an interference effect associated with radiative capture can be observed only if the study selects a single mode of decay, or only a very few.

The aim of the present experiment was to measure the relative intensity of individual capture gamma rays as a function of neutron energy in the vicinity of the Pt^{195} resonances at 11.9 and 19.6 ev, both of which are known[2] to have $J = 1$.

The measurements were made with the Argonne fast chopper[3] operated at a speed of 15 000 rpm. The sample, a piece of normal platinum 6 in. × 12 in. × 0.080 in., was mounted 25 m from the chopper at an angle of about 22° to the beam. The over-all time-of-flight resolution of the system was 0.16 μsec/m. The capture gamma rays were detected by a NaI(Tl) scintillator, 6 in. long by 8 in. in diameter, whose output was fed to an analog-to-digital converter. All of the digitalized pulse heights and the time differences corresponding to the energies of the captured neutrons were recorded on magnetic tape in the ANL three-parameter analyzer.[4] In order to be able to correct for the effects of possible gamma-ray summing, two experiments were performed, one with the crystal $5\frac{3}{8}$ in. from the center of the sample, and another with the crystal $10\frac{3}{8}$ in. from the sample. However, both this series of experiments and others[5] performed for the purpose of determining partial radiation widths show that for platinum no such correction is necessary.

For the two Pt^{195} resonances being considered, the easiest transition to observe is the one directly from the initial state to the ground state. The relative intensity for this transition may be studied by means of the ratio R_0/R_γ, where R_0 is the intensity of pulses (in a given time channel) for which the height is in the neighborhood of the binding energy and R_γ is the intensity of pulses in a broad band at a much lower energy. It is assumed that, because of the complexity of the capture γ-ray cascade, R_γ is a measure of the rate of neutron capture. The experimental values for the ratio R_0/R_γ are shown in Fig. 1. The point (indicated by ×) shown for $E = 0.0253$ ev was the result of a separate experiment performed with the rotor of the chopper stationary. Although the quantity of interest in this experiment is the relative strength of the ground-state transition compared with the total capture in resonances of Pt^{195} with total angular momentum $J = 1$, the ratio R_0/R_γ is a measure of the fraction of this transition in the total capture in all isotopes of platinum. However, over the energy region dominated by the 11.9- and 19.6-ev resonances, the difference between these ratios is not significant; the other isotopes make a significant difference only for the experimental point

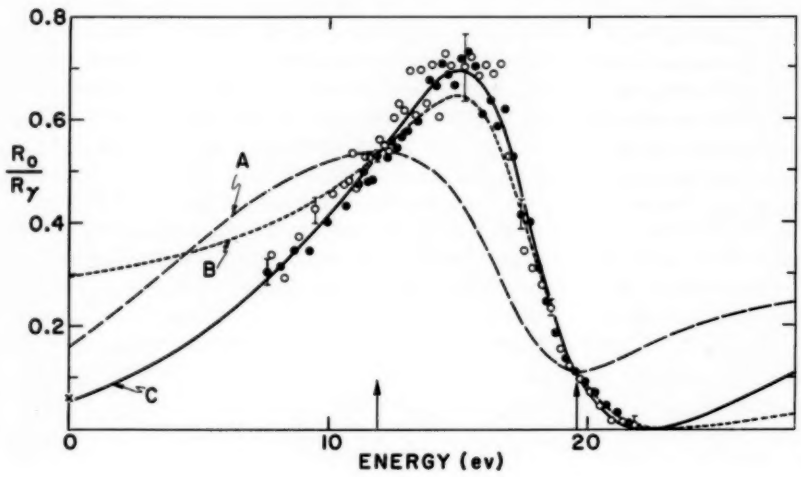

FIG. 1. The relative strength of the 7.92-Mev ground-state transition in Pt^{196} following neutron capture in platinum as a function of neutron energy. The open circles are the result of an experiment in which the distance from sample to detector was $10\frac{5}{8}$ in., the solid circles from one in which this distance was $5\frac{5}{8}$ in. The indicated errors are standard statistical errors. Curve *A* is the shape of the variation expected if no interference occurs between levels of the same *J*. Curve *B* shows the shape expected if the components associated with the resonances at 11.9 and 19.6 ev (indicated by arrows) interfere, and the contributions from other levels are ignored. Curve *C* is the expected shape if all of the levels listed in Table I are included and interference is allowed between all levels of the same *J*.

at thermal energy.

Along with the data shown in Fig. 1 are three curves computed on the basis of a simple multilevel formula[6] applicable to the present case in which $\Gamma \ll D$. Curve *A* shows the shape obtained on the assumption that no interference exists. Curve *B* was computed for the case of interference between the 11.9- and 19.6-ev resonances with no others included. Curve *C* shows the shape obtained if all resonances of the same *J* are allowed to interfere. The parameters used

Table I. The resonance parameters used in computing the curves of Fig. 1. The partial radiation widths $\Gamma_{\gamma 0}{}^*$, although of the order of magnitude of the absolute partial radiation width $\Gamma_{\gamma 0}$, must be considered meaningful only with respect to each other; the absolute values are of no importance here. The quantity in the last column is proportional to the wave amplitude.

E_0 (ev)	J	$\Gamma_n{}^0$ (ev)	Γ_γ (ev)	$\Gamma_{\gamma 0}{}^*$ (ev)	$\lvert\sigma_0\Gamma_{\gamma 0}{}^*\lvert E\rvert^{1/2}\Gamma^{-1}\rvert^{1/2}$
-13.6[a]	0	0.0302[a]	0.100[b]	0.0	0.0
or					
-13.0[a]	1	0.0092[a]	0.100[b]	≤0.00001	+3.2
11.9	1[c]	0.0034[d]	0.112[d]	0.00505[e]	+43.5
19.6	1[c]	0.0016[d]	0.100[d]	0.00095[e]	-15.9
67.4[f]	1[e]	0.0044	0.100[b]	0.0039[e]	-42.5

[a]Chosen so that the contribution to the thermal capture cross section would be consistent with the measured value for Pt^{195}.
[b]Assumed.
[c]See reference 2.
[d]John R. Waters, Phys. Rev. 120, 2090 (1960).
[e]See reference 5.
[f]See reference 7.

in the computation are listed in Table I. A few remarks about some of these parameters are relevant. Since the known positive energy levels do not account for the measured thermal capture cross section for Pt^{195}, a bound level needs to be included in the computations to obtain results consistent with the experimental data. On the assumption that $\Gamma_\gamma = 0.100$ ev, a set of parameters E_0 and Γ_n^0 was selected for this level, for each possible value of J, which provides the correct amount of capture at thermal energies. A value of the partial radiation width $\Gamma_{\gamma 0}$ and the sign of the wave amplitude were selected for the set with $J = 1$ that gave a proper fit to the data. (An equally good fit can be obtained with the opposite sign and correspondingly different $\Gamma_{\gamma 0}$.) Of course, $\Gamma_{\gamma 0} = 0$ for $J = 0$. No obvious choice can be made between these solutions, so all sets of parameters have been included in the table. There are known to be two resonances in Pt^{195} near 68 ev.[7] Studies of the capture gamma rays that result from neutron capture in these resonances suggest that only the higher energy resonance of the pair has $J = 1$.[5] An area analysis of some unpublished transmission data, under the assumption that $\Gamma_\gamma = 0.100$, leads to the estimate $\Gamma_n = 0.136$ ev for this resonance.

On the basis of the excellent agreement between the data and curve C and the obvious disagreement between the data and the curve A, it can be concluded that interference does occur between radiative transitions associated with neutron resonances of the same J. Curve B merely strengthens the argument by showing that the dominant features of the data (the maximum between the resonances and more importantly the minimum above) are accounted for by consideration of only the well-known nearby resonances and are not strongly dependent on the parameters of the less well-known distant resonances.

Since the number ν of channels available for this process of radiative capture to a particular final state has been the subject of much debate during the past few years, it is of interest to emphasize that the present results are consistent with a single-channel process. Furthermore, the improvement in the quality of the fit brought about by the inclusion of the 68-ev resonance strengthens the argument that $\nu = 1$, and certainly requires that ν be a number very near one, if not equal to it, since the interference between three neighboring levels would be very unlikely if the process could proceed through many channels.

---

*Work performed under the auspices of the U. S. Atomic Energy Commission.

[1]A. M. Lane and R. G. Thomas, Revs. Modern Phys. 30, 257 (1958); C. E. Porter and R. G. Thomas, Phys. Rev. 104, 483 (1956).

[2]L. M. Bollinger, R. E. Coté, and T. J. Kennett, Phys. Rev. Letters 3, 376 (1959).

[3]L. M. Bollinger, R. E. Coté, and G. E. Thomas, Proceedings of the Second International Conference on the Peaceful Uses of Atomic Energy, Geneva, 1958 (United Nations, Geneva, 1958), Vol. 14, p. 239.

[4]M. G. Strauss and C. C. Rockwood, Bull. Am. Phys. Soc. 6, 241 (1961).

[5]L. M. Bollinger, R. E. Coté, J. P. Marion, and R. T. Carpenter (to be published).

[6]H. Feshbach, C. E. Porter, and V. F. Weisskopf, Phys. Rev. 96, 448 (1954).

[7]G. E. Thomas, Argonne National Laboratory Report ANL-6072 (unpublished), p. 4.

STUDY OF RESONANCES OF THE Σ-π SYSTEM*

Margaret H. Alston, Luis W. Alvarez, Philippe Eberhard,† Myron L. Good,‡
William Graziano, Harold K. Ticho,‖ and Stanley G. Wojcicki
Lawrence Radiation Laboratory and Department of Physics, University of California, Berkeley, California
(Received May 8, 1961; revised manuscript received May 31, 1961)

Recently a $T=1$ resonance in the Λ-π system, called Y_1^*, has been observed with a mass of 1385 Mev.[1-6] Two types of resonances have been predicted that might relate this observation to other elementary-particle interactions: (1) $P_{3/2}$ resonances in the Λ-π and Σ-π systems predicted by global symmetry,[7,8] corresponding to the $(\frac{3}{2},\frac{3}{2})$ resonance of the π-N system, (2) a spin-$\frac{1}{2}$ Y-π resonance resulting from a bound state in the $\overline{K}$-N system.[9,10] The position and the width of the observed Y_1^* resonance agree with both theories, but since the spin and parity have not yet been determined, we cannot distinguish between the two theoretical interpretations.

Global symmetry[11] (including a phase-space factor) predicts a branching ratio $R=(Y_1^{*\pm}\to\Sigma^0+\pi^\pm)/(Y_1^{*\pm}\to\Lambda^0+\pi^\pm)=(Y_1^{*\pm}\to\Sigma^\pm+\pi^0)/(Y_1^{*\pm}\to\Lambda^0+\pi^\pm)=\frac{1}{4}(0.225)\sim 5\%$. The $\overline{K}$-N bound-state model suggests values of R considerably larger than 5%. However, when nonzero effective ranges are taken into account,[12] R can become quite small, especially if the Σ-Λ parity should be odd.

To investigate these possibilities, we have continued our study of K^--p interactions at 1.15 Bev/c in the Lawrence Radiation Laboratory 15-in. hydrogen bubble chamber by studying events in which a Σ is observed. The total cross sections for these interactions are shown in Table I; only statistical errors are indicated. The separation of $\Sigma^\pm+\pi^\mp+\pi^0$ and $\Sigma^\pm+\pi^\mp+2\pi^0$ events was difficult because many of the latter events will also fit the first hypothesis. The numbers given in Table I and in the mass plots below were corrected to account for this ambiguity. The correction factor was estimated by using our $\Sigma^\pm+\pi^\mp+\pi^+\pi^-$ events.

To obtain an upper limit for the branching ratio, R, we combined the Σ-2π events into different charge states of the Σ-π system. All charged Σ hyperons were observed; however, in the Σ^0 cases only two-thirds of the events were observable because of the neutral decays of the Λ^0. Furthermore, we had estimated that about one-third of the $\Sigma^0\pi^+\pi^-$ events also fitted a $\Lambda\pi^+\pi^-$ interpretation and had been included in already published data.[1] Consequently each $\Sigma^0\pi^+\pi^-$ event was given a weight of 2.25. The resultant mass spectra are shown in Fig. 1. In the cases of $(\Sigma$-$\pi)^+$ and $(\Sigma$-$\pi)^-$ there appears to be no excess of events in the region of $M=1385$ Mev. Using the number of $(\Lambda$-$\pi^+)$ and $(\Lambda$-$\pi^-)$ events with 1355 Mev$<M_{\Lambda\text{-}\pi}<$1415 Mev from reference 1, and assuming that all charged Σ-π systems in the same mass regions of Fig. 1 are Y_1^*, we obtain $R_{\max}\leq 8\%$. This treatment yields an unrealistic upper limit, since there is no evidence of any peaking above background. The $\Sigma^\pm+\pi^\mp+2\pi^0$ events possibly misidentified as $\Sigma^\pm+\pi^\mp+\pi^0$ (or vice versa) do not fall into the mass band used in this analysis.

We conclude that the Σ/Λ branching ratio R for the strong decay of the $T=1$ Y_1^* is at most a few percent and is consistent with zero. This result agrees with the value of R obtained by Bastien et al.[13] As indicated above, this value of R does not rule out either the global symmetry or the $\overline{K}$-N bound-state model of the Y_1^* resonance.

Next, we wish to report the results of our study of the three reactions:

$$K^-+p\to\Sigma^++\pi^-+\pi^-+\pi^+, \quad (1)$$

$$K^-+p\to\Sigma^-+\pi^++\pi^++\pi^-, \quad (2)$$

$$K^-+p\to\Sigma^0+\pi^0+\pi^++\pi^-. \quad (3)$$

Reactions (1) and (2) are readily identified and measured, but reaction (3) cannot be identified unambiguously. Accordingly, we discuss first the results pertaining to reactions (1) and (2). In a search for possible Σ-π resonances, we have

Table I. Cross sections for the Σ-producing interactions at 1.15 Bev/c.

Reaction	No. of events (uncorrected)	Cross sections (mb)
$K^-+p\to\Sigma^-+\pi^+$	87	1.40 ±0.16
$\to\Sigma^++\pi^-$	84	1.34 ±0.18
$\to\Sigma^++\pi^-+\pi^0$	57	0.97 ±0.16
$\to\Sigma^-+\pi^++\pi^0$	54	0.83 ±0.20
$\to\Sigma^0+\pi^++\pi^-$	27	0.97 ±0.20
$\to\Sigma^++\pi^-+\pi^0+\pi^0$	13	0.18 ±0.06
$\to\Sigma^-+\pi^++\pi^0+\pi^0$	9	0.12 ±0.05
$\to\Sigma^++\pi^++\pi^-+\pi^-$	19	0.19 ±0.06
$\to\Sigma^-+\pi^-+\pi^++\pi^+$	13	0.12 ±0.05

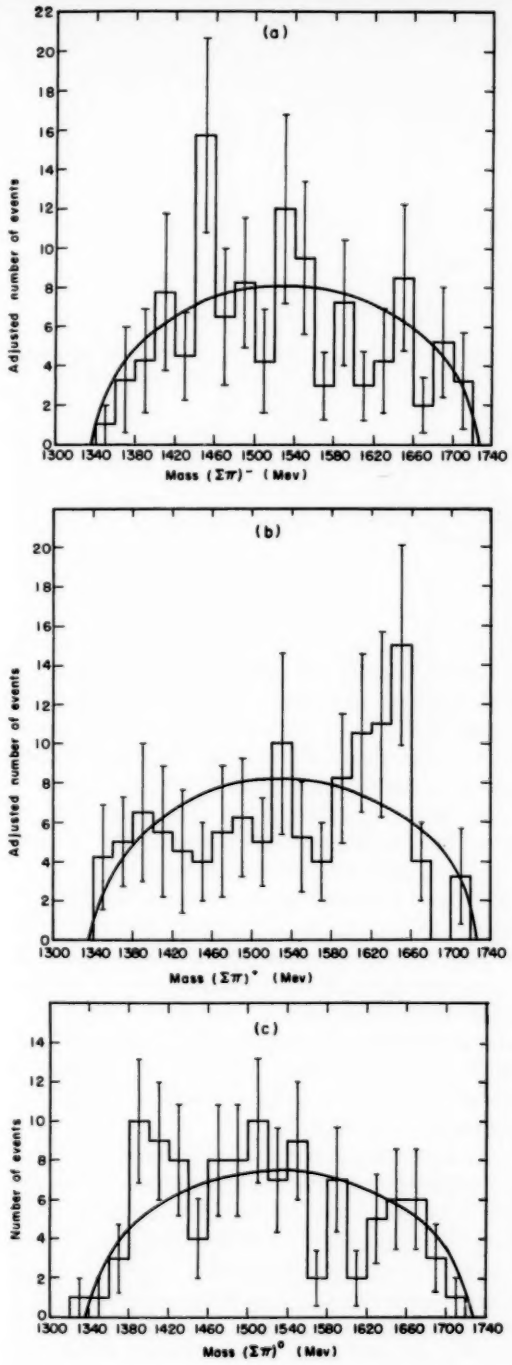

FIG. 1. Mass plots of the charged and neutral Σ-π systems, including curves representing phase-space distributions. (a) Mass of $(\Sigma\text{-}\pi)^-$, from the reactions: $K^- + p \to \Sigma^0 + \pi^- + \pi^+$ or $\Sigma^- + \pi^0 + \pi^+$. (b) Mass of $(\Sigma\text{-}\pi)^+$, from the reactions: $K^- + p \to \Sigma^0 + \pi^+ + \pi^-$ or $\Sigma^+ + \pi^0 + \pi^-$. (c) Mass of $(\Sigma\text{-}\pi)^0$, from the reactions: $K^- + p \to \Sigma^+ + \pi^- + \pi^0$ or $\Sigma^- + \pi^+ + \pi^0$.

plotted in Fig. 2 histograms of the invariant masses of the Σ and each of the three pions in reactions (1) and (2). Figure 2(b) refers to the Σ and pion of like charge; Fig. 2(a) to the Σ and each of the pions of unlike charge. For this reason twice as many events appear in Fig. 2(a) as in Fig. 2(b). The plotted curves are mass distributions expected on the basis of a uniform phase-space population. The histogram of Fig. 2(b) agrees with the phase-space curve, but the Σ and unlike-charged pion distribution appears to exhibit an anomaly, indicating a concentration of events with a Σ-π mass of about 1405 Mev. A more detailed investigation of the distribution of our events in the four-particle phase space suggests that it is quite unlikely that we are dealing with a statistical accident. In fact, in practically every event one of the neutral Σ-π systems has a mass which lies in the resonance region. If one interprets the observed distribution as a resonance, its peak corresponds to a mass of 1405 Mev, and its full width at half maximum is about 20 Mev after unfolding experimental errors.

To investigate further the possibility of a Σ-π resonance, we studied the 39 two-prong events associated with a Λ that did not fit the $K^- + p \to \Lambda + \pi^+ + \pi^-$ or $K^- + p \to \Sigma^0 + \pi^+ + \pi^-$ interpretations. These events could be:

$$K^- + p \to \Sigma^0 + \pi^+ + \pi^- + \pi^0, \quad (3)$$

$$K^- + p \to \Lambda + \pi^+ + \pi^- + \pi^0, \quad (4)$$

$$K^- + p \to \Sigma^0 + \pi^+ + \pi^- + \pi^0 + \pi^0, \quad (5)$$

$$K^- + p \to \Lambda + \pi^+ + \pi^- + \pi^0 + \pi^0. \quad (6)$$

Identification is very difficult because only reaction (4) is sufficiently overconstrained to permit a kinematical fit. Furthermore, most of the events that are actually examples of reaction (3) fit hypothesis (4), but generally with a larger χ^2 value.

Of the 39 events, 16 had $\chi^2 \geq 2$ when kinematically fitted to the one-constraint hypothesis (4). Most of these events are probably due to reaction (3), since a priori only 17% of the events due to reaction (4) should have $\chi^2 \geq 2$. Also, only one example of the reaction $K^- + p \to \Lambda + \pi^+ + \pi^- + \pi^+ + \pi^-$ and no examples of $K^- + p \to \Sigma^\pm + \pi^\mp + \pi^+ + \pi^- + \pi^0$ were observed; thus reactions (5) and (6) are probably rare. Even though a kinematical fit to hypothesis (3) is impossible, one can obtain the invariant mass of the Σ^0-π^0 system from the incident K^- momentum and the measured momenta of the two charged pions. However, since no kinematic constraints can be imposed on such

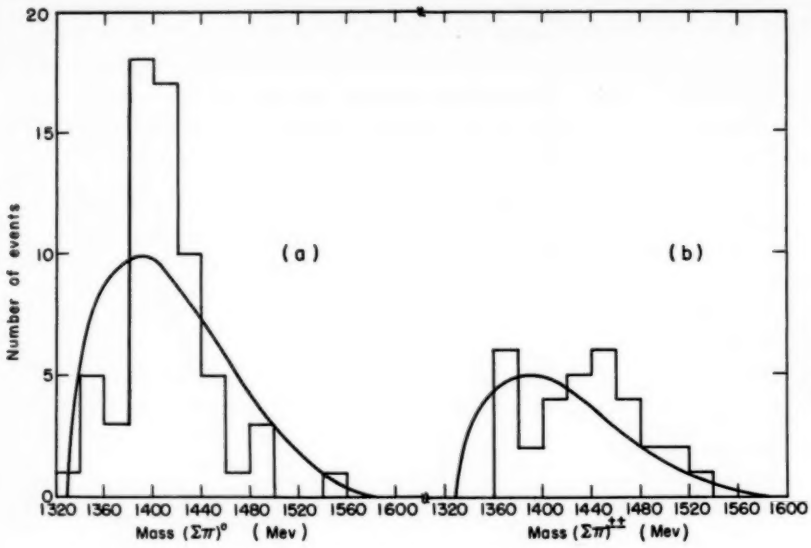

FIG. 2. Mass plots of the neutral and doubly charged Σ-π systems.

events, the experimental errors will, in general, be larger than for fitted events and fluctuate more widely. Therefore, the data are better represented by ideograms.

Figure 3(a) shows the ideogram of the mass distribution of the 16 events with $\chi^2 \geq 2$. The three events with $M < 1320$ Mev can be interpreted as the tail of the χ^2 distribution of reaction (4); the four events with $M > 1450$ Mev are probably due to reactions (5) and (6). The remaining nine events fall into a narrow band centered at about 1386 Mev and are most probably due to reaction (3). The plotted curve is the mass distribution of Σ^0-π^0 systems based on phase space and normalized to nine events. It is worth emphasizing that due to our experimental errors of ~20 Mev, the actual peak is expected to be somewhat sharper than shown.

Figure 3(b) shows the corresponding distribution for the events with $\chi^2 < 2$. In order to permit a direct comparison with Fig. 3(a), again only the measured momenta of the charged pions were used to obtain the mass ideogram. The measured distribution appears to agree with that expected from phase space for $\Lambda\pi^0\pi^+\pi^-$ events. No anomaly at $M \sim 1390$ Mev is observed. Thus there does not appear to be any evidence of the $T=1$ Y_1^{*0} resonance in the $\Lambda\pi^0\pi^+\pi^-$ data. Furthermore, if one fits all 39 events to the $\Lambda\pi^0\pi^+\pi^-$ hypothesis and then calculates the Λ-π^0, Λ-π^+, and Λ-π^- masses from the fitted values, there is still no evidence for the Y_1^* resonance. In particular, the peak of Fig. 3(a) vanishes. Thus we cannot attribute the observed peaks in the mass distribution shown in Figs. 2(a) or 3(a) to the Y_1^* resonance, especially in view of the low Σ/Λ branching ratio discussed above. Because of this and the selection criterion used in isolating the events of Fig. 3(a), the nine events probably represent a Σ^0-π^0 resonance linked by charge independence to the Σ^+-π^- and Σ^--π^+ resonance already discussed.

It is easy to show that the branching ratio $\beta = N_{\Sigma^0\pi^0}/(N_{\Sigma^+\pi^-} + N_{\Sigma^-\pi^+})$ uniquely determines the isotopic spin of the resonance. For $T=2$, 1, or 0, we have $\beta = 2$, 0, or $\frac{1}{2}$, respectively. Neglecting possible backgrounds, and correcting for neutral decays and escape of the Λ hyperons in the Σ^0-π^0 case, we have $\beta = 0.6 \pm 0.2$. Hence, the isotopic spin of the indicated resonance is zero, and we will call it Y_0^*.

One difficulty of our interpretation of the data is the difference in mass of 19 Mev ± 6 Mev between the two peaks of Figs. 2(a) and 3(a). However, since there are two identical pions in the charged Σ cases and not in the Σ^0 cases, it is possible that the effect of Bose statistics could cause a shift of the peaks. Also, from the fact that the charged Σ can resonate with either of the two unlike-charged pions, one would expect interference effects between the two resonant amplitudes. Another possibility is interference between the resonance and nonresonant backgrounds. Both these interferences might alter the observed positions of the peaks. Electromag-

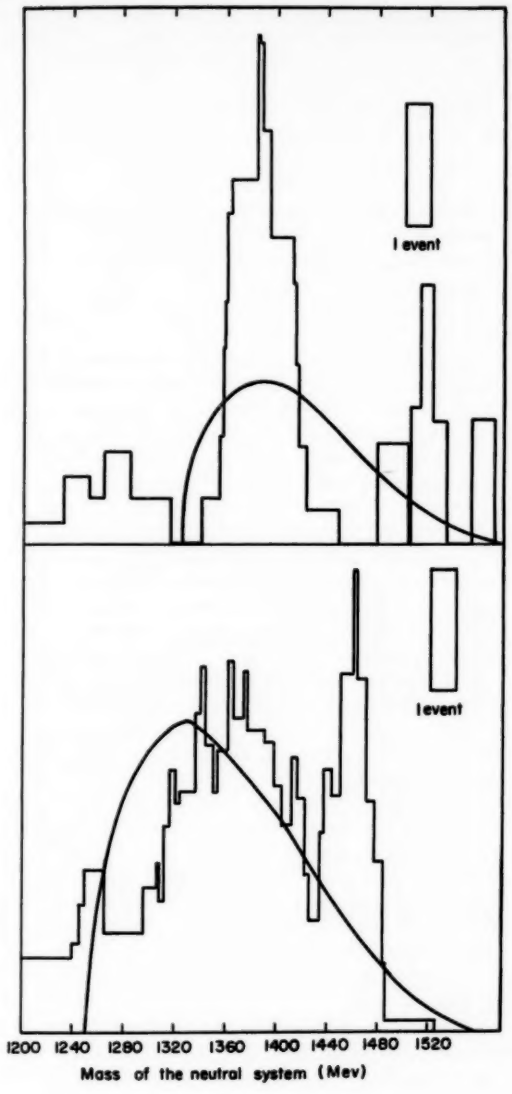

FIG. 3. Ideograms of the missing mass for the 39 events in which a Λ and two charged pions were observed and neutral pions were also produced. (a) Events with $\chi^2 \geq 2$ for the $\Lambda\pi^0\pi^+\pi^-$ hypothesis. The superimposed curve is the phase-space distribution for the $\Sigma^0\pi^0\pi^+\pi^-$ reaction normalized to nine events. (b) Events with $\chi^2 < 2$ for the $\Lambda\pi^0\pi^+\pi^-$ hypothesis. The superimposed curve is the expected $\Lambda\pi^0\pi^+\pi^-$ phase-space distribution.

netic mass differences in the Σ^+-π^-, Σ^--π^+, and Σ^0-π^0 have a negligible effect on the position of the peaks if one assumes transition probabilities that are proportional to the decay momentum.

The Y_0^* could also be produced in the events in which the final state consists of a Σ and two pions. If it is produced, it should appear in the $(\Sigma$-$\pi)^0$ mass plot given in Fig. 1(c). No significant peak is observed; however, the number of events in this region of the mass plot is uncertain because of the difficulty of correcting for $\Sigma^\pm\pi^\mp\pi^0\pi^0$ production. The absence of the Y_0^* in this final state ($Y_0^* + \pi$) could be easily understood if the interaction took place mainly through the $T=0$ initial channel. The equality of the cross sections for Σ-2π reactions producing Σ of all charges (Table I) is consistent with this possibility. A stronger test of this possibility is provided by the interaction $\overline{K}^0 + p$ (a pure $T=1$ state) currently being studied by Martin et al.[4]

We believe that our data for Σ and three pions are most naturally interpreted by invoking a $T=0$ Σ-π resonance. However, both because of the small number of events involved and the complexity of the final state, we cannot regard the evidence as conclusive. Evidence for a $(\Sigma^\pm$-$\pi^\mp)$ resonance has been obtained by Eisenberg et al., who have studied K^--meson interactions in emulsion and find a peaking in the $(\Sigma$-$\pi)^0$ mass spectrum at 1405 Mev.[14] This peaking could be attributed to a Y_0^*. In addition, Schult and Capps have recently invoked a $T=0$ resonance at a mass of about 1410 Mev to explain the hyperon branching ratio in low-energy K^--d interactions.[15]

Dalitz and Tuan have shown that the (b^-) solution for the scattering lengths in $\overline{K}$-N low-energy interactions will result in a Σ-π resonance in the $T=0$ state.[9] Recent values for the zero-energy $\overline{K}$-N scattering lengths obtained by Dalitz[16] using the data presented by Alvarez at the Kiev Conference,[17] indicate that this resonance will be at 1415 ± 3 Mev, with a half-width ($\Gamma/2$) of about 20 Mev. If this explanation of the $T=0$ resonance is correct, it should have $J=\frac{1}{2}$; the observed $T=1$ resonance could be the resonance predicted by global symmetry with $J=\frac{3}{2}$.[18] Dalitz has pointed out that the values of the (a^-) solution given in reference 9 are consistent with both a $T=1$ and a $T=0$ $Y\pi$ resonance[19]; both of these resonances should then have $J=\frac{1}{2}$.

The authors wish to thank the many members of the Bevatron and bubble chamber crews and the scanners who made this experiment possible. We also thank Professor R. H. Dalitz, Professor A. Pais, Professor B. Sakita, and Professor S. Treiman for several helpful discussions. One of us (P.E.) wishes to thank the Philippe's Foundation,

Inc., and the Commisariat à l'Energie Atomique of France for a fellowship.

---

*Work done under the auspices of the U. S. Atomic Energy Commission.

†Presently at the Laboratoire de Physique Atomique, Collège de France, Paris, France.

‡Presently at the University of Wisconsin, Madison, Wisconsin.

‖Presently at the University of California at Los Angeles, Los Angeles, California.

[1]M. Alston, L. Alvarez, P. Eberhard, M. Good, W. Graziano, H. Ticho, and S. Wojcicki, Phys. Rev. Letters 5, 520 (1960).

[2]O. Dahl, N. Horwitz, D. Miller, J. Murray, and P. White, Phys. Rev. Letters 6, 142 (1961).

[3]J. P. Berge, P. Bastien, O. Dahl, M. Ferro-Luzzi, J. Kirz, D. H. Miller, J. J. Murray, A. H. Rosenfeld, R. D. Tripp, and M. Watson, Phys. Rev. Letters 6, 557 (1961).

[4]H. Martin, L. Leipuner, W. Chinowsky, F. Shively, and R. Adair, Phys. Rev. Letters 6, 283 (1961).

[5]M. M. Block, E. B. Brucker, R. Gessaroli, T. Kikuchi, A. Kovacs, C. M. Meltzer, R. Kraemer, M. Nussbaum, A. Pevsner, P. Schlein, R. Strand, H. O. Cohn, E. M. Harth, J. Leitner, L. Lendinara, L. Monari, and G. Puppi, Nuovo cimento (to be published).

[6]R. Ely, S. Fung, G. Gidal, Y. Pan, W. Powell, and H. White, Bull. Am. Phys. Soc. 6, 291 (1961).

[7]M. Gell-Mann, Phys. Rev. 106, 1297 (1957).

[8]P. Amati, A. Stanghellini, and B. Vitali, Phys. Rev. Letters 5, 524 (1960); Nuovo cimento 13, 1143 (1959).

[9]R. Dalitz and S. F. Tuan, Phys. Rev. Letters 2, 425 (1959).

[10]R. Dalitz, Phys. Rev. Letters 6, 239 (1961).

[11]Ph. Meyer, J. Prentki, and Y. Yamaguchi, Phys. Rev. Letters 5, 442 (1960).

[12]J. L. Shaw (private communication).

[13]P. Bastien, M. Ferro-Luzzi, and A. H. Rosenfeld, this issue [Phys. Rev. Letters 6, 702 (1961)].

[14]Y. Eisenberg, G. Yekutieli, P. Abrahamson, and D. Kessler (private communciation).

[15]R. L. Schult and R. H. Capps, Phys. Rev. 122, 1659 (1961).

[16]R. H. Dalitz, Lawrence Radiation Laboratory Report UCRL-9580, 1961 [Revs. Modern Phys. (to be published)].

[17]L. W. Alvarez, paper presented at the Ninth Annual International Conference on High-Energy Physics, Kiev, July, 1959 (unpublished); Lawrence Radiation Laboratory Report UCRL-9354, 1960 (unpublished).

[18]A. Pais has pointed out to us that if the Y_1^* should turn out to be the resonance predicted by global symmetry, the question arises whether the existence of Y_0^* could have anything to do with the global symmetry as well. This is certainly not the case because, if the Y_0^* is related to the global symmetry hypothesis, then there should be a corresponding $T=\frac{1}{2}$ π-N resonance with $Q\sim 160$ Mev. Thus the existence of a Y_0^* may indicate that the assumption of global symmetry is wrong. However, another possibility is that this symmetry could be valid in the P-wave but not the S-wave pion-baryon interaction.

[19]R. H. Dalitz (private communication).

SIGMA DECAY MODES OF PION-HYPERON RESONANCES*

Pierre Bastien, Massimiliano Ferro-Luzzi,† and Arthur H. Rosenfeld

Lawrence Radiation Laboratory and Department of Physics, University of California, Berkeley, California

(Received May 12, 1961)

During a study of K^-p interactions in the Lawrence Radiation Laboratory 15-inch hydrogen bubble chamber, we have analyzed a total of 249 three-body reactions of the type

$$K^- + p \to \Sigma^+ + \pi^- + \pi^0, \qquad (1)$$

and

$$K^- + p \to \Sigma^- + \pi^+ + \pi^0, \qquad (2)$$

at incident K^- momenta of 760 and 850 Mev/c. Reactions (1) and (2) are interesting in view of the existence of the resonant pion-hyperon state Y_1^*,[1] which is now known to influence strongly reactions such as

$$K^- + p \to \Lambda + \pi^+ + \pi^-. \qquad (3)$$

It is of interest to compare the $\Sigma^\pm$ production via reactions (1) and (2) with the Λ production via (3) to obtain the Σ/Λ branching fraction R for Y_1^*.

Another interesting feature of reactions (1) and (2) is related to the fact that the dominant decay mode $Y_1^* \to \Lambda + \pi$ is accessible only to the Y_1^* of isotopic spin 1. However, pion-hyperon resonances in other isotopic spin states such as Y_0^* and Y_2^* can decay into $\Sigma + \pi$. Alston et al. have already reported evidence for a singlet resonance Y_0^*, and we present more Y_0^* data in the second half of this Letter. Additional data on $Y^{*0} \to \Sigma^\pm + \pi^\mp$ have also been reported by Eisenberg et al.[3]

On the subject of the branching ratio of Y_1^*, both current theories agree in predicting values of R largely undetermined but generally "small."[4,5] In particular, global symmetry favors R of the order of a few percent with an upper limit of 25%,[4] while

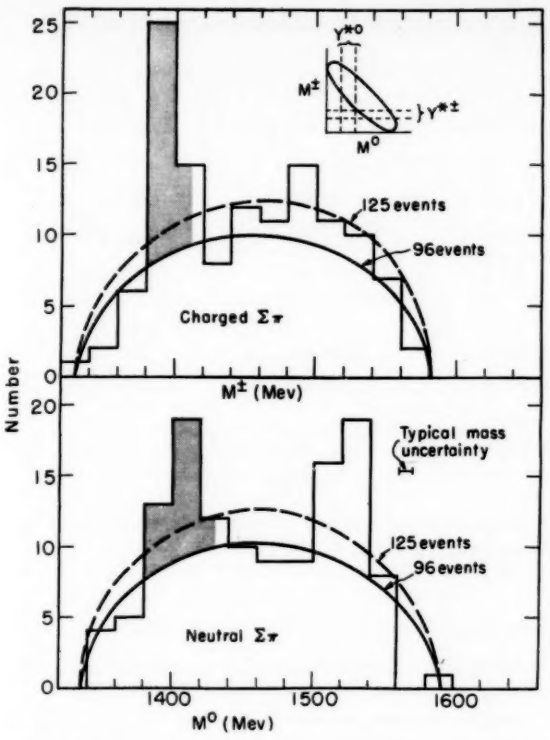

FIG. 1. Upper histogram: Sum of the mass spectrum for the $\Sigma^+\pi^0$ and $\Sigma^-\pi^0$ systems based on 49 reactions (1) and 76 reactions (2) at $P_K = 850$ Mev/c. Lower histogram: Sum of $\Sigma^+\pi^-$ and $\Sigma^-\pi^+$ masses from the same reactions. The dashed curve represents phase space normalized to all 125 events. The solid curve allows for the subtraction of the shaded areas in the Y^* peaks. For clarity, only the phase space for reaction (2) is shown; the difference from that for reaction (1) is negligible. The shaded area for charged $\Sigma\pi$ ranges from 1380 to 1410 Mev, which are the limits seen experimentally in the $Y_1^{*\pm} \to \Lambda + \pi^\pm$ mass distribution[1]; the neutral shading runs from 1380 to 1430, as suggested by Alston et al.[2] for the Y_0^*.

the $\bar{K}N$ "bound-state" model yields generally larger values of R,[5] even if no real lower limit exists because of the present uncertainty concerning the $\Lambda\Sigma$ parity and the validity of the zero-effective-range theory 50 Mev below the $\bar{K}N$ threshold.

Our kinematics program, "Kick," easily separates the three-body reactions (1) and (2) from the topologically similar two-body reactions $K^- + p \to \Sigma^\pm + \pi^\mp$, and from the four-body reactions $K^- + p \to \Sigma^\pm + \pi^\mp + \pi^0 + \pi^0$. A Dalitz plot of the 125 fitted three-body events produced at 850 Mev/c shows the now familiar highly populated bands corresponding to a mass of 1385 Mev for the $\Sigma\pi$ system. Figure 1 shows the mass histograms of these events. A small sketch at the upper right represents the scatter diagram in mass space, from which these histograms were projected. The shaded area in the conspicuous $M^\pm$ peak is easily attributed to the decay mode $Y^{*\pm} \to \Sigma^\pm + \pi^0$. (In fact, as we shall discuss below, we are forced to conclude that it is only a statistical fluctuation.) From the same hopeful point of view one can explain the broader peak at the right of the $M^\pm$ histogram as the $Y^{*0} \to \Sigma^\pm + \pi^\mp$ band projected sideways (see sketch). The dashed lines in Fig. 1 represent phase space, normalized to the total number of events. They are seen to be a rather poor fit to the histograms, thus displaying more quantitatively the extra population in the Y^* bands. In the neutral histogram of Fig. 1 some suggestion of a peak appears at 1500 to 1540 Mev, which is where Y_2^* is expected. However, this is not supported either by our data at 760 Mev/c or by the data for reactions (1) and (2) of Alston et al. at 1150 Mev/c,[2] nor is it borne out by the configuration of events on any of the Dalitz plots. For the rest of this Letter, we shall discuss only the peaks near 1385 Mev and assume that they can be explained in terms of Y_1^* and perhaps the singlet Y_0^* which, according to Alston et al., shows up in the mass region of 1380 to 1430 Mev, partly overlapping Y_1^*.[2] Note that the charged peak can come from $Y_1^{*\pm}$ only, whereas the neutral peak is the sum of contributions from Y_1^{*0} and Y_0^*. We shall discuss the unique charged peak first and determine from it the Y_1^* branching fraction, R.

In the 850-Mev/c column of Table I, the number of events in the shaded area have been used to compute $R^\pm$, which is defined as

$$R^\pm = \frac{n(Y^{*+} \to \Sigma^+\pi^0) + n(Y^{*-} \to \Sigma^-\pi^0)}{n(Y^{*+} \to \Lambda\pi^+) + n(Y^{*-} \to \Lambda\pi^-)}.$$

Charge symmetry requires

$$R^\pm = R^0 = \frac{n(Y^{*+} \to \Sigma^0\pi^+) + n(Y^{*-} \to \Sigma^0\pi^-)}{n(Y^{*+} \to \Lambda\pi^+) + n(Y^{*-} \to \Lambda\pi^-)}.$$

Values of R^0 derived at various momenta[1,2] from the study of the reaction $K^- + p \to \Sigma^0 + \pi^+ + \pi^-$ are also given in row E of Table I. The 124 events at 760 Mev/c have been treated in the same way and are displayed in Fig. 2. At this momentum neither the Dalitz plot nor the histograms show such a convincing peak structure; the solid lines in Fig. 2 represent phase space and are seen to fit the data adequately. Nevertheless some real peaking may be present, particularly because at

Table I. Data from $K^- + p \rightarrow \Sigma^{\pm} + \pi^{\mp} + \pi^0$.

	P_K(lab) (Mev/c)	760	850	1150[a]
A.	Total number of events	124	125	111
B.	$\sigma(\Sigma^-\pi^+\pi^0) + \sigma(\Sigma^+\pi^-\pi^0)$ (mb)	0.9 ±0.2	1.7 ±0.3	1.8 ±0.2
$Y_1^{*\pm} \rightarrow \Sigma^{\pm} + \pi^0$				
C.	Events in shaded area	6 ±7	20 ±7	−3 ±5
D.	$R^{\pm}$ (%)	2 ±2	15 ±6	−2 ±3
E.	R^0(from $\Sigma^0\pi^+\pi^-$) (%)	1 ±5	−5 ±5	unreliable[b]
$Y^{*0} \rightarrow \Sigma^{\pm} + \pi^{\mp}$				
F.	Events in shaded area	17 ±8	16 ±8	9 ±10
G.	$\sigma(K^- + p \rightarrow Y^{*0} + \pi^0)$ (mb)	0.12 ±0.06	0.22 ±0.11	0.15 ±0.17
H.	$\sigma(K^- + p \rightarrow Y_1^{*\pm} + \pi^{\mp})$ (mb)	2.4 ±0.15	1.9 ±0.2	3.1 ±0.4

[a]From Alston et al., reference 2.

[b]The data of row E are plagued with the difficulty of Λ vs Σ^0 separation; the fraction of ambiguous events increases quickly with beam momentum, and at 1150 Mev/c only an upper limit $R^0 < 8\%$ can be stated.

760 Mev/c the Y^* bands in the mass scatter diagram are less well separated, so that they are less easily resolved and are also subject to the interference effects already well known to occur in reaction (3) at the same beam momentum.[6]

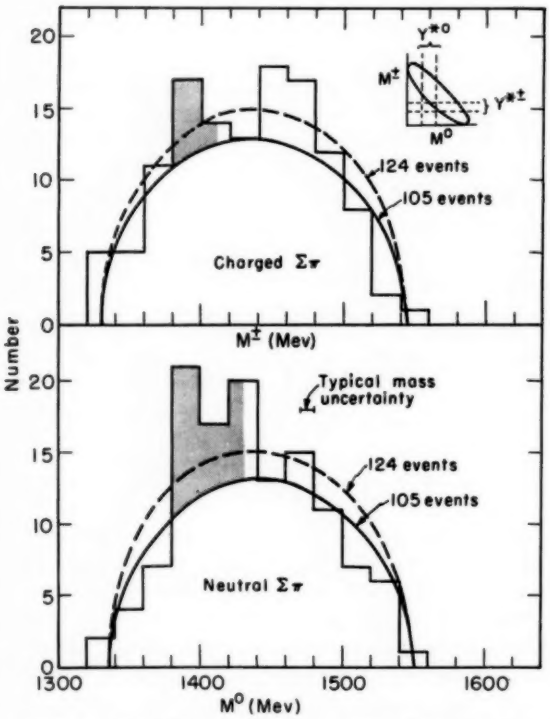

FIG. 2. Data from 55 reactions (1) and 69 reactions (2) at $P_K = 760$ Mev/c. The same considerations as for Fig. 1 apply here.

The five values of the branching fraction R shown in rows D and E of Table I can now be combined to give an average of $(2 \pm 2)\%$. This average must be used with some reservation, since the five input data are not very consistent; their χ^2 value is 8 (its average expected value is 4), and the probability for this fluctuation is only about 10%. However, it is consistent with the value $\approx(6 \pm 2)\%$ observed from the reaction $K^- + d \rightarrow \Sigma^- + \pi^0 + p$ by Levine et al.[7] Therefore, we are inclined to believe that there is substantial evidence that R is less than a few percent and conclude that the 850-Mev/c charged peak is a fluctuation. If R only is a few percent, we can show now that very few of the events in the neutral peak can be attributed to Y_1^{*0}. The argument is as follows: In the production reaction $K^- + p \rightarrow Y^* + \pi$, the $I = 1$ channel cannot produce any Y_1^{*0}, and the $I = 0$ channel gives equal numbers of Y_1^{*0}, Y_1^{*+}, and Y_1^{*-}. From this it can easily be shown that in order to explain the neutral peaks as $Y_1^{*0} \rightarrow \Sigma^{\pm} + \pi^{\mp}$, we must assume that the production is dominantly in the $I = 0$ channel and $R \sim 10\%$. However, Dalitz and Miller have given good arguments in favor of the predominance of the $I = 1$ channel,[6] and furthermore we have just concluded that R is only a few percent.

We then interpret the neutral peaks either as a statistical fluctuation or as evidence for the sing-

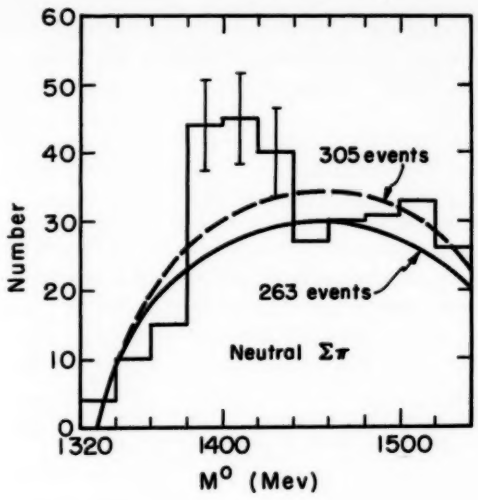

FIG. 3. Combined histogram of 305 $\Sigma^{\pm}\pi^{\mp}$ pairs at 760, 850, and 1150 Mev/c. The neutral pairs from Figs. 1 and 2 have been added to those in Fig. 1(c) of Alston et al. (1150 Mev/c).[2] The dashed curve is the sum of the dashed phase-space curves of our Figs. 1 and 2 and Fig. 1(c) of Alston et al.[2] The solid curve is the sum of our solid curves (in which we assume the existence of a neutral peak containing 17 events at 760 Mev/c and 16 at 850 Mev/c) and a corresponding curve that assumes 9 events at 1150 Mev/c, as shown in Table I.

let Y_0^* reported by Alston et al.[2] The excess events in the neutral peaks at each of the three momenta are listed in row F of Table I. The a priori probability for this fluctuation is actually quite small; however, such probabilities can give illusory results, so we prefer to illustrate the situation through Fig. 3, which is a combined mass histogram of all the currently available $\Sigma^{\pm}\pi^{\mp}\pi^0$ data. It does seem to constitute mild support for Y_0^*. In this connection two disconcerting facts should be noted: (a) The Y_0^* production cross section $\sigma(Y_0^*)$ (row G of Table I) is rather small in comparison with that of Y_1^* (row H). (b) If Y_0^* shows up so strongly in the two small-statistics, four-body final states reported by Alston et al.,[2] it is disappointing that the larger three-body samples do not confirm it more strongly.

This work is part of a study of low-energy K^-p interactions carried out in collaboration with J. P. Berge, O. Dahl, J. Kirz, D. H. Miller, J. J. Murray, R. D. Tripp, and M. Watson. We thank L. W. Alvarez and many members of his group for their help. In particular, we want to acknowledge close collaboration with the group who ran the 1150-Mev/c experiment: M. H. Alston, L. W. Alvarez, P. Eberhart, M. L. Good, W. Graziano, H. K. Ticho, and S. G. Wojcicki.

---

*Work done under the auspices of the U. S. Atomic Energy Commission.

†National Academy of Sciences Fellow.

[1]For a list of references on Y_1^*, see the review articles by M. H. Alston and M. Ferro-Luzzi, and by R. K. Adair, Revs. Modern Phys. (to be published).

[2]M. Alston, L. W. Alvarez, P. Eberhard, M. L. Good, W. Graziano, H. K. Ticho, and S. G. Wojcicki, this issue [Phys. Rev. Letters 6, 698 (1961)].

[3]Y. Eisenberg, G. Yekutieli, P. Abrahamson, and D. Kessler (private communication).

[4]D. Amati, B. Vitale, and A. Stanghellini, Phys. Rev. Letters 5, 524 (1960).

[5]R. H. Dalitz, Phys. Rev. Letters 6, 239 (1961).

[6]R. H. Dalitz and D. H. Miller, Phys. Rev. Letters 6, 562 (1961).

[7]R. D. Levine, J. J. Murray, D. H. Miller, and J. Schwartz (private communication).

INVERSE PHOTOPRODUCTION REACTION $\pi^- + p \rightarrow \gamma + n$ IN FLIGHT

G. Gatti, P. Hillman,* W. C. Middelkoop, T. Yamagata,† and E. Zavattini
CERN, Geneva, Switzerland
(Received May 31, 1961)

The cross section for the photoproduction of pions off free neutrons has in the past been extracted, somewhat precariously, from analysis of photoproduction off deuterium.[1,2] We have now measured the absolute value of the cross section for the process $\pi^- + p \rightarrow \gamma + n$, from which the free-neutron photoproduction cross section is immediately calculable using the principle of detailed balance. The experiment was performed at 90° c.m. angle and a pion energy of 72 Mev, which corresponds to a photon c.m. energy of 182 Mev, 53 Mev above threshold. The cross section was measured by detecting the neutrons in a plastic scintillation counter (10 cm thick and 17.6 cm diameter) whose efficiency has been measured.

In order to discriminate against the much more probable charge-exchange reaction $\pi^- + p \rightarrow \pi^0 + n$, the energy of the neutrons was measured by time of flight. The time zero was given by the incident pions. In order to reduce this and other backgrounds even further, a coincidence was also required with the γ ray, which was detected in a large lead-glass total absorption Čerenkov counter. All three pulses (incident pion, neutron, and photon) were displayed on a travelling wave oscilloscope and photographed. The film traces were read on IEP, a track-measuring instrument of CERN, after which the CERN Ferranti "Mercury" computer was used to analyze the results and to apply various small corrections. The final time-of-flight spectrum is shown in Fig. 1. The three peaks originate from (1) the photons from neutral pion decay, (2) the neutrons from the inverse photoproduction reaction, and (3) the neutrons from the charge-exchange reaction.

The beam intensity was monitored by an argon-filled ionization chamber[3] calibrated at low intensity against a scintillator telescope. The beam composition was measured by a glycerol Čerenkov counter and found to be $(35.7 \pm 1.0)\%$ pions, $(10.7 \pm 1.0)\%$ muons, and $(53.6 \pm 1.5)\%$ electrons.

The neutron counter efficiency was measured in a separate experiment. The same liquid hydrogen target as used in the main experiment was placed in a beam of neutrons from 190-Mev proton bombardment of a bakelite target inside the cyclotron. The protons knocked out of the hydrogen were detected in a telescope whose energy threshold and channel width had a spatial variation, such that the corresponding scattered neutrons nearly reproduced the spatial and energy distributions of the neutron incident on the neutron counter in the main experiment. The neutron counter was placed in this flux and the fraction of counts in the proton counter which coincided with counts in the neutron counter was measured. In this way the loss of neutrons which were scattered out in the target and target walls in the main experiment was automatically taken into account. The neutron counter efficiency, at a bias equivalent to about 5-Mev recoil protons and for an average neutron

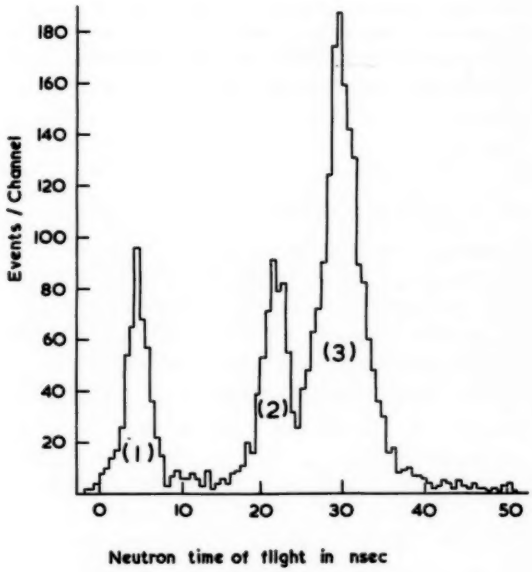

FIG. 1. Neutron time-of-flight spectrum. The peaks are (1) the photons from decay of neutral pions from the charge-exchange reaction, (2) the neutrons from the inverse photoproduction reaction with an average kinetic energy of 26.9 Mev, and (3) the neutrons from the charge-exchange reaction with an average kinetic energy of 13.4 Mev. An average time-of-flight path of 1.45 m was used.

energy of 26.9 Mev, was found to be $(13.6 \pm 0.7)\%$.

The final cross section of 70 ± 7 μb sr^{-1} is based on 505 events (after an empty-target background subtraction of 80 events). This 10% total error is mainly due to a 6% statistical error, a 5% error due to lack of separation between the peaks (2) and (3), an estimated 5% error in the calibration of the neutron counter efficiency, and a 3% error in the measured pion flux. Using the principle of detailed balance, a value of 20.1 ± 2.0 μb sr^{-1} is obtained for a_0^-. This is the 90° differential cross section divided by the statistical factor $W = qq_0(1+k/M)^{-2}$, where q and q_0 are the pion momentum and total energy, k the photon energy (all c.m.), and M the nucleon mass (in units $\mu_\pi = \hbar = c = 1$). Figure 2 shows our result together with those for a_0^+ (the process $\gamma + p \to \pi^+ + n$), and the values of a_0^- obtained by Adamovich et al.[1] from analysis of the process $\gamma + d \to \pi^- + p + p$. Also shown are the predictions of dispersion relation theory as given by Chew, Goldberger, Low, and Nambu[4] and as calculated by Hamilton and Woolcock[5] with parameters $f^2 = 0.08$ and $N^{(-)} = 0$. The π^-/π^+ ratio at our photon energy becomes 1.34 ± 0.15, where we used an a_0^+ value of 15.0×10^{-30} cm^2 sr^{-1} as derived from values of Beneventano et al.[6] and Barbaro et al.[7] at nearby energies. This value of π^-/π^+ is in good agreement with the CGLN dispersion theory. However, it is interesting to note that the experimental values of both a_0^- and a_0^+ deviate from the theoretical curves in the same manner around our photon energy. A strong p-wave π-π resonance, which was introduced to explain the nucleon form factors[8,9] and for which an indication was recently found from pion-proton inelastic scattering,[10] is expected to contribute to the photomeson production and to modify the CGLN dispersion relations. Particularly, it has been shown by Ball[11] and by Kawaguchi et al.[12] that the π^-/π^+ ratio at threshold is sensitive to the strength of π-π interaction, but more experiments on a_0^- at lower energies are required to clarify this point.

The guidance and encouragement of Professor G. Bernardini throughout the experiment has been essential to this work. The warm support of Professor P. Preiswerk is acknowledged with gratitude. We thank Dr. Goldschmidt-Clermont who kindly arranged the use of IEP. The help of G. Sicher and B. Smith is gratefully acknowledged as is the competence of the cyclotron, IEP, and hydrogen liquefier staffs.

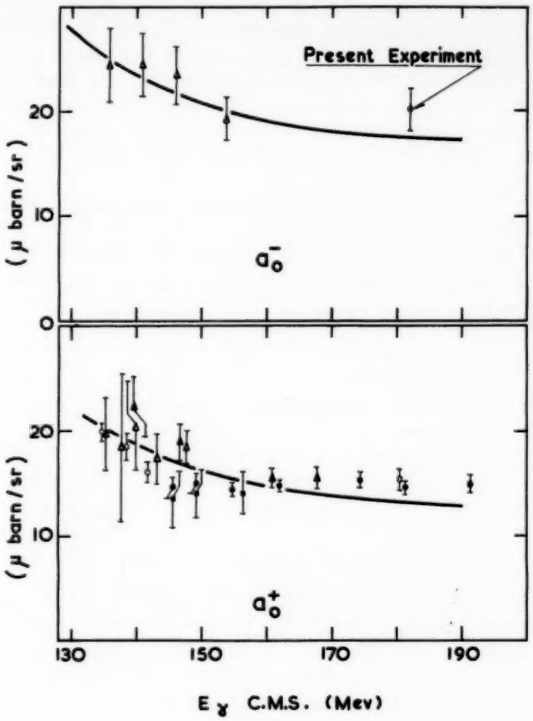

FIG. 2. Values of the π^- and π^+ photoproduction coefficients a_0^- and a_0^+, respectively. ⊙-present experiment; △-Adamovich et al., reference 1; ●-Beneventano et al., reference 6; □-Barbaro et al., reference 7; ▲-J. G. Rutherglen, J. Walker, D. Miller, and G. M. Patterson, Proceedings of the 1960 Annual International Conference on High-Energy Physics at Rochester (Interscience Publishers, New York, 1960); ○-J. E. Leiss, C. S. Robinson, and S. Penner, Phys. Rev. 98, 201 (1955); and as reported by G. Bernardini, Proceedings of the Ninth Annual Conference on High-Energy Nuclear Physics, Kiev, 1959 (unpublished); ■-G. M. Lewis and R. E. Azuma, Proc. Phys. Soc. (London) 73, 873 (1959). The theoretical curves in both figures are the dispersion relations of Chew et al., reference 4, as calculated by Hamilton and Woolcock, reference 5, with $f^2 = 0.08$ and $N^{(-)} = 0$.

---

*Now at Physics Department, Weizmann Institute, Rehovoth, Israel; Ford Foundation Postdoctoral Fellow.

†Ford Foundation Postdoctoral Fellow.

[1]M. J. Adamovich, E. G. Gorzhevskaya, V. G. Larionova, V. M. Popava, S. P. Kharlamov, and F. R. Yagudina, J. Exptl. Theoret. Phys. (U.S.S.R.) 38, 1078 (1960) [translation: Soviet Phys.-JETP 11, 779 (1960)].

[2]W. P. Swanson, D. C. Gates, T. L. Jenkins, and R. W. Kenney, Phys. Rev. Letters 5, 336, 339 (1960).
[3]D. Harting, J. C. Kluyver, and A. Kusumegi, CERN Report 60-17, 1960 (unpublished). We thank Dr. D. Harting for the use of his ionization chamber.
[4]G. F. Chew, M. L. Goldberger, F. E. Low, and Y. Nambu, Phys. Rev. 106, 1345 (1957); referred to as CGLN.
[5]J. Hamilton and W. S. Woolcock, Phys. Rev. 118, 291 (1960).
[6]M. Beneventano, G. Bernardini, D. Carlson-Lee, G. Stoppini, and L. Tau, Nuovo cimento 4, 323 (1956).
[7]A. Barbaro, E. L. Goldwasser, and D. Carlson-Lee, Bull. Am. Phys. Soc. 4, 23 (1959).
[8]R. Hofstader and R. Herman, Phys. Rev. Letters 6, 293 (1961).
[9]W. R. Frazer and J. R. Fulco, Phys. Rev. 117, 1609 (1960).
[10]J. A. Anderson, V. X. Bang, P. G. Burke, D. D. Carmony, and N. Schmitz, Phys. Rev. Letters 6, 365 (1961).
[11]J. S. Ball, Phys. Rev. Letters 5, 73 (1960).
[12]M. Kawaguchi, M. Miyamoto, and Y. Fujii, Nuovo cimento 20, 408 (1961).

COUPLED S- AND P-WAVE SOLUTIONS FOR PION-PION SCATTERING

B. H. Bransden* and J. W. Moffat†
CERN, Geneva, Switzerland
(Received March 27, 1961)

In a recent paper by Moffat,[1] a set of coupled equations was derived for the inverse partial-wave amplitudes on the basis of the partial-wave analysis of Chew and Mandelstam.[2] We present here the results of a numerical iteration of these equations when coupled S and P waves are treated, and all but two-pion exchange mechanisms are neglected. Up to and including P waves there occur two S-wave subtraction constants, $a_0^I = A_0^I(-\frac{2}{3})$, one P-wave subtraction constant, $a_1^1 = A_1^1(-\frac{2}{3})$, and a constant ξ_1, generated by the P-wave threshold behavior.

By using crossing symmetry, Chew and Mandelstam[2] have deduced that so long as D and higher waves are small the following five conditions hold at $\nu = -\frac{2}{3}$:

$$\tfrac{1}{5}a_0^0 = \tfrac{1}{2}a_0^2 = -\lambda, \tag{1}$$

$$\tfrac{2}{3}a_0^{2\prime} = -\tfrac{1}{3}a_0^{0\prime} = a_1^{1\prime}, \tag{2}$$

$$a_0^{0\prime\prime} - \tfrac{5}{2}a_0^{2\prime\prime} = 27a_1^1 + 18a_1^{1\prime}. \tag{3}$$

All other derivative conditions which may be deduced at the symmetry point depend mainly on the omitted higher partial waves.

The system of equations for the inverse amplitude was programmed for an iterative solution on the CERN mercury computer, supplying λ, the effective pion-pion coupling constant, as a parameter. The constants a_1^1 and ξ_1 are determined by imposing the two crossing-symmetry conditions (2). The solutions, as functions of the single parameter λ, are used to determine the quantities entering (3). The extent to which the condition (3) is satisfied is a test of the consistency of the theory, and, as we shall see, this does not impose any limitations on the values of λ employed. If the solutions are to be consistent with the Mandelstam representation, no complex poles may occur in $A_l(\nu)$. It has been verified that no such poles occur for the solutions presented in this Letter.

Seven or eight interation cycles were found to be sufficient to determine the inverse amplitudes to better than 1%, when starting from given values of ξ_1 and a_1^1. By varying ξ_1 and a_1^1 in a systematic manner until Eqs. (2) were satisfied to 1-2%, these constants and the calculated phase shifts for a given λ were found to be of the same order of accuracy. In a preliminary calculation[3] the conditions (2) were only satisfied to 15%, but this accuracy has been found to be insufficient to obtain a quantitatively correct set of phase shifts.

The numerical calculations have shown clearly that the range of λ is limited. For each negative λ (corresponding to attractive S-wave forces) with $|\lambda| \leq 0.5$, a single positive value of ξ_1 can be found so that conditions (2) are satisfied. These solutions are characterized by a very small P-wave phase shift and correspond to those computed by Chew, Mandelstam, and Noyes.[4] However, these solutions with positive ξ_1 completely fail to satisfy condition (3) and do not, therefore, represent cases of physical interest. For negative values of λ, other solutions are found having a negative value of ξ_1. For values of $|\lambda| \geq 0.45$ a bound state in the $I = 0$ state occurs ($\cot\delta_0^0$ becomes negative near zero energy), but

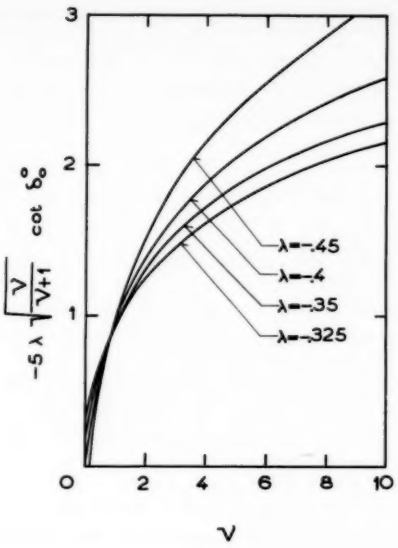

FIG. 1. $(-5\lambda)[\nu/(\nu+1)]^{1/2}\cot\delta_0^0$ as a function of ν, for different values of λ. Note that $\cot\delta_0^0$ for $\lambda=-0.45$ becomes negative near $\nu=0$.

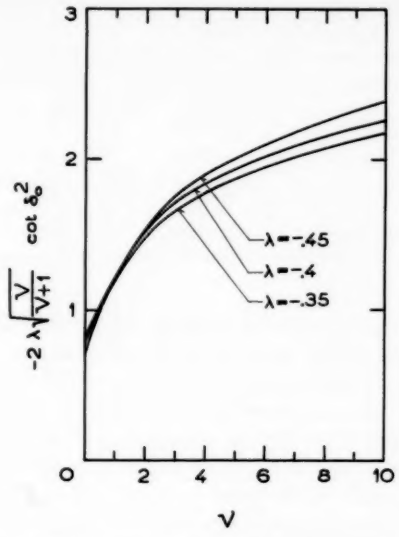

FIG. 2. $(-2\lambda)[\nu/(\nu+1)]^{1/2}\cot\delta_0^2$ as a function of ν, for different values of λ. The curve for $\lambda=-0.325$ is close to that for $\lambda=-0.35$ and is not shown in the interests of clarity.

for smaller values of $|\lambda|$ this disappears and the solutions are characterized by large P-wave phase shifts. The solutions with negative ξ_1 are all found to satisfy the second derivative condition (3), and therefore represent acceptable physical solutions.

Solutions of the coupled equations for positive λ (repulsive S-wave forces) with $\lambda>0.25$ fail to satisfy conditions (2). For $\lambda<0.25$ the iterative procedure adopted becomes unstable and we have been as yet unable to determine whether solutions exist. The calculated values of $-5\lambda[\nu/(\nu+1)]^{1/2}\cot\delta_0^0$, $-2\lambda[\nu/(\nu+1)]^{1/2}\cot\delta_0^2$, and $[\nu^3/(\nu+1)]^{1/2}\cot\delta_1^1$ are displayed in Figs. 1, 2, and 3 for $-0.45\leq\lambda\leq-0.325$, and the corresponding values of a_1^1 and ξ_1 are shown in Table I. Results for smaller values of $|\lambda|$ and full details of the calculations will be published elsewhere. It should be noted that the $I=0$ phase shifts are much larger than $I=2$ phase shifts at low energies, and that the S-wave scattering lengths become smaller as the resonance position moves towards smaller energies. (This can be observed for the S-wave scattering lengths α_0, α_2, which have been included in Table I.) For $|\lambda|<0.45$, $\cot\delta_1^1$ passes through zero from positive to negative values, this giving rise to a P-wave resonant cross section. The resonance positions ν_R and the

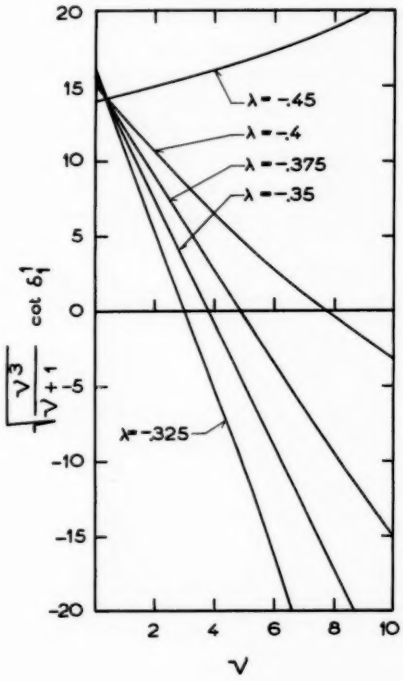

FIG. 3. $[\nu^3/(\nu+1)]^{1/2}\cot\delta_1^1$ as a function of ν, for different values of λ.

Table I. Calculated values of a_1^1, ξ_1, resonance parameters ν_R, Γ, and S-wave scattering lengths α_0, α_2.

λ	a_1^1	ξ_1	ν_R	Γ	α_0	α_2
-0.45	-0.0529	-21.2	...	...	-68.0	+1.24
-0.40	-0.0442	-22.5	7.7	6.0	+33.7	1.05
-0.375	-0.0413	-22.9	4.8(5)	2.5	16.4	0.96
-0.35	-0.0397	-23.4	3.8	1.7(5)	10.8	0.87
-0.325	-0.0373	-24.1	3.0	1.0	7.5	0.79

corresponding total widths Γ are also included in Table I [the total width Γ is related to the reduced width γ by $\Gamma = (\nu_R^3/(\nu_R+1))^{1/2}\gamma$].

The P-wave resonance suggested by Frazer and Fulco[5] was at $\nu_R = 1.5$ with a reduced width $\gamma = 0.4$, but more recently Bowcock et al.[6] and Frautschi[7] have found that on the basis of π-N scattering the resonance position ν_R should be further out at $\nu_R = 4.6$ with a reduced width $\gamma = 0.2$ and $\gamma = 0.4$, respectively. The value $\nu_R = 4.6$ is given by our calculated phase shifts for $|\lambda| = 0.37$ with an associated reduced width $\gamma = 0.5$. The calculated S-wave scattering lengths do not agree with the analysis of 3-pion τ decay,[8,9] but as this analysis is based on the assumption of small S-wave scattering lengths (i.e., α_0, $\alpha_2 \ll 1$), the calculated values are not necessarily in disagreement with experiment.

The authors wish to record their gratitude to CERN for its hospitality while this work was in progress, and to thank the staff of the CERN Mercury computer for their cooperation.

*On leave of absence from The University, Glasgow, Scotland.

†Permanent address: RIAS, Baltimore, Maryland.

[1]J. W. Moffat, Phys. Rev. 121, 926 (1961); afterwards referred to as I. The notation and units of this paper are used throughout.

[2]G. F. Chew and S. Mandelstam, Phys. Rev. 119, 467 (1960); G. F. Chew and S. Mandelstam, University of California Radiation Laboratory Report UCRL-9126, March, 1960 (unpublished).

[3]B. H. Bransden and J. W. Moffat, CERN Report 339/TH.158 (unpublished).

[4]G. F. Chew, S. Mandelstam, and H. P. Noyes, Phys. Rev. 119, 478 (1960).

[5]W. R. Frazer and J. R. Fulco, Phys. Rev. 117, 1609 (1960).

[6]J. Bowcock, W. N. Cottingham, and D. Lurié, Nuovo cimento 16, 918 (1960), and Phys. Rev. Letters 5, 386 (1960).

[7]S. C. Frautschi, Phys. Rev. Letters 5, 159 (1960).

[8]N. N. Khuri and S. B. Treiman, Phys. Rev. 119, 1115 (1960).

[9]R. F. Sawyer and K. C. Wali, Phys. Rev. 119, 1429 (1960).

ERRATUM

INELASTIC SCATTERING OF 18.9-Mev NUCLEONS FROM THE 9.6-Mev STATE OF C^{12}. E. Bradford and B. A. Robson [Phys. Rev. Letters 6, 550 (1961)].

The calculation giving Fig. 1 contains an error. The results of a corrected calculation for $\alpha_1 = 0.917$, $\alpha_2 = -0.399$, $\alpha_3 = 0$ are shown in the following diagram. The conclusions of the Letter remain unchanged.

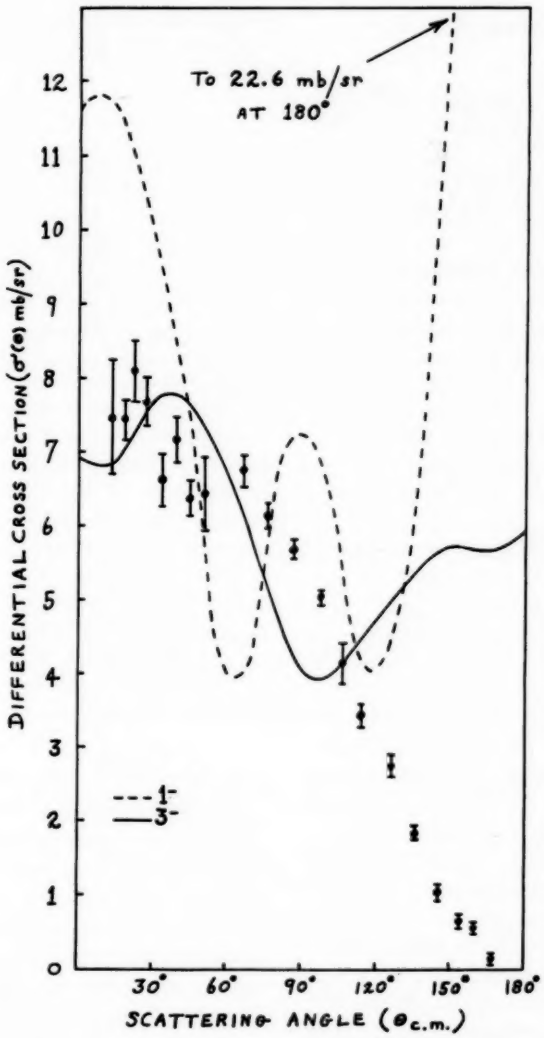

FIG. 1. Inelastic nucleon scattering from the 9.6-Mev state of C^{12}. The points are the experimental results of Peelle for 18.9-Mev protons. The theoretical curves are for 18.9-Mev neutrons. The curves for 3^- and 1^- are normalized at 60° and 50°, respectively.

ABSTRACTS

In this section are printed the abstracts of Articles that have been forwarded to The American Institute of Physics for publication in THE PHYSICAL REVIEW. In quoting information obtained from this section before the appearance of the corresponding Article, reference should be made to "Physical Review (to be published)" rather than to this Journal.

NONLINEAR, TIME-DEPENDENT, PLASMA OSCILLATIONS. David Montgomery, University of Wisconsin, Madison, Wisconsin (Received April 6, 1961).

The Laplace-transform technique employed by Landau to solve the problem of the first-order motions in an unbounded, rarified, electron plasma is modified to solve the problem to arbitrarily high order. The transforms of the nth-order contributions are expressible in terms of convolution integrals involving only terms up to order n-1. The method is applied to second order for the case of square-integrable disturbances.

ANOMALIES IN IONIZATION COEFFICIENTS AND IN UNIFORM FIELD BREAKDOWN IN ARGON FOR LOW VALUES OF E/p. D. E. Golden and L. H. Fisher, Department of Physics, New York University, University Heights, New York, New York (Received March 21, 1961; revised manuscript received May 4, 1961).

Prebreakdown ionization currents in argon have been measured in uniform fields for low values of the ratio of field strength to pressure E/p [5 to 12 volts (cm mm Hg)$^{-1}$]. Currents obtained with varying electrode separation d at constant E/p and constant p could not be analyzed to yield values of the Townsend coefficients α/p and γ. Currents obtained with varying p at constant E/p and constant d could be analyzed to yield values of α/p and γ, but such currents yielded coefficients which depend on d. The dependence of the values of α/p on d is attributed to the production of highly excited atoms by resonance radiation at some distance from the positions where the electrons lose their energy; these highly excited atoms then produce molecular ions and electrons in collisions with ground-state argon atoms. The secondary mechanism and the dependence of γ on d is associated with resonance radiation. Sparking potential measurements in argon made by varying both p and d for values of pd corresponding to breakdown for the above range of E/p show deviations from Paschen's law.

Disregarding the above anomalies, the values of α/p are smaller than the earlier measurements of Kruithof and Penning by as much as a factor of 15 at $E/p=5$ ($d=4$ cm). At this value of E/p (and of d), the value of $\exp(\alpha d)$ at breakdown is only 1.05, and the value of γ is about 20. At larger values of E/p, the present values of α/p become independent of d and approach theirs. The sparking potentials obtained are significantly larger than those obtained by Kachickas and Fisher. This is shown to be due to the condition of the cathode surface.

VELOCITY-DEPENDENT CORRELATIONS IN THE STATISTICAL DISTRIBUTION OF THE ELECTRIC MICROFIELD IN A PLASMA. Amiram Ron, Department of Physics and Faculty of Electrical Engineering, Technion-Israel Institute of Technology, Haifa, Israel, and G. Kalman, Department of Physics, Technion-Israel Institute of Technology, Haifa, Israel (Received April 6, 1961).

The polarization of a plasma in the neighborhood of a moving ion depends on the ion velocity. This affects the distribution of the stochastic field acting upon the ion. Correction to the Holtsmark distribution due to the complete test particle–field particle correlation including this dynamic effect is calculated up to the order e^2. The result is: (1) shift toward smaller fields, (2) anisotropy, and (3) velocity dependence, which is not necessarily equal to the zero-velocity effect even on the average.

MAGNETIC ANOMALY IN $FeTiO_3$-αFe_2O_3 SYSTEM BY MÖSSBAUER EFFECT. S. L. Ruby, Radiation and Nucleonics Laboratory, Westinghouse Electric Corporation, East Pittsburgh, Pennsylvania, and G. Shirane, Research Laboratories, Westinghouse Electric Corporation, East Pittsburgh, Pennsylvania (Received April 13, 1961).

The solid solutions $(1-x)FeTiO_3-xFe_2O_3$ exhibit strong ferrimagnetic moments for the compositions $x<0.6$, where the Fe and Ti ions are ordered in the alternate (111) layers. The anom-

aly revealed by the Mössbauer measurements is that the ferrimagnetic phase consists of ferrimagnetic clusters surrounded by paramagnetic media. The size of these clusters decreases with increasing temperature or increasing local concentration of Ti. The isomer shift of $FeTiO_3$ is 1.2 mm/sec at room temperature as expected for Fe^{2+}, although the quadrupole splitting of 0.62 mm/sec is smaller than that observed in other ferrous environments.

PRODUCTION OF VACANCIES IN PULSED GOLD. James J. Jackson and James S. Koehler, University of Illinois, Urbana, Illinois (Received April 3, 1961).

Pulse heating experiments were done on 2-mil diameter pure gold wires in an attempt to obtain information on the sources for lattice vacancies. About a quarter or less of the vacancies are generated at the wire surface during the first few milliseconds. The fraction is smaller for longer times. The majority are produced at dislocations. From the high initial rate of production one infers that the jog energy in gold is equal to or less than 1.10 ev. The details of the creation and diffusion of vacancies are described. Annealing experiments on pulsed wires are consistent with the idea that dislocations act both as sources and sinks for vacancies.

ELECTRON WAVE FUNCTIONS IN METALLIC SODIUM. Joseph Callaway, Department of Physics, University of California, Riverside, California (Received April 10, 1961).

Wave functions to order k^2 are presented for electrons in metallic sodium. The calculation is an application of the cellular method. The empirical potential of Prokofjew was employed.

ELECTRICAL CONDUCTION IN p-TYPE TITANIUM SESQUIOXIDE. J. Yahia and H. P. R. Frederikse, National Bureau of Standards, Washington, D. C. (Received March 31, 1961; revised manuscript received May 25, 1961).

The Hall effect, thermoelectric power, and electrical conductivity have been measured as a function of temperature in crystals of p-type titanium sesquioxide. A transition is observed at about 450°K. Below this temperature the crystals behave like semiconductors, while above it the conductivity is apparently metallic.

The behavior below 450°K is in line with antiferromagnetic ordering. The effective mass of the holes is found to be about $5m_0$ and the average Hall mobility 5 cm^2/volt-sec at room temperature. It is claimed that these values, combined with the fact that the Hall effect is measurable, support the assumption of conduction in a narrow $3d$ band.

HYPERFINE SPECTRUM OF CHROMIUM-53 IN Al_2O_3. R. W. Terhune and J. Lambe, Scientific Laboratory, Ford Motor Company, Dearborn, Michigan, and C. Kikuchi and J. Baker, Nuclear Engineering Department, University of Michigan, Ann Arbor, Michigan (Received April 7, 1961).

Electron nuclear double resonance techniques were used to observe the hyperfine spectrum of Cr^{53} in Al_2O_3. Through analysis of the spectrum at zero degrees a positive value of 48.5 ± 0.1 Mc/sec was obtained for the hyperfine coupling constant and minus 0.85 ± 0.04 Mc/sec for the quadrupole coupling constant. From this a value of minus 0.03 barn was deduced for the quadrupole moment of Cr^{53}.

COLOR CENTERS AND RADIATION-INDUCED DEFECTS IN Al_2O_3. Paul W. Levy, Brookhaven National Laboratory, Upton, New York (Received April 5, 1961).

The peak energy E_0 and full width U, in ev, of the color centers in Al_2O_3 before irradiation are: $E_0 = 5.45$, $U = 0.6$; $E_0 = 4.84$, $U = 0.54$; with an indication of a band at $E_0 > 6.2$, $U > 0.4$. Irradiation of 3×10^4 r produces saturation of the gamma-ray-induced bands which occur at $E_0 = 5.45$, $U = 1.25$; $E_0 = 3.08$, $U = 1.50$, and probably an additional band at $E_0 = 4.28$, $U = 0.70$. Reactor irradiation produces bands at $E_0 = 6.02$, $U = 0.60$; $E_0 = 5.35$, $U = 0.40$; $E_0 = 4.85$, $U = 0.54$; $E_0 = 4.21$, $U = 0.80$; $E_0 = 3.74$, $U = 0.88$; $E_0 = 2.64$, $U = 0.64$; and $E_0 = 2.00$, $U = 0.44$.

Curves of color center concentration versus irradiation time for the reactor-induced bands at $E_0 = 6.02$, $E_0 = 5.35$, and $E_0 = 4.85$, can be ac-

curately represented by a saturating exponential plus a linear increase. This behavior is predicted by a simple theory which assumes that the color centers are formed by the coloring of defects present prior to and increased by irradiation and possibly by the coloring of additional centers formed only by radiation damage. The measured rate of defect formation could be consistent with current radiation damage theories; however, several inaccurately known parameters preclude a meaningful comparison.

GYROMAGNETIC RATIO OF PYRRHOTITE. G. G. Scott, Research Laboratories, General Motors Corporation, Warren, Michigan, and André J. P. Meyer, Pierre Weiss Laboratory, Institute of Physics, University of Strasbourg, Strasbourg, France (Received April 7, 1961).

The gyromagnetic ratio of pyrrhotite was determined by measurements of the Einstein–de Haas effect. The value obtained for g' is $1.9 \pm 15\%$.

EXTRAORDINARY HALL EFFECT MEASUREMENTS ON Ni, SOME Ni ALLOYS, AND FERRITES. Jerome M. Lavine, Research Division, Raytheon Company, Waltham, Massachusetts (Received April 14, 1961).

Extraordinary Hall effect measurements over a wide range of temperature are reported for 99.9 Ni, 99.4 Ni, 95 Ni, several 80% Ni alloys, Fe_3O_4, and $(NiO)_{0.75}(FeO)_{0.25}(Fe_2O_3)$. The resistivity ρ of all samples over the same temperature range is also reported. At high temperatures, the extraordinary Hall coefficient R_1 for 99.9 Ni is proportional to ρ^2 as predicted by theory. However, the dependence upon ρ is smaller in the 99.9 Ni sample at lower temperatures and in the samples with higher impurity concentration at all temperatures. The 80% Ni samples exhibit positive R_1 while R_1 in the high-concentration Ni samples is negative. R_1 for both ferrites is negative below about 400°C and positive above this temperature.

The theoretical work on metals generally indicates that R_1 is proportional to ρ^2 and the constant of proportionality r is weakly temperature-dependent and of the order of unity. In the high-concentration Ni samples, r is negative, of the order of unity, and exhibits a significant temperature dependence at low temperatures. In the 80% Ni samples, r is positive and of the order of 10^{-2}. At room temperature, r is of the order of 10^{-3} in Fe_3O_4 and of the order of 10^{-6} in $(NiO)_{0.75}(FeO)_{0.25}(Fe_2O_3)$. In both ferrites, r is strongly temperature-dependent. The change of sign of r with temperature observed in both ferrites has not been previously observed in metals or alloys.

UNPAIRED SPIN DENSITY IN ORDERED Fe_3Al. S. J. Pickart, U. S. Naval Ordnance Laboratory, Silver Spring, Maryland and Brookhaven National Laboratory, Upton, New York, and R. Nathans, Brookhaven National Laboratory, Upton, New York (Received March 7, 1961).

A precise determination of the magnetic form factor of the ordered alloy Fe_3Al has been made by diffraction of polarized neutrons from a single crystal. Some forty-three reflections in the angular range $\sin\theta/\lambda \leq 0.9$ A^{-1} have been examined and show characteristic departures from a smooth single-valued function, indicating that the unpaired electron density in the unit cell is not spherically symmetric. The data are analyzed in two ways: by comparison with form factors calculated from free-atom Hartree-Fock wave functions including crystal-field splitting effects, and by two-dimensional Fourier projections of the unpaired spin density. The analysis indicates that, while the radial spin density of the two types of iron atom in the lattice is similar, their orbital symmetry is different. The results are discussed with reference to various theories of the electronic structure in transition metals.

PRESSURE DEPENDENCE OF THE MICROWAVE RESONANCE PROPERTIES OF SOME SPINEL AND GARNET FERRITES. I. P. Kaminow* and R. V. Jones, Gordon McKay Laboratory, Harvard University, Cambridge, Massachusetts (Received March 15, 1961).

The anisotropy field, g value, and linewidth of several spinel and garnet ferrites have been measured at X band and room temperature as functions of hydrostatic pressure to 10^4 kg/cm^2. The crystals studied include yttrium, ytterbium, and erbium iron garnet; magnesium ferrite (with different distributions of Mg^{2+} ions on A and B sites); and $Ni_{1-z}Co_zFe_2O_4$ with $z = 0$, 0.05, and 0.10. The pressure dependence of magnetization was

measured using magnetostatic mode methods in the narrow-linewidth materials, yttrium iron garnet, and magnesium ferrite.

The complexity of the crystal structure and magnetic interactions makes any quantitative interpretation very difficult. However, the observations can be understood qualitatively in terms of the volume dependence of the crystalline fields and the exchange interactions. In the case of erbium iron garnet, the volume dependence of the ferric-rare earth exchange constant is calculated; and, in the case of nickel cobalt ferrite, a simple explanation is offered for the observed volume dependence of the Co^{2+} anisotropy.

The contribution of thermal lattice vibrations to the linewidth in yttrium iron garnet is discussed, and the possibility of an anisotropic spin-orbit interaction is considered.

*Now at Bell Telephone Laboratories, Holmdel, New Jersey.

CYCLOTRON RESONANCE AND de HAAS–van ALPHEN OSCILLATIONS OF AN INTERACTING ELECTRON GAS. Walter Kohn, University of California at San Diego, La Jolla, California (Received April 5, 1961).

An electron gas with short-range interactions is considered in the presence of a uniform magnetic field. It is shown that (1) the cyclotron resonance frequency is independent of the interaction; (2) for a two-dimensional gas, the de Haas–van Alphen period is independent of the interaction. The low-lying excited states are briefly discussed.

SPECULAR REFLECTION IN THE DIFFRACTION OF SLOW ELECTRONS NEAR NORMAL INCIDENCE. J. P. Hobson and I. H. Khan, Radio and Electrical Engineering Division, National Research Council, Ottawa, Canada (Received April 14, 1961).

During experiments on the diffraction of slow electrons (0-180 ev) at normal incidence, a diffracted beam was observed corresponding to the direction of specular reflection; i.e., straight back along the incident direction. This beam had properties indicating that it should not be considered as a limiting case of beams diffracted at other colatitude angles. Maxima in reflected intensity of this beam were observed at 4-, 16-, and 31-ev incident energy. The target used was a single crystal of tungsten with the (110) face exposed. Ultra-high-vacuum techniques were employed.

RESISTIVITY AND THERMOELECTRIC POWER OF TRANSITION METALS IN COPPER-GOLD ALLOYS. M. D. Blue, Honeywell Research Center, Hopkins, Minnesota (Received April 7, 1961).

Resistivity and thermoelectric power measurements on CuAu alloys containing dilute amounts of Co, Fe, and Mn are discussed. An analysis of these measurements using the thermoelectric power formula of Mott leads to values of the scattering cross sections of transition elements and their derivatives with respect to energy in good agreement with the values obtained for these elements with Cu or Au as solvent. The results indicate that contributions to resistance due to disorder scattering and impurity scattering are additive in these alloys.

SUPERCONDUCTING CRITICAL FIELD OF TANTALUM AS A FUNCTION OF TEMPERATURE AND PRESSURE. C. H. Hinrichs* and C. A. Swenson, Institute for Atomic Research and Department of Physics, Iowa State University, Ames, Iowa (Received April 13, 1961).

The results of precise critical field measurements on tantalum samples which show "soft" superconducting behavior are given along with direct measurements of the pressure effect, $(\partial H_c/\partial P)_T$, as a function of temperature. The BCS theory is used as a guide in the extrapolation of these data to absolute zero from 1.1°K. The advantages of using an H^2 vs T^2 representation for both the critical field and pressure effect data are discussed, and it is shown that if both sets of data can be represented in terms of power series [H^2 or $(\partial H_c{}^2/\partial P)_T$ vs T^2] over a limited range of temperature, it is then possible to write down explicit power-series expressions for the differences in the thermodynamic functions between the normal and superconducting states over this same temperature range. The electronic contributions to the specific heats and the thermal expansions for tantalum are calculated from the experimental data. The results

can be interpreted to show that the thermodynamic properties of superconducting tantalum cannot be expressed in the form of a law of corresponding states involving the zero-field transition temperature.

*Now at the Linfield Research Institute, McMinnville, Oregon.

SUPERCONDUCTIVITY OF α AND β MERCURY. J. E. Schirber and C. A. Swenson, Institute for Atomic Research and Department of Physics, Iowa State University, Ames, Iowa (Received April 13, 1961).

Precise critical field measurements and a direct measurement of $(\partial H/\partial P)_T$ as a function of temperature were made on physically identical samples of α and β Hg. The purpose of these measurements was to obtain data on the effects of crystal structure on the properties of superconductors, and to permit the calculation of various thermodynamic quantities difficult to obtain in any other way. The critical fields of the two phases were found to be identical when expressed in terms of the reduced variables H/H_0 and T/T_C. No generalizations of this type could be found to explain the pressure effects. The advantages of an H^2 vs T^2 and $\partial H^2/\partial P$ vs T^2 analysis for extrapolation to absolute zero are stressed. The critical fields of several representative superconductors are compared with the critical field predicted by the BCS theory, using a plot that emphasizes the detailed shape of the curves at low temperatures. This plot also can be interpreted in terms of the θ/T_c dependence of the width of the energy gap. The agreement between calorimetric and critical field determinations of the electronic specific heat in the normal state is shown to be improved by using the H^2-T^2 extrapolation.

EFFECT OF PERIODIC ADIABATIC TIME VARIATIONS ON INTERACTING SYSTEMS. H. Suhl, Physics Department, University of California, La Jolla, California (Received April 3, 1961).

It is shown that a many-particle system subject to periodic adiabatic variation of certain of its parameters is to a certain extent equivalent to a non-time-varying system with a radically modified interaction between the particles. The particular case of an electron gas in a metal is discussed in some detail.

DIFFUSION ALONG SMALL-ANGLE GRAIN BOUNDARIES IN SILICON. H. J. Queisser, K. Hubner, and W. Shockley, Shockley Transistor, Unit of Clevite Transistor, Palo Alto, California (Received April 5, 1961).

Diffusion fronts in samples containing grain boundaries are spike-shaped. Velocity of spike advance and angle between spike and boundary are measured. The "spike velocity method" of analysis permits evaluation of two effective widths, W_D and W_0, which describe the diffusion properties of the boundary. This method has been used to analyze data on phosphorus diffusion into boron-doped silicon at 1200°C and 1050°C. It is concluded that an enhanced diffusion current flows along each dislocation of the grain boundary over a cross section less than one Burgers-vector square. The diffusion current density is about 300 000 times that of the bulk. This corresponds to an energy of 1.5 ev by which grain boundary diffusion is favored over the bulk diffusion. This enhancement is believed to be caused by enrichment of phosphorus and also partly by the extra concentration of vacancies near the dislocation cores. Some possible extensions of the studies to include saturation effects at the dislocation cores are discussed.

SOME NEW INTERRELATIONS IN THE PROPERTIES OF SOLIDS. Johannes N. Plendl, Electronics Research Directorate, Air Force Cambridge Research Laboratories, Office of Aerospace Research, Hansom Field, Bedford, Massachusetts (Received October 3, 1960; revised manuscript received February 13, 1961).

The lattice vibration spectrum of a solid can be characterized by one single frequency, which is defined as "the frequency of the center of gravity" of this spectrum or simply "center frequency." From its equality with the characteristic frequency of specific heat we have recently derived the "center law of the lattice vibration spectra." In assuming now that in a lattice, at equilibrium, the hypothetical maximum of vibrational energy (kinetic energy) of

an atom (ion) pair equals the total cohesive energy (potential energy), and at the same time considering the anharmonicity of lattice vibrations, we derive a basic interrelation between center frequency and total cohesive energy. It constitutes a substantial extension of the above "center law." Its validity has been illustrated for 26 solid compounds of six different lattice structures which cover almost the entire range of lattice vibration spectra of solids. This interrelation allows a first determination of thus far inaccessible data of cohesive energy for solids of extremely high sublimation temperatures, such as silicon carbide, boron nitride, and the two types of diamond. Detailed study of the anharmonicity of lattice vibrations results in additional interrelations, such as one between exponent of repulsion and "related mass" [=reduced mass of the vibrating atom (ion) pairs related to argon], one between exponent of repulsion and "relative compressibility" (change of compressibility with pressure over compressibility), and thus one between "relative compressibility" and "related mass." In combining the two interrelations of center frequency, namely that with characteristic temperature and that with cohesive energy, we derive an interrelation between characteristic temperature and total cohesive energy. Examination of the relationship between anharmonicity and atomic behavior suggests a classification of solids according to their different anharmonic force characteristics. The solids can have either a soft or linear or hard force characteristic, dependent on the configuration which they resemble in the periodic chart of the atoms. The underlying concept of anharmonicity deduced in this paper helps to understand the physical properties of solids from an atomistic point of view.

ELASTIC CONSTANTS OF CsBr, CsI, RbBr, and RbI. K. Reinitz,* Rensselaer Polytechnic Institute, Troy, New York (Received February 14, 1961; revised manuscript received May 12, 1961).

The elastic constants of two body-centered halides, CsBr and CsI, were determined as a function of temperature from 300°K to 73°K. The velocity measurements were obtained with an ultrasonic interferometer constructed according to the design principles of Williams and Lamb. Room-temperature constants of RbBr and RbI samples were also measured. The values of C_{11}, C_{12}, and C_{44} in units of 10^{11} dynes/cm^2 at 22°C for these salts are given in the following table:

	C_{11}	C_{12}	C_{44}
CsBr	3.097	0.903	0.7500
CsI	2.434	0.636	0.6316
RbBr	3.15	0.493	0.384
RbI	2.54	0.407	0.276

The temperature dependence of all the cesium salt constants was negative and nearly linear over the temperature range investigated. It was found that with decreasing temperatures C_{44} increased more rapidly than C_{12} for the two cesium salts examined.

The elastic constant data of the sodium chloride type halides, compiled from the literature, are compared with those of the cesium chloride type salts.

*Now at Delco Radio, Kokomo, Indiana.

INTERPRETATION OF LOW-ENERGY ELECTRON DIFFRACTION PATTERNS OF ADSORBED GASES. Ernst Bauer, Michelson Laboratory, China Lake, California (Received March 27, 1961).

Recent observations of the adsorption of oxygen on nickel are interpreted in terms of double scattering processes instead of the single scattering mechanism which has been used in all previous interpretations. This permits a simple explanation of the observed variation of the intensity of the diffraction pattern with electron energy and provides a plausible understanding of the early stages of adsorption.

ELECTRONIC STRUCTURE OF THE F CENTER IN LiCl. R. F. Wood* and J. Korringa, The Ohio State University, Columbus, Ohio (Received April 14, 1961).

The electronic structure of the F-center lattice defect in LiCl is investigated with calculations based on the usual model of the F center proposed by de Boer. The ground- and excited-state wave functions and energies of the trapped electron are determined by two different methods. First, the method of linear combination of atomic orbit-

als (LCAO) is used. This method is capable of yielding good results but the complexity of the necessary calculations is great. In an effort to avoid this complexity, the method of vacancy-centered wave functions is investigated. Very simple wave functions are used in this method with satisfactory results. The coefficient of the hyperfine interaction of the F-center electron with the nearest neighbor lithium ion and the oscillator strength of the optical transition are calculated. The distortions of the lattice in the vicinity of the F center are calculated. A very small outward movement of the first and second nearest neighbors occurs in the ground state. The situation in the excited state is complicated by the "p-type" symmetry of the F-electron wave function. In this case, the two nearest neighbor lithium ions located on the symmetry axis of the wave function are found to undergo a large displacement outward from the vacancy. The other four nearest neighbors displace inward toward the center of the vacancy. The results of the calculations are discussed and detailed comparisons with other work of a similar nature are given.

*Present address: Quantum Chemistry Group, University of Uppsala, Uppsala, Sweden.

ANTIFERROMAGNETIC LINEAR CHAIN. L. F. Mattheiss,* Solid-State and Molecular Theory Group, Massachusetts Institute of Technology, Cambridge, Massachusetts (Received February 1, 1961).

Many-electron configuration interaction calculations have been carried out on a system of six hydrogen atoms arranged in a regular hexagonal array with a variable lattice spacing. The approximate wave functions for this system have been expressed as linear combinations of the $(2\times6)!/(6!)^2=924$ determinantal functions which can be formed from atomic 1s functions. In this manner, the effects of ionic configurations containing as many as three pairs of doubly filled orbitals have been introduced into the calculations. All three- and four-center integrals have been taken into account. The nonorthogonality of hydrogenic 1s orbitals localized about different atomic sites has been removed by transforming to a set of orthonormal Wannier functions. The principal result of these calculations is the fact that the effects of configuration interaction can be represented quite accurately at large internuclear separations in terms of a parameter J' (analogous to a nearest neighbor exchange integral) which assumes a negative value in a nonferromagnetic system such as this one. This provides a justification for the use of the Heisenberg exchange operator $-2J'(\sum_i \vec{s}_i\cdot\vec{s}_{i+1}-\frac{1}{4})$ to describe the magnetic interaction at large separations in this system. In addition, these results show that this system of hydrogen atoms is bound with respect to six separated atoms, but not with respect to three molecules. The ground-state wave function is a singlet at all internuclear separations. The general form of the curves representing energy as a function of internuclear separation shows a striking similarity to those obtained for the hydrogen molecule.

*Now at Cavendish Laboratory, Cambridge University, Cambridge, England.

EFFECTIVE EXCHANGE INTEGRAL. L. F. Mattheiss,* Solid-State and Molecular Theory Group, Massachusetts Institute of Technology, Cambridge, Massachusetts (Received February 1, 1961).

The magnetic properties of a linear chain of monovalent atoms are investigated from the point of view of perturbation theory. The many-electron wave functions for the system are expanded as linear combinations of determinantal functions which are eigenfunctions of S^2 and S_z. These determinantal functions are constructed from orthonormal one-electron orbitals of the Wannier type so that the nearest neighbor exchange integral is positive definite and approaches zero at large lattice spacings. The secular equation is set up using the method of the Dirac vector model. By means of the Kramers perturbation technique, the interaction of ionic states with those arising from the ground configuration is represented by means of an effective Hamiltonian operator with its associated matrix. The results of this treatment are analogous to those obtained by Paul in that an analytic expression is found for an effective nearest neighbor exchange integral J'. This quantity is represented as the difference between the positive-definite exchange integral and additional terms from ionic states. The present treatment defines in a fairly precise manner the type configurations which contribute to this effective exchange integral and the limits for which this parameterization is valid. The results of this analysis are compared with those obtained from

recent calculations on a system of six hydrogen atoms.

*Now at Cavendish Laboratory, Cambridge University, Cambridge, England.

STIMULATED OPTICAL EMISSION IN FLUORESCENT SOLIDS. I. THEORETICAL CONSIDERATIONS. T. H. Maiman,* Hughes Research Laboratories, a division of Hughes Aircraft Company, Malibu, California (Received January 27, 1961; revised manuscript received May 17, 1961).

An analysis of stimulated emission processes in fluorescent solids is presented. The kinetic equations are discussed and expressions for pumping power and effective temperature of the exciting source are given in terms of the material parameters. A comparison of excitation intensity for three- and four-level systems is given. The spectral width of the stimulated radiation is discussed with particular attention to imperfect crystals.

*Now at Quantatron, Inc., 2520 Colorado Avenue, Santa Monica, California.

STIMULATED OPTICAL EMISSION IN FLUORESCENT SOLIDS. II. SPECTROSCOPY AND STIMULATED EMISSION IN RUBY. T. H. Maiman,* R. H. Hoskins,* I. J. D'Haenens, C. K. Asawa, and V. Evtuhov, Hughes Research Laboratories, a division of Hughes Aircraft Company, Malibu, California (Received January 27, 1961).

Optical absorption cross sections and the fluorescent quantum efficiency in ruby have been determined. These data have been used to correlate calculations with the analysis of the preceding paper. Stimulated emission from ruby under pulsed excitation has been studied in some detail; the observations are found to depend strongly on the perfection of the particular crystal under study. A peak power output of approximately 5 kw, total output energy of near one joule, beam collimation of less than 10^{-2} radian, and a spectral width of individual components in the output radiation of about 6×10^{-4} A at 6943 A have been measured. It is suggested that mode instabilities due to temperature shifts and a time-varying magnetic field are contributing to an oscillatory behavior of the output pulse.

*Now at Quantatron, Inc., 2520 Colorado Avenue, Santa Monica, California.

DIAMAGNETIC SUSCEPTIBILITY OF PYROLYTIC GRAPHITE. D. B. Fischbach, Jet Propulsion Laboratory, California Institute of Technology, Pasadena, California (Received April 12, 1961).

The diamagnetic susceptibilities of some pyrolytic graphites deposited at 2100-2300°C have been measured at room temperature. As-deposited sampled had significantly larger susceptibilities than that of well-graphitized carbons or single-crystal graphite. Heat treatment at temperatures above 2300°C caused the total susceptibility to decrease to a minimum value, then rise and level out at a value characteristic of graphite, as a function of treatment temperature. The relationship of the susceptibility behavior to the structure of the pyrolytic graphite is discussed.

PRESSURE DEPENDENCE OF THE ELASTIC SHEAR CONSTANTS OF Li. A. L. Jain, Case Institute of Technology, Cleveland, Ohio (Received April 14, 1961).

The elastic shear constants, $C = C_{44}$ and $C' = \frac{1}{2}(C_{11} - C_{12})$, of lithium have been measured as a function of pressure at room temperature. The measured values of $d\ln C/d\ln r$ and $d\ln C'/d\ln r$ are -4.1 and -2.8, respectively. This inequality of the two pressure variations is contrary to the situation found in sodium, where the two coefficients were equal. Theoretically, the two coefficients are expected to be the same, if only the electrostatic interaction between the electrons and the ions is responsible for the elastic stiffness of the metal. The different behavior in lithium can be understood in terms of the extra contribution to the shear constants arising due to the change in the Fermi energy of the electrons on shearing.

THERMODYNAMICS OF DIRTY SUPERCONDUCTORS. D. J. Kenworthy* and D. ter Haar, The Clarendon Laboratory, Oxford, Great Britain (Received April 7, 1961).

We use a method due to Tsekhmistrenko to eliminate from the Fröhlich Hamiltonian the electron-phonon interaction term. We then evaluate the thermodynamic properties of a superconductor described by this Hamiltonian, using a formalism developed by Zubarev and

Tserkovnikov which is based on a paper by Bloch and De Dominicis. We introduce an extra term in the Hamiltonian to take the impurity scattering into account and study the effect of this extra term on the transition temperature. For the product of the mean free path and the relative change in the transition temperature we find values of 7×10^{-6}, 9×10^{-6}, and 8×10^{-6} cm for Sn, In, and Al, respectively.

*Present address: Department of Mathematics, McMaster University, Hamilton, Ontario, Canada.

ENERGY LOSSES IN A MANY-BODY SYSTEM. Stanley Engelsberg, Department of Physics, University of Illinois, Urbana, Illinois (Received March 27, 1961).

The energy loss problem is formulated in such a way as to include all losses simultaneously. The lifetime and energy losses of a particle in a well-defined single-particle state with small transition probability are found to be related to the self-energy operator. As an illustration of the application of the relation obtained, a derivation of the Bethe sum rule and the Čerenkov losses is given for a particle incident on a many-body system.

HARTREE-FOCK ATOMIC WAVE FUNCTIONS FROM Cu^{+} TO Kr^{+8}. W. W. Piper, General Electric Research Laboratory, Schenectady, New York (Received April 12, 1961).

Hartree-Fock atomic wave functions have been calculated and tabulated for the ground-state configurations of Cu^{+} through Kr^{+8}. Interpolation functions for this configuration have also been tabulated.

"REPULSION OF ENERGY LEVELS" IN COMPLEX ATOMIC SPECTRA. R. E. Trees, National Bureau of Standards, Washington, D. C. (Received April 4, 1961).

Rosenzweig and Porter have shown a "repulsion of energy levels" in spacing distributions determined from energy levels in complex atomic spectra. The present paper extends their work by showing that these spacing distributions can be determined from calculated positions of the levels in these spectra. Since calculated data are available for spectra where the observed data are scarce or incomplete, this partially overcomes limitations imposed by statistical inaccuracy when direct use is made of the observed data. The equivalence of the two approaches is demonstrated by showing that calculated data for Ta II yield the same spacing distribution as obtained from observed data for Ta II and Re I combined. These are complex spectra in which a fully developed repulsion effect is present. A similar demonstration of equivalence is carried out for spectra of Ru I and Mo I, where the repulsion effect is in an intermediate state of development. The results also indicate that numbers easily evaluated from the radial parameters of the theory will indicate roughly the degree of repulsion, replacing to some extent the need for an explicit calculation of the spacing distribution.

PARAMETERS α AND β IN THE SPECTRA OF THE IRON GROUP. Richard E. Trees, National Bureau of Standards, Washington, D. C., and Chr. Klixbüll Jørgensen, Cyanamid European Research Institute, Cologny, Geneva, Switzerland (Received April 4, 1961).

The parameters α and β in the low even configurations of iron-group spectra are qualitatively explained as effects of the interaction with configurations having two $3p$ electrons excited from the argon-type core to $3d$ states. Quantitatively, the parameters are too large by a factor of two when the interaction integrals are taken equal to the exchange integrals of Watson's self-consistent field calculations. The parameters are too small when the exchange integrals are evaluated from observed data in the $3p^{5}3d$ configuration of Ca III.

NEW HAFNIUM ISOTOPE, Hf^{182}. J. Wing, B. A. Swartz, and J. R. Huizenga, Argonne National Laboratory, Argonne, Illinois (Received April 3, 1961).

A new isotope of hafnium, Hf^{182}, has been produced by double neutron capture in Hf^{180} in the intense neutron flux of the Materials Testing Reactor (MTR). Mass spectrometric analysis of the irradiated hafnium gave a Hf^{182}/Hf^{180} atom ratio of 0.00147 ± 0.00001. The new isotope decays with a half-life of $(9\pm2)\times10^{6}$ years by β^{-}

emission predominantly to a 271-kev level in Ta^{182}. The number of 271-kev gamma rays per β^- disintegration is 0.84 ± 0.10. The $\log(ft)$ for the beta transition to the Ta^{182} ground state is >15, indicating that this transition is at least third forbidden. The neutron capture cross section of Hf^{181} is 40^{+40}_{-20} barns.

PARITY CONSERVATION IN NUCLEAR REACTIONS: SEARCH FOR α DECAY OF THE 8.88-Mev STATE IN O^{16}. R. E. Segel, J. W. Olness, and E. L. Sprenkel, Aeronautical Research Laboratory, Dayton, Ohio (Received April 13, 1961).

A search has been carried out for the parity-nonconserving α decay of the 8.88-Mev (2^-) state in O^{16} by examining the alpha-particle spectrum following N^{16} β decay. An upper limit of $\Gamma_\alpha/\Gamma_\gamma < 2\times10^{-6}$ was determined which is shown to lead to the estimate that $\mathfrak{F}^2 \leq 2\times10^{-12}$. The alpha-particle group corresponding to disintegration of the broad 9.58-Mev (1^-) state was observed and the $\log ft$ for the β decay to this state found to be 6.8 ± 0.1, the slow transition rate being in accord with a shell-model prediction that the 9.58-Mev state is due to a three-nucleon excitation. The shape of the alpha spectrum was fitted with a Breit-Wigner analysis.

NEW ISOTOPE, Al^{30}. E. L. Robinson and O. E. Johnson, Physics Department, Purdue University, Lafayette, Indiana (Received April 6, 1961).

Scintillation measurements were made of the beta and gamma radiation from high-purity natural silicon targets after bombardment with fast neutrons produced by the $Li^7(d,n)Be^8$ reaction ($E_n \lesssim 24$ Mev). In addition to well-known radiations, a beta spectrum with an end point of 5.05 ± 0.25 Mev and two gamma rays with energies of 2.26 ± 0.03 Mev and 3.52 ± 0.03 Mev were observed. These gamma rays and the beta group decayed, within experimental error, with the same half-life, 3.27 ± 0.20 sec. The assignment of this activity to Al^{30} and the proposed decay scheme are supported by considerations involving the decay schemes of the well-known isotopes produced, half-life studies using portions of both the beta and gamma spectra, the features of experimental beta and gamma spectra, and nuclear systematics. Strong beta transitions to the first and second excited states of Si^{30} are inferred by the experimental gamma spectrum and nuclear systematics. A weak beta transition ($<2\%$) to the ground state can not be excluded by this investigation. Possible spin and parity assignments for the ground state of Al^{30} are 1+, 2+, and 3+. A weak argument is made against a spin 1 assignment. The results of this investigation can not be used to reduce the ambiguity of the spin assignment further. The resulting Al^{30}-Si^{30} mass difference is 7.29 ± 0.25 Mev.

SPECTROSCOPY OF GAMMA RADIATION FROM Nd^{144}, Sr^{88}, and Pb^{207}. J. E. Monahan, S. Raboy, and C. C. Trail, Argonne National Laboratory, Argonne, Illinois (Received March 27, 1961).

The energies of the cascade gamma rays in Nd^{144} are found to be 1487.0 ± 1.1 kev and 696.7 ± 0.6 kev and the measured energy of the cross-over transition is 2186.0 ± 2.2 kev. The agreement of these results is used to justify the claim of 0.1% accuracy for the scintillation spectrometer with anticoincidence annulus for the measurement of gamma-ray energies in the interval from 0.5 Mev to roughly 3.0 Mev. An energy of 570.8 ± 0.5 kev is obtained for the low-energy radiation from Pb^{207}, and energies of 1836.2 ± 1.7 kev and 898.7 ± 0.8 kev are reported for two Sr^{88} gamma rays. Also measurements are given for the relative intensities of the 2.18-Mev, 1.48-Mev, and 0.696-Mev gamma rays of Nd^{144}, the relative intensities of the 1.8-Mev and 0.898-Mev transitions in Sr^{88}, and the relative intensities of the 1.06-Mev and 0.57-Mev transitions in Pb^{207}.

MEAN LIFE OF THE 1.61-Mev LEVEL OF Mg^{25}. V. K. Rasmussen, F. R. Metzger, and C. P. Swann, Bartol Research Foundation of the Franklin Institute, Swarthmore, Pennsylvania (Received April 10, 1961).

Nuclear resonance fluorescence techniques have been used to measure the mean life of the 1.61-Mev level of Mg^{25} and the 1.83-Mev level of Mg^{26}. The exciting γ radiation was obtained by bombarding metallic Mg^{25} and Mg^{26} targets with 4.0- and 4.4-Mev protons. For the Mg^{25} level, assumed to be $7/2^+$, the self-absorption of the resonance radiation gives $\tau = (2.5^{+0.6}_{-0.4}) \times 10^{-14}$ sec. The angular distribution for the reso-

nance scattering was found to be $1+(0.42\pm0.03)\times P_2(\cos\theta)+(0.03\pm0.003)P_4(\cos\theta)$, where the errors given are statistical only. For other reasons it is believed that the correct coefficient of the P_4 term is approximately zero. For the Mg^{26} level, the apparent resonance scattering cross section combined with some previous estimates of slowing-down times for the excited nuclei gives $\tau=(7\pm3)\times10^{-13}$ sec. Further evidence as to the collective nature of these nuclei and of Al^{27} is discussed. Support is given to the suggestion of the Chalk River group that the 1.61-Mev Mg^{25} and the 2.21-Mev Al^{27} levels are the $7/2^+$ second members of $K=5/2^+$ rotational bands based on the ground states. For the Mg^{25} level, a spin and parity assignment of $7/2^+$ is required to obtain agreement between the quadrupole transition probability from these measurements and that found by Coulomb excitation.

TEST OF THE ξ APPROXIMATION IN SOME FIRST-FORBIDDEN $2^-\rightarrow2^+$ β TRANSITIONS. R. M. Steffen, Department of Physics, Purdue University, Lafayette, Indiana (Received April 11, 1961).

The β-γ directional correlations of the first-forbidden nonunique $2^-\rightarrow2^+$ β transitions of K^{42}, Sb^{122}, and Au^{198} were investigated and compared with the predictions of the ξ approximation, whose range of applicability is discussed. Upper limits for the contribution of the tensor-type matrix element $\int B_{ij}$ to the β transitions were estimated on the basis of the modified B_{ij} approximation.

The anisotropy coefficient $A_2(W)$ in the β-γ directional correlation involving the 1.98-Mev β transition of K^{42} varies from $A_2(1.66)=-0.009\pm0.002$ to $A_2(4.60)=-0.049\pm0.002$. The energy dependence of $A_2(W)$ deviates from the predictions of the ξ approximation by about 40% over the measured energy range. A rough estimate of the upper limit for the contribution from the $\int B_{ij}$ component is $|C_A\int B_{ij}|<0.3(|V_0|+|Y_1|)$ (in the notation of Kotani).

The anisotropy factor $A_2(W)$ of the β-γ directional correlation involving the 1.40-Mev β transition of Sb^{122} varies from $A_2(1.96)=+0.035\pm0.003$ to $A_2(3.5)=-0.081\pm0.004$. The energy dependence of $A_2(W)$ is well represented by the factor $\lambda_2(Z,W)\times(W^2-1)/W$ as predicted by the ξ approximation. The upper limit of the $\int B_{ij}$ contribution to this β transition is estimated as $|C_A\int B_{ij}|<0.15|Y_1|$ or $|C_A\int B_{ij}|<0.2|V_0|$.

The anisotropy factor $A_2(W)$ of the Au^{198} β-γ directional correlation involving the 0.96-Mev β transition varies between $A_2(1.39)=+0.0076\pm0.0010$ and $A_2(2.78)=+0.0286\pm0.0010$, and its energy dependence agrees very well with the predictions of the ξ approximation. The upper limit for the $\int B_{ij}$ matrix element is estimated as $|C_A\int B_{ij}|<0.1|Y_1|$.

HIGH-RESOLUTION MEASUREMENTS OF THE $O^{16}(p,\alpha)N^{13}$ EXCITATION FUNCTION. H. A. Hill, E. L. Haase, and D. B. Knudsen, Palmer Physical Laboratory, Princeton University, Princeton, New Jersey (Received April 10, 1961).

The $O^{16}(p,\alpha)N^{13}$ activation cross section was measured from 12 to 18 Mev with an energy resolution of 30 kev. The results are essentially the same as obtained by Whitehead and Foster and Rouse using poorer resolution except for one very narrow resonance. As the proton energy increases through this resonance, the cross section first rises 7% to a maximum, then drops 33% to a minimum, and finally rises 6%. The peak and valley have a width at half maximum of 30 kev and the peak and valley are separated by 60 kev. The proton energy at halfway down the drop was determined using the limp-wire technique to be 14.600 ± 0.020 Mev. This resonance is well suited for calibration purposes. A qualitative interpretation of the results is made using the "cluster model."

$O^{16}(p,\alpha)N^{13}$ ANGULAR DISTRIBUTIONS AT 13.5-18.1 Mev. Donald R. Maxson,* Palmer Physical Laboratory, Princeton University, Princeton, New Jersey (Received April 10, 1961).

Angular distributions of alpha particles from the $O^{16}(p,\alpha)N^{13}$ ground-state reaction were measured with an ionization chamber at 10 bombarding energies from 13.5 to 18.1 Mev. The angular distributions are oscillatory but not of the form predicted by the plane wave pickup or knock-on theories, and the variation with energy is more pronounced than would be expected for a simple direct reaction. The excitation curve has a minimum at $E_p\simeq16.5$ Mev, and the angular distributions are markedly different above and below that energy. The $O^{16}(p,\alpha)N^{13*}$(2.4-Mev) reaction is also strongly energy dependent, and the $O^{16}(p,p)O^{16}$ elastic scattering cross section is

quite energy sensitive at large angles. The energy dependence of the scattering cross section at 125 degrees appears to be correlated with the $O^{16}(p,\alpha)N^{13}$ excitation function.

*Present address: Department of Physics, Brown University, Providence 12, Rhode Island.

EXCITATION FUNCTIONS FOR LITHIUM-6 INDUCED REACTIONS ON ALUMINUM-27. Inge-Maria Ladenbauer,* Ivor L. Preiss, and Carl E. Anderson,† Yale University, New Haven, Connecticut (Received April 5, 1961).

Excitation functions for a number of Li^6-induced reactions on Al^{27} have been studied using stacked-foil techniques and the Li^6 ion beam from the Yale heavy-ion accelerator. Excitation functions corresponding to radioactive residual nuclei P^{32}, P^{30}, Si^{31}, Al^{29}, Al^{28}, Mg^{27}, Na^{24}, and Na^{22} have been measured in the Li^6 range from 1 to 63.3 Mev. The data strongly suggest that the P^{32}, P^{30}, and Si^{31} result from compound-system processes and the Na^{22} and Na^{24} from a predominant direct-knockout process. In the cases of Al^{28} and Al^{29} both compound-system and direct-pickup reaction amplitudes contribute to the reaction yield.

*On leave from the University of Vienna, Analytical Chemical Institute, Vienna, Austria.

† Present address: Applied Physics Laboratory, The Johns Hopkins University, Baltimore, Maryland.

NEUTRONS AND GAMMA RAYS FROM THE BOMBARDMENT OF O^{16} by He^3. K. L. Dunning and J. W. Butler, Nucleonics Division, U. S. Naval Research Laboratory, Washington, D. C. (Received April 11, 1961).

The threshold energy for the $O^{16}(He^3,n)Ne^{18}$ reaction has been measured. The value obtained, 3.811 ± 0.015 Mev, determines the mass of Ne^{18} to be 18.011446 ± 0.000014 amu (O^{16} standard, 1960 mass tables). The slow-fast ratio method for the observation of neutron thresholds was employed at bombarding energies from the ground-state threshold to 5.6 Mev, corresponding to a region of excitation in the residual nucleus from zero to 1.5 Mev. No excited states in Ne^{18} were identified. The bombardment of O^{16} by He^3 also produced the reactions $O^{16}(He^3,p)F^{18}$ and $O^{16}(He^3,\alpha)O^{15}$. Energy spectra were obtained by means of a scintillation spectrometer for gamma rays resulting from certain transitions in F^{18} and O^{15}. For 4.5-Mev He^3 particles impinging on a 1-Mev thick target of TiO_2, gamma rays of the following energies were observed and attributed to F^{18}: 0.652 ± 0.007, 0.939 ± 0.005, 1.041 ± 0.005, 1.17 ± 0.01, 1.61 ± 0.02, 1.68 ± 0.02, 2.09 ± 0.01, 2.51 ± 0.01, 2.65 ± 0.05, 3.06 ± 0.05, 3.35 ± 0.10?, and 3.84 ± 0.10 Mev. The following gamma rays were also observed and attributed to O^{15}: 5.25 ± 0.05, 6.22 ± 0.10, and 6.87 ± 0.10 Mev.

$C^{14}(d,n)N^{15}$ REACTION. Ren Chiba,* University of Wisconsin, Madison, Wisconsin (Received January 25, 1961).

Differential cross sections for ground-state neutrons from the $C^{14}(d,n)N^{15}$ reaction have been measured at $E_d = 3.53$ Mev and 2.786 Mev by a neutron spectrometer. A stripping peak implying $l_p = 1$ is observed. The excitation function of the ground-state neutrons has been measured from $E_d = 1.2$ Mev to $E_d = 3.53$ Mev. A number of resonances were found corresponding to virtual states of N^{16}. The angular distributions of neutrons associated with the 5.28-, 5.31-Mev doublet (unresolved) and 6.33-Mev levels of N^{15} were measured by photographic emulsion technique. A stripping peak characteristic of $l_p = 0$ corresponds to the unresolved doublet, and $l_p = 1$ to the 6.33-Mev state. The excitation function for all neutrons from $C^{14}(d,n)N^{15}$ was measured both by "slow" and by "fast" neutron counters. Several possible slow-neutron thresholds were found corresponding to excited states of N^{15}. The sensitivity of the slow-neutron threshold technique was checked by the $O^{16}(d,n)F^{17}$. Accurate values of these thresholds are reported.

*Present address: Nippon Atomic Industry Group Company, Ltd., Tokyo, Japan.

EVIDENCE FOR AN ISOMERIC STATE OF Y^{90}. W. L. Alford, D. R. Koehler, and C. E. Mandeville,* Army Rocket and Guided Missile Agency, Redstone Arsenal, Alabama (Received April 6, 1961).

The recently reported activity induced by neutron bombardment of niobium has been produced by 14-Mev neutrons and by neutrons of energy less than 6 Mev on both niobium and zirconium. In each case, chemical separation showed the

activity to be due to an isotope of yttrium. Two coincident gamma rays having energies of 0.200 and 0.485 Mev and a half-life of 3.1 ± 0.1 hours were observed; these observations were in agreement with earlier results. The activity appears very similar to that which has been previously attributed to the decay of Y^{92}. However, threshold considerations and the failure to observe by means of a thin-window Geiger counter any beta emission associated with this gamma activity point to an isomeric state of Y^{90}. Experiments with separated isotopes of Zr^{90} and Zr^{92} support this assignment.

*Present address: Physics Department, University of Alabama, University, Alabama.

FISSION OF GOLD WITH 112-Mev C^{12} IONS: A YIELD-MASS AND CHARGE-DISTRIBUTION STUDY. H. Marshall Blann,* Lawrence Radiation Laboratory, University of California, Berkeley, California (Received October 4, 1960; revised manuscript received May 12, 1961).

Fission-product cross sections have been measured radiochemically and mass-spectrometrically for gold bombarded with 112-Mev C^{12} ions. Cross sections for 43 nuclides have been measured for elements from nickel to barium. Thirty-six yields are either primary fission-product yields (independent yields) or have been corrected (with less than 25% correction) so as to represent independent yields. The independent yields have been empirically systematized, and a yield-mass curve has been constructed. The yield-mass curve is compared with the yield-mass curves obtained from the fission of bismuth with 22-Mev and 190-Mev deuterons. The yield systematics indicate that the sum of the mass numbers of complementary fission products is 13 ± 1 amu less than that of the compound nucleus, and the sum of the charges of complementary fission products is two units less than that of the compound nucleus. By thermodynamic arguments it is shown that the loss of charge was carried by an alpha particle, not by protons.

The most probable charge of the fission products as a function of mass number has been determined empirically and compared with theoretical prediction. The charge-dispersion curve (fraction chain yield vs $Z-Z_p$) may be fitted well by the Gaussian $y = \exp[-(Z-Z_p)^2/0.9]/(0.9\pi)^{1/2}$. Experimental yields on both sides of $Z-Z_p = 0$ support the symmetry of the charge-dispersion curve that many workers have assumed.

*Present address: University of Rochester, Rochester, New York.

CONVERSION OF MUONIUM INTO ANTIMUONIUM. G. Feinberg, Columbia University, New York, New York, and S. Weinberg, University of California, Berkeley, California (Received April 3, 1961).

A detailed analysis is made of the possible conversion of muonium into antimuonium in various environments. An assumed $\bar{\mu}e\bar{\mu}e$ weak interaction of the usual form and strength gives a probability of 2.5×10^{-5} in vacuum, even in the presence of reasonable external electric fields. In a solid the probability is less by at least 10, and probably 20, orders of magnitude. In an inert gas the probability is roughly to be divided by the numbers of collisions during a muon lifetime, and hence is quite small unless the pressure at room temperature is less than about 10^{-4} atmosphere. Lowering the temperature does not help. A possible experiment is suggested.

INELASTIC ELECTRON-DEUTERON SCATTERING CROSS SECTIONS AT HIGH ENERGIES. II. FINAL-STATE INTERACTIONS AND RELATIVISTIC CORRECTIONS. Loyal Durand, III, Brookhaven National Laboratory, Upton, New York (Received March 30, 1961; revised manuscript received May 11, 1961).

Measurements of the cross section $d^2\sigma/(d\Omega_e dE_e')$ for the inelastic electron-deuteron scattering process $e+d \rightarrow e+n+p$ have been used to determine the electromagnetic structure of the neutron. The effects on the theoretical cross section of interactions between the outgoing nucleons are examined in detail using the methods of a previous paper. The transition matrix elements connecting the initial state of the two-nucleon system (the deuteron) to a final state with specified total, orbital, and spin angular momenta are calculated using approximate wave functions which are matched to the experimentally determined neutron-proton scattering phase shifts. While individual matrix elements may be drastically changed by the distortion of the final-state wave functions by the neutron-proton interaction, the over-all correc-

tions to the peak value of the cross section are found to be small (-1 to -2%) for electron momentum transfers in the range $q = 3.4 - 2.6$ f^{-1}. The precise magnitude of the corrections is somewhat uncertain because of the approximate nature of the wave functions, but it is unlikely either that they are large, or that the corrections could become positive. The effects of final-state interactions on the cross section $d^2\sigma/(d\Omega_e dE_e')$ are also examined for final electron energies near the upper limit of the inelastic continuum. In this region, the nucleons emerge with low relative momenta, and, in agreement with the predictions of Jankus, the cross section is found to be drastically changed by the strong interactions in the final S states. However, it is shown that the presence in the neutron-proton interaction of a strongly repulsive core results in a considerable diminution of the cross section relative to the predictions of Jankus for large values of q. This lowering of the cross section has been observed by Kendall et al. Results obtained with approximate repulsive core wave functions provide a reasonable fit both to the inelastic cross section near the end point, and to the deuteron electromagnetic form factor obtained from elastic electron-deuteron scattering. Finally, the relativistic theory of inelastic electron-deuteron scattering is examined using the methods of dispersion relations. It is found that in the region of the large peak, the cross section $d^2\sigma/(d\Omega_e dE_e')$ is given essentially correctly by a nonrelativistic calculation using a modified Hamiltonian, provided the results are interpreted correctly with respect to the kinematics. The approximations inherent in the calculation are examined in detail. The resulting cross section differs significantly from the modified Jankus cross section which has been used in the analysis of the high-energy electron-deuteron scattering data obtained by the Stanford group. It is found that the apparent values of the neutron charge form factor F_{1n} are reduced essentially to zero for q^2 in the range 5 f$^{-2} \leq q^2 \leq 20$ f^{-2} when relativistic correction, the effects of the deuteron D-state scattering, and the effects of final-state interactions are taken into account. Corresponding reductions in the value of the neutron anomalous magnetic moment form factor F_{2n} range up to about 30%, and bring F_{2n} into closer agreement with F_{2p}. A complete reanalysis of the experimental data will be necessary.

S-WAVE PION-NUCLEON SCATTERING. Jack L. Uretsky, Physics Department, Purdue University, Lafayette, Indiana (Received November 17, 1960; revised manuscript received May 18, 1961).

The Mandelstam relations for pion-nucleon scattering are used to obtain equations for the s-wave partial wave amplitudes in the two isotopic spin states. The solutions of these equations are investigated in the approximation where only the one-nucleon contributions and the unitarity integral are kept. It is found that there are no solutions of the form N/D without complex zeros, and that this is a consequence of the large size of the one-nucleon terms. A comparison with experiment is made which suggests that the dominant contribution to the $T = 3/2$ s-wave amplitude (other than the one-nucleon contribution) comes from a region of the complex energy plane that is outside the physical region for the related processes (π-π into NN and "crossed" π-N scattering). An Appendix is devoted to discussing the available experimental data and they are found to be consistent with a scattering length (δ/k at threshold) of 0.098 ± 0.004 in the $T = 3/2$ state.

X-RAY DEFICIENCY IN MESONIC ATOMS. Y. Eisenberg, The Weizmann Institute of Science, Rehovoth, Israel, and D. Kessler, Israel Atomic Energy Establishment, Rehovoth, Israel (Received February 23, 1961; revised manuscript received May 9, 1961).

We present an analysis of π-mesonic atoms, based upon cascade calculations taking into account the known processes of radiation, Auger transitions, and nuclear absorption. This analysis, together with the previous one on μ-mesonic atoms, is intended to provide a deeper insight into the unsolved problem of the deficiency of x rays in mesonic atoms. It is shown that the π-mesonic L x-ray yields (for $Z \leq 20$) are quite insensitive to the strength of nuclear absorption and depend only upon the chosen initial meson population of the higher levels. Similarly, the ratios of basic (K_α, L_α, etc.) to higher x-ray yields, both for μ and π mesons, depend strongly on the initial distribution. The best agreement between the calculations and experiment was obtained for a "modified statistical" initial population of the form $(2l+1)e^{al}$, with $a = 0.2$, in the

$n = 14$ level. From the existing experimental data on π-mesonic K x rays, the mean life of the π meson in nuclear matter was deduced: $\tau_c = 2.75 \times 10^{-23}$ sec. Within the framework of the present theory we are still unable to account for the x-ray deficiency in the light atoms. However, it is shown that the quantum loss as a function of energy is different for π- and μ-mesonic atoms, and therefore it is very probably due to a real physical effect. Furthermore, by comparing our predicted Auger electron yields with the experimental data, we can rule out any hypothetical simple Auger process in which the full energy of the "missing" quantum is given to a single electron.

SECONDARY COSMIC-RAY PHOTONS BELOW CASCADE ENERGY. Kinsey A. Anderson, Department of Physics, University of California, Berkeley, California (Received April 7, 1961).

Investigations with small unshielded scintillation crystals carried through the atmosphere by balloons show large fluxes of photons in the energy region 30 to 300 kev in equilibrium with the primary cosmic-ray beam. At 90 g cm^{-2} depth the flux is about 22 photons $cm^{-2}\,sec^{-1}$ compared with a charged particle flux determined from a Geiger tube of 1.9 $cm^{-2}\,sec^{-1}$ at this same depth. The photon flux at zero depth, taken to be the albedo of this secondary cosmic-ray component, has been estimated by extrapolation to be 8 photons $cm^{-2}\,sec^{-1}$ greater than 30 kev.

PHOTOPRODUCTION OF CHARGED π MESONS FROM NUCLEI. W. Melville McClelland,* Laboratory of Nuclear Studies, Cornell University, Ithaca, New York (Received March 6, 1961).

The photoproduction of charged π mesons by a 1000-Mev bremsstrahlung beam has been studied for the elements Be, C, Al, Cu, and Pb. Mesons with energies in the range 100 to 400 Mev emerging from the targets at angles of 58° and 115° were detected, and absolute measurements for the cross section are given. An optical model for the nucleus was employed to predict absolute upper and lower limits for the nuclear cross section, and reasonable agreement with the data was obtained. The measured cross sections had a dependence on the target atomic weight of $A^{3/4}$ and this result lay between the limits predicted by the model. The experimental nuclear π^-/π^+ ratio exhibited the general behavior of this quantity for deuterium, but the model could make no prediction here. The results seem to be consistent with an optical-model treatment of an assumed initial production of mesons throughout the nuclear volume, and no recourse to a surface production mechanism was found to be necessary.

*Present address: Lawrence Radiation Laboratory, University of California, Livermore, California.

ANGULAR DISTRIBUTION OF PROTONS FROM π^--p SCATTERING AT 900 Mev. Bogdan C. Maglić, Bernard T. Feld, and Carol A. Diffey, Physics Department and Laboratory for Nuclear Science, Massachusetts Institute of Technology, Cambridge, Massachusetts (Received April 10, 1961).

The shape of the π^--p differential scattering cross section in the backward hemisphere should be sensitive to the nature of the "resonances" assumed to be responsible for the peaks in the total cross section at 600 and 900 Mev. The angular distribution of protons scattered in the forward hemisphere by pions of kinetic energy around 925 Mev, corresponding to pion c.m. angles from 65 deg to 150 deg, was obtained by placing nuclear emulsions close to liquid hydrogen and by measuring the direction angle and the grain count of every proton track. It is shown that the sensitivity of emulsions in the temperature region $22°K < T < 90°K$ does not drop below 85% of the sensitivity at 300°K. The resulting distribution is consistent with the assignment of $D_{3/2}{}^{1/2}$ and $F_{5/2}{}^{1/2}$, respectively, for the 600- and 900-Mev levels.

FORMATION OF N^{13} IN HIGH-ENERGY NUCLEAR REACTIONS. I. Dostrovsky, The Weizmann Institute of Science, Rehovoth, Israel and Chemistry Department, Brookhaven National Laboratory, Upton, New York, Z. Fraenkel, The Weizmann Institute of Science, Rehovoth, Israel, and J. Hudis, Chemistry Department, Brookhaven National Laboratory, Upton, New York (Received April 10, 1961).

Experimental cross sections are reported for the formation of N^{13} in the bombardment of Zn, In, Pb, and U with protons of 0.9-, 1.9-, and 2.9-

Bev energy. These values are compared with theoretical N^{13} emission cross sections for proton energies of 0.84 and 1.84 Bev. The calculations are based on the evaporation model. The previously described Monte Carlo procedure was modified in order to obtain better statistical accuracy for the calculated N^{13} cross sections. Previously computed emission cross sections for He^6, Li^8, and Be^7 were also recomputed using the modified Monte Carlo procedure. The cross sections were computed for three different formulations of the interaction radius. Good fit with the experimental He^6, Li^8, and Be^7 cross sections is obtained when the smaller values for the interaction radius are used. However, the fit with the experimental N^{13} values is not good enough to exclude processes other than evaporation as contributing to the experimentally observed cross sections.

PRODUCTION OF STRANGE PARTICLES IN p-p COLLISIONS AT 2.85 Bev. R. I. Louttit, T. W. Morris, D. C. Rahm,* R. R. Rau, A. M. Thorndike, and W. J. Willis, Brookhaven National Laboratory, Upton, New York, and R. M. Lea, The City College of New York, New York, New York (Received April 12, 1961).

From a sample of 98 hyperon production events observed in a liquid hydrogen bubble chamber the partial cross sections for various final states are found to be: $\Sigma^+K^+n-0.047$, $\Sigma^+K^0p-0.030$, $\Sigma^0K^+p-0.013$, $\Lambda^0K^+p-0.051$, $\Sigma^-K^+p\pi^+-0.003$, $\Sigma^+KN\pi-0.004$, $(\Lambda^0\Sigma^0)K^+p\pi^0-0.011$, $(\Lambda^0\Sigma^0)K^0p\pi^+-0.014$, $(\Lambda^0\Sigma^0)K^+n\pi^+-0.002$, all in millibarns. For the first four processes the values are in general agreement with those calculated by Ferrari using a one-pion-exchange model. Only one example of K-pair production was observed, indicating a cross section less than 0.01 millibarn.

*Now on leave at Centre d'Etudes Nucléaires de Saclay, Saclay, France.

EVOLUTION OF A QUASI-STATIONARY STATE. Rolf G. Winter, Department of Physics, The Pennsylvania State University, University Park, Pennsylvania (Received April 10, 1961).

To elucidate the time development of quasi-stationary states, a simple barrier penetration problem has been studied. Both approximate expressions and numerical results for some parameters were obtained for the decay rate. First, irregular oscillations occur for a short time. Second, the exponential region follows. Third, further oscillations occur during which the decay rate dips to negative values, so that the probability of finding the undecayed system increases briefly at several times. Fourth and finally, the decay rate decreases like an inverse power of the time.

DYNAMICAL THEORY FOR STRONG INTERACTIONS AT LOW MOMENTUM TRANSFERS BUT ARBITRARY ENERGIES. Geoffrey F. Chew and Steven C. Frautschi, Lawrence Radiation Laboratory and Department of Physics, University of California, Berkeley, California (Received March 30, 1961).

Starting from the Mandelstam representation, it is argued on physical grounds that "strips" along the boundaries of the double spectral regions are likely to control the physical elastic scattering amplitude for arbitrarily high energies at small momentum transfers. Pion-pion scattering is used as an illustration to show how the double spectral functions in the nearest strip regions may be calculated, and an attempt is made to formulate an approximate but "complete" set of dynamical equations. The asymptotic behavior of the solutions of these equations is discussed, and it is shown that if the total cross section is to approach a constant at large energies then at low energy the S-dominant $\pi\pi$ solution is inadmissible. A principle of "maximum strength" for strong interactions is proposed, and it is argued that such a principle will allow large low-energy phase shifts only for $l \leq l_{max}$, where $l_{max} \sim 1$.

THEORY OF π-N SCATTERING IN THE STRIP APPROXIMATION TO THE MANDELSTAM REPRESENTATION. Virendra Singh* and B. M. Udgaonkar,† Lawrence Radiation Laboratory, University of California, Berkeley, California (Received April 7, 1961).

The strip approximation to the Mandelstam representation is applied to the π-N problem, and the basic equations given. The asymptotic behavior of the invariant amplitudes in the physical regions is discussed in terms of the unitarity

condition on partial-wave amplitudes, the constancy of high-energy scattering cross sections, and the Pomeranchuk theorem, and it is shown to imply that no subtractions should be necessary except in the $J = 1/2$ wave of the π-N channel and the $J = 0$ wave of the $\pi + \pi \rightarrow N + \bar{N}$ channel. This obviates the difficulties encountered by earlier workers when they subtracted higher waves.

*On deputation from Tata Institute of Fundamental Research, Bombay, India.

†On deputation from Atomic Energy Establishment, Trombay, India.

THEORY OF STRONG-INTERACTION SYMMETRY. Murray Gell-Mann, California Institute of Technology, Pasadena, California (Received March 27, 1961).

We attempt once more, as in the global symmetry scheme, to treat the eight known baryons as a supermultiplet, degenerate in the limit of a certain symmetry but split into isotopic spin multiplets by a symmetry-breaking term. Here we do not try to describe the symmetry violation in detail, but we ascribe it phenomenologically to the mass differences themselves, supposing that there is some analogy to the μ-e mass difference. The symmetry is called unitary symmetry and corresponds to the "unitary group" in three dimensions in the same way that charge independence corresponds to the "unitary group" in two dimensions. The eight infinitesimal generators of the group form a simple Lie algebra, just like the three components of isotopic spin. In this important sense, unitary symmetry is the simplest generalization of charge independence. The baryons then correspond naturally to an eight-dimensional irreducible representation of the group; when the mass differences are turned on, the familiar multiplets appear. The pion and K meson fit into a similar set of eight particles, along with a predicted pseudoscalar meson χ^0 having $I = 0$. The pattern of Yukawa couplings of π, K, and χ is then nearly determined, in the limit of unitary symmetry.

The most attractive feature of the scheme is that it permits the description of eight vector mesons by a unified theory of the Yang-Mills type (with a mass term). Like Sakurai, we have a triplet ρ of vector mesons coupled to the isotopic spin current and a singlet vector meson ω^0 coupled to the hypercharge current. We also have a pair of doublets M and $\bar{M}$, strange vector mesons coupled to strangeness-changing currents that are conserved when the mass differences are turned off. There is only one coupling constant, in the symmetric limit, for the system of eight vector mesons. There is some experimental evidence for the existence of ω^0 and M, while ρ is presumably the famous $I = 1$, $J = 1$, π-π resonance.

A ninth vector meson coupled to the baryon current can be accommodated naturally in the scheme.

The most important prediction is the qualitative one that the eight baryons should all have the same spin and parity and that the pseudoscalar and vector mesons should form "octets," with possible additional "singlets."

If the symmetry is not too badly broken in the case of the renormalized coupling constants of the eight vector mesons, then numerous detailed predictions can be made of experimental results.

The mathematics of the unitary group is described by considering three fictitious "leptons," ν, e^-, and μ^-, which may or may not have something to do with real leptons. If there is a connection, then it may throw light on the structure of the weak interactions.

HYPERVIRIAL THEOREMS FOR VARIATIONAL WAVE FUNCTIONS. Saul T. Epstein, Department of Physics, University of Nebraska, Lincoln, Nebraska, and Joseph O. Hirschfelder, Theoretical Chemistry, University of Wisconsin, Madison, Wisconsin (Received March 24, 1961).

It is shown that a sufficient condition for an optimal energy variational wave function ψ_0 to satisfy the hypervirial relation $(\psi_0, [H, W]\psi_0) = 0$ is for the trial function ψ to admit variations of the form $\partial\psi/\partial a = (i/\hbar)W\psi$. Here H is the Hamiltonian, W is a Hermitian operator, and a is a variational parameter. Explicit forms of such trial functions are exhibited for several W's. The case in which W generates a point transformation of the coordinates is discussed in detail. Conditions are given for the existence of simultaneous hypervirial theorems.

FURTHER CONSIDERATIONS ON ELECTROMAGNETIC POTENTIALS IN THE QUANTUM THEORY. Y. Aharonov, Department of Physics, Brandeis University, Waltham, Massachusetts, and D. Bohm, H. H. Wills Physics Laboratory, Univer-

sity of Bristol, Bristol, England (Received April 6, 1961).

In this article we discuss in further detail the significance of potentials in the quantum theory, and in so doing, we answer a number of arguments that have been raised against the conclusions of our first paper on the same subject. We then proceed to extend our treatment to include the sources of potentials quantum mechanically, and we show that when this is done, the same results are obtained as those of our first paper, in which the potential was taken to be a specified function of space and time. In this way, we not only answer certain additional criticisms that have been made of the original treatment, but we also bring out more clearly the importance of the potential in the expression of the local character of the interaction of charged particles and the electromagnetic field.

TRANSFER OF HELICITY IN RADIATION AND ABSORPTION OF HIGH-ENERGY PHOTONS. R. H. Pratt, Institute of Theoretical Physics, Department of Physics, Stanford University, Stanford, California (Received April 7, 1961).

Nearly complete transfer of momentum between a high-energy electron (or positron) and a photon in a Coulomb field implies that helicity is also transferred. This is not a consequence of conservation of total angular momentum but, rather, of spin angular momentum, and follows from a demonstration that it is possible to use free-particle spinors (though not free wave functions) for the high-energy particles. Polarization correlations of the lower energy particle in such a process are discussed. Applications are made to bremsstrahlung, pair production, photoeffect, and one-photon pair annihilation.

ANNOUNCEMENTS

Supplement

Beginning with the issue of July 1, the "Abstracts of Articles to be published in The Physical Review" will be printed as a loose insert. This will make bound volumes of Physical Review Letters about 150 pages thinner.

Five-Year Index

A useful five-year cumulative AUTHOR INDEX of THE PHYSICAL REVIEW and PHYSICAL REVIEW LETTERS has been prepared and will be available for distribution after July 1. The price to members of the American Physical Society will be $2; to nonmembers $3. Orders for copies should be sent to The American Institute of Physics, 335 East 45 Street, New York 17, New York. A convenient order form will be enclosed with the July 1 issue of Physical Review Letters.

AUTHOR INDEX TO VOLUME 6

References with (E) are to Errata

ADAIR, R. K. (see Martin, H. J.) 283
AGARWAL, S. P. (see Pomerantz, M. A.) 362
ALBERT, RICHARD D. and LUISA F. HANSEN. 10-Mev proton reaction cross sections for Cu^{63} and Cu^{65} 13
ALERS, G. A. and D. L. WALDORF. Variation of the elastic moduli at the superconducting transition 677
ALFORD, W. P. and J. B. FRENCH. Isotopic spin admixtures in $Ge^{66} \rightarrow Ga^{66} \rightarrow Zn^{66}$ β transitions 119
ALLEN, M. A. and G. S. KINO. Interaction of an electron beam with a fully ionized plasma 163
ALPERIN, HARVEY A. Aspherical $3d$ electron distribution in Ni^{++} 55
ALSTON, MARGARET H., LUIS W. ALVAREZ, PHILIPPE EBERHARD, MYRON L. GOOD, WILLIAM GRAZIANO, HAROLD K. TICHO, and STANLEY G. WOJCICKI. Resonance in the K-π system 300
———, LUIS W. ALVAREZ, PHILIPPE EBERHARD, MYRON L. GOOD, WILLIAM GRAZIANO, HAROLD K. TICHO, and STANLEY G. WOJCICKI. Study of resonances of the Σ-π system 698
ALVÄGER, TORSTEN (see Ryde, Hans) 475
ALVAREZ, LUIS W. (see Alston, Margaret H.) 300; 698
AMBLER, E. (see Hoppes, D. D.) 115
AMELINCKX, S. (see Ruedl, E.) 530
ANDERSON, A. C., G. L. SALINGER, W. A. STEYERT, and J. C. WHEATLEY. Specific heat and thermal boundary resistance of liquid He^3 331
———, G. L. SALINGER, and J. C. WHEATLEY. Thermal conductivity of liquid He^3 443
ANDERSON, JERRY A., VO X. BANG, PHILIP G. BURKE, D. DUANE CARMONY, and NORBERT SCHMITZ. Experimental results on the π-π cross section 365
ARP, V. D., R. H. KROPSCHOT, J. H. WILSON, W. F. LOVE, and R. PHELAN. Superconductivity of Nb_3Sn in pulsed fields of 185 kilogauss 452
AUFFRAY, J. P. Deuteron electric quadrupole moment 120
BACKENSTOSS, G., B. D. HYAMS, G. KNOP, P. C. MARIN, and U. STIERLIN. Helicity of μ^- mesons from π-meson decay 415
BALL, JAMES S. and DAVID Y. WONG. $N\bar{N} \rightarrow \pi\pi$ amplitude and the electromagnetic structure of the nucleon 29
BALTAY, C. (see Stonehill, D.) 624
BANG, VO X. (see Anderson, Jerry A.) 365
BARDEEN, J. Tunnelling from a many-particle point of view 57
BARISH, BARRY C., RICHARD J. KURZ, PAUL G. McMANIGAL, VICTOR PEREZ-MENDEZ, and JULIUS SOLOMON. Pion production by negative pions 297
BARNES, R. G., W. H. JONES, JR., and T. P. GRAHAM. Large anisotropic Knight shifts in intermetallic compounds 221; 506(E)
BARNES, W. S., D. W. MARTIN, and E. W. McDANIEL. Mass spectrographic identification of the ion observed in hydrogen mobility experiments 110
BARNETT, C. F., J. L. DUNLAP, R. S. EDWARDS, G. R. HASTE, H. POSTMA, J. A. RAY, R. G. REINHARDT, W. J. SCHILL, R. M. WARNER, and E. R. WELLS. Lifetimes of fast ions in the plasma of DCX 589
BARSHAY, S. and H. PENDLETON, III. π-Λ resonance and the sigma hyperon 421
BARTKE, J., R. BÖCK, R. BUDDE, W. A. COOPER, H. FILTHUTH, Y. GOLDSCHMIDT-CLERMONT, F. GRARD, G. R. MacLEOD, A. MINGUZZI-RANZI, L. MONTANET, W. G. MOORHEAD, D. R. O. MORRISON, S. NILSSON, C. PEYROU, B. W. POWELL, J. TREMBLEY, D. WISKOTT, I. BERTANZA, C. FRANZINETTI, I. MANELLI, V. SILVESTRINI, G. BRAUTTI, M. CESCHIA, and L. CHERVOSANI. Charged hyperon production by 16-Gev/c π^- mesons 303
BASTIEN, PIERRE, MASSIMILIANO FERRO-LUZZI, and ARTHUR H.

ROSENFELD. Sigma decay modes of pion-hyperon resonances 702
—— (see Berge, J. P.) 557
BAUMINGER, R., S. G. COHEN, A. MARINOV, and S. OFER. Hyperfine interactions in the ground state and first excited state of Dy^{161} in dysprosium iron garnet 467
BEARDEN, A. J., F. L. RIBE, G. A. SAWYER, and T. F. STRATTON. X-ray continua and line spectra from highly stripped atoms in a magnetically compressed plasma 257
BÉG, MIRZA A. BAQI and PAUL C. De CELLES. K-π resonance and lifetime of the K' particle 145; 428(E)
BELL, WILLIAM E. and ARNOLD L. BLOOM. Observation of forbidden resonances in optically driven spin systems 623
—— and ARNOLD L. BLOOM. Optically driven spin precession 280
BELLEMANS, A. and M. De LEENER. Ground-state energy of an electron gas in a lattice of positive point charges 603
BENDT, P. J. and T. A. OLIPHANT. Hydrodynamics of helium II in annular geometry 213
BENNETT, W. R., JR. (see Javan, A.) 106
BERGE, J. P., P. BASTIEN, O. DAHL, M. FERRO-LUZZI, J. KIRZ, D. H. MILLER, J. J. MURRAY, A. H. ROSENFELD, R. D. TRIPP, and M. B. WATSON. Pion-lambda resonance (Y_1^*) 557
BERGIA, S., A. STANGHELLINI, S. FUBINI, and C. VILLI. Electromagnetic form factors of the nucleon and pion-pion interaction 367
BERGSTRÖM, J., S. HOLMBERG, and B. LEHNERT. Experiments on the energy balance and confinement of a magnetized plasma 525
BERKELMAN, K., G. CORTELLESSA, and A. REALE. Search for the ω^0 in photoproduction 234
BERLINCOURT, T. G., R. R. HAKE, and D. H. LESLIE. Superconductivity at high magnetic fields and current densities in some Nb-Zr alloys 671
—— (see Thorsen, A. C.) 617
BERNARD, W. (see Neuringer, L. J.) 455
BERNSTEIN, JEREMY and REINHARD OEHME. Consequences of a scalar $\Sigma\Lambda\pi$ coupling 639
BERTANZA, I. (see Bartke, J.) 303
BETTERTON, J. O., JR., R. W. BOOM, G. D. KNEIP, R. E. WORSHAM, and C. E. ROOS. Superconductivity of Nb_3Sn in a pulsed magnetic field 532
BHAVSAR, P. D. (see Winckler, J. R.) 488
BIR, G. L. (see Pikus, G. E.) 103
BIRGE, ROBERT W. (see Fowler, William B.) 134
BLAMONT, J. E., T. M. DONAHUE, and M. L. LORY. Measurement of the temperature in the upper atmosphere to 150 km in a rocket experiment 403
BLATT, J. M. (see Derrick, G.) 69
BLOCH, B. L. (see Maier, E. J.) 417
BLOOM, ARNOLD L. (see Bell, William E.) 280; 623
BÖCK, R. (see Bartke, J.) 303
BOLLINGER, L. M. (see Coté, R. E.) 695
—— (see Jackson, H. E.) 187
BONNAL, JEAN-FRANÇOIS, GEORGES BRIFFOD, and CLAUDE MANUS. Enhanced diffusion and oscillations in weakly ionized plasmas 665
BOOM, R. W. (see Betterton, J. O., Jr.) 532
BRADFORD, E. and B. A. ROBSON. Inelastic scattering of 18.9-Mev nucleons from the 9.6-Mev state of C^{12} 550; 711(E)
BRANSDEN, B. H. and J. W. MOFFAT. Coupled S- and P-wave solutions for pion-pion scattering 708
BRAUTTI, G. (see Bartke, J.) 303
BRAY, P. J. (see Kim, Y. W.) 4
BREIT, G., K. E. LASSILA, H. M. RUPPEL, and M. H. HULL, JR. Two-pion exchange interaction 138
BRIFFOD, GEORGES (see Bonnal, Jean-François) 665
BUDDE, R. (see Bartke, J.) 303
BUDINI, PAOLO and LUCIANO FONDA. Pion-pion interaction from threshold anomalies in K^+ decay 419
BUEHLER, E. (see Kunzler, J. E.) 89
BURGER, JEAN-PAUL and MICHAEL ALAN TAYLOR. Anomalies in the magnetic susceptibility and electrical resistivity of vanadium 185
BURGESS, J. H. (see Rhodes, R. S.) 462
BURKE, PHILIP G. (see Anderson, Jerry A.) 365
BURSTEIN, E., D. N. LANGENBERG, and B. N. TAYLOR. Superconductors as quantum detectors for microwave

and sub-millimeter-wave radiation 92
—— (see Stiles, P. J.) 667

CAPPS, RICHARD H. K^- absorption and the $K\Sigma N$ parity 375
CARMICHAEL, H., J. F. STELJES, D. C. ROSE, and B. G. WILSON. Cosmic-ray neutron increase from a flare on the far side of the sun 49
CARMONY, D. DUANE (see Anderson, Jerry A.) 365
CARRUTHERS, P. Pion-nucleon interaction in the region of the higher resonances 567
CASAL, F. G. (see Vette, J. I.) 334
CASPARI, M. E., S. FRANKEL, D. RAY, and G. T. WOOD. Direction of internal magnetic fields in rare earth ions 345
CASTLE, J. G., JR., B. S. CHANDRASEKHAR, and J. A. RAYNE. Cyclotron resonance in indium 409
—— (see McAvoy, B. R.) 618
CESCHIA, M. (see Bartke, J.) 303
CHAMBERS, R. H. and J. SCHULTZ. Dislocation relaxation spectra of cold-worked body-centered cubic transition metals 273
CHAN, CHIA-HWA. Spin of the K' 383
CHANDRASEKHAR, B. S. and J. A. RAYNE. Limiting value of Debye temperature for superconducting and normal indium from low-temperature elastic constants 3
—— (see Castle, J. G., Jr.) 409
CHANG, F. C. Formation of alpha clusters in even-even nuclei 414
CHARPAK, G., F. J. M. FARLEY, R. L. GARWIN, T. MULLER, J. C. SENS, V. L. TELEGDI, and A. ZICHICHI. Measurement of the anomalous magnetic moment of the muon 128
CHERVOSANI, L. (see Bartke, J.) 303
CHINOWSKY, W. (see Martin, H. J.) 283
CLARK, G. (see Hersil, J.) 22
COCCONI, G., A. N. DIDDENS, E. LILLETHUN, and A. M. WETHERELL. Elastic and quasi-elastic collisions of protons with momenta between 9 and 25 Gev/c 231
COHEN, S. G. (see Bauminger, R.) 467
COLEMAN, SIDNEY and SHELDON LEE GLASHOW. Electrodynamic properties of baryons in the unitary symmetry scheme 423
CONNOLLY, P. L., J. G. McEWEN, and J. OREAR. Elastic scattering of muons in nuclear emulsion 554
COOPER, LEON N. Superconductivity in the neighborhood of metallic contacts 689
COOPER, W. A. (see Bartke, J.) 303
CORENZWIT, E. (see Geballe, T. H.) 275
CORTELLESSA, G. (see Berkelman, K.) 234
COTÉ, R. E. and L. M. BOLLINGER. Interference in the radiative capture of neutrons 695
—— (see Jackson, H. E.) 187
COURANT, H. (see Stonehill, D.) 624
COVINGTON, ARTHUR E. and GLADYS A. HARVEY. 10.7-cm solar noise burst of November 20, 1960 51
CRANSHAW, T. E. (see Johnson, C. E.) 450
CRAWFORD, F. W. Electrostatic sound wave modes in a plasma 663
CUFF, K. F. (see Kuglin, C. D.) 177
CUMMING, J. B., A. M. POSKANZER, and J. HUDIS. Loss of C^{11} from plastic foils and its effect on cross-section measurements 484; 646(E)

DAHL, ORIN I., NAHMIN HORWITZ, DONALD H. MILLER, JOSEPH J. MURRAY, and PAUL G. WHITE. Influence of the $\Lambda\pi$ resonance on correlations in the reaction $K^- + d \to \Lambda + \pi^- + p$ 142
—— (see Berge, J. P.) 557
DALITZ, R. H. $\bar{K}$-nucleon bound-state interpretation of the 1385-Mev π-Λ resonance 239
—— and DONALD H. MILLER. Bose statistics and Y^* production and decay in K^--p collisions 562
DANIELIAN, A. Ground state of an Ising face-centered cubic lattice 670
DAUENBAUGH, C. E. (see Palmer, D. R.) 170
DAUNT, J. G. and J. L. OLSEN. Compressibility, zero-point energy, and specific heat in superconductors 267
DAVIS, D. H., R. D. HILL, B. D. JONES, B. SANJEEVAIAH, J. ZAKRZEWSKI, and J. P. LAGNAUX. Elastic scattering of low-energy K^- mesons on protons 132

DAVIS, L. R., C. E. FICHTEL, D. E. GUSS, and K. W. OGILVIE. Rocket observations of solar protons on September 3, 1960 492
DAY, GENE F. (see La Force, Richard Conley) 226
DAZEY, M. H. (see Josephson, Vernal) 33(E)
DeBENEDETTI, S., G. LANG, and R. INGALLS. Electric quadrupole splitting and the nuclear volume effect in the ions of Fe^{57} 60
De CELLES, PAUL C. (see Bég, Mirza A. Baqi) 145; 428(E)
DELAVIGNETTE, P. (see Ruedl, E.) 530
De LEENER, M. (see Bellemans, A.) 603
DERR, V. E., J. J. GALLAGHER, R. E. JOHNSON, and A. P. SHEPPARD. Microwave emission from an optically pumped atomic system 572(E)
DERRICK, G., D. MUSTARD, and J. M. BLATT. Binding energy of the triton 69
DESAI, BIPIN R. Low-energy pion-pion S-wave phase shifts 497
De TOLLIS, B. and A. VERGANELAKIS. Pion-pion interaction in the photoproduction of neutral pions with polarized γ rays 371
DEVLIN, G. E. (see Schawlow, A. L.) 96
DEVLIN, THOMAS J. (see Wood, Calvin D.) 481
de VRIES, C. (see Hofstadter, R.) 290
DIDDENS, A. N. (see Cocconi, G.) 231
DOMBEY, NORMAN. Intermediate boson production in pion-proton collisions 66
DONAHUE, T. M. (see Blamont, J. E.) 403
DOUGLASS, D. H., JR. Magnetic field dependence of the superconducting energy gap 346
DOYLE, W. T. and W. L. WILLIAMS. Resolved isotropic hyperfine structure of the electron paramagnetic resonance absorption of F centers in NaH 537
DUGGAL, S. P. (see Pomerantz, M. A.) 123
DUNGEY, J. W. Interplanetary magnetic field and the auroral zones 47
DUNLAP, J. L. (see Barnett, C. F.) 589
DURAND, LOYAL, III. Inelastic electron-deuteron scattering and the electromagnetic structure of the neutron 631

EARL, JAMES A. Cloud-chamber observations of primary cosmic-ray electrons 125
EBERHARD, PHILIPPE (see Alston, Margaret H.) 300; 698
——— (see Fowler, William B.) 134
EDELSTEIN, A. S. (see Rhodes, R. S.) 462
EDELSTEIN, R. M. (see Maier, E. J.) 417
EDWARDS, H. H. (see Sherrill, M. D.) 460
EDWARDS, R. S. (see Barnett, C. F.) 589
ELLETT, M. R. (see Kuglin, C. D.) 177
ELLIOTT, R. O. (see Gschneidner, K. A., Jr.) 218
ELY, ROBERT (see Fowler, William B.) 134
ERWIN, A. R., R. MARCH, W. D. WALKER, and E. WEST. Evidence for a π-π resonance in the $I=1$, $J=1$ state 628
ESCOBAR, I. (see Hersil, J.) 22

FAIRBANK, HENRY A. (see Strongin, Myron) 404
——— (see Vignos, James H.) 265; 646(E)
FARLEY, F. J. M. (see Charpak, G.) 128
FAWCETT, E. Fermi surface topology of even-valent metals from their magnetoresistance anisotropy 534
FEINBERG, G. and S. WEINBERG. Law of conservation of muons 381
FELDMAN, D. W. (see McAvoy, B. R.) 618
FELDMAN, G. (see Wali, K. C.) 644
FERRELL, RICHARD A. Anomalous lattice specific heat of superconductors 541
FERRO-LUZZI, MASSIMILIANO (see Bastien, Pierre) 702
——— (see Berge, J. P.) 557
FESHBACH, H., E. LOMON, and A. TUBIS. Proton-proton interaction 635
FICHTEL, C. E. and D. E. GUSS. Heavy nuclei in solar cosmic rays 495
——— (see Davis, L. R.) 492
FICKINGER, W. (see Stonehill, D.) 624
FILTHUTH, H. (see Bartke, J.) 303
FILZ, ROBERT (see Yagoda, Herman) 626
FOLEN, V. J., G. T. RADO, and E. E. STALDER. Anisotropy of the magnetoelectric effect in Cr_2O_3 607
FONDA, LUCIANO (see Budini, Paolo) 419
FORMAN, R. Electrical conduction and breakdown in high-pressure rare gases 594
FOWLER, E. C. (see Stonehill, D.) 624
FOWLER, WILLIAM B., ROBERT W. BIRGE, PHILIPPE EBERHARD, ROBERT ELY, MYRON L. GOOD, WILSON M. POWELL, and HAROLD K. TICHO. Ξ^- production by K^- mesons 134

FRANKEL, S. (see Caspari, M. E.) 345
FRANZINETTI, C. (see Bartke, J.) 303
FRANZINI, PAOLO and JACK STEINBERGER. Leptonic decay of a Σ^- hyperon 281
FREEMAN, A. J. and R. E. WATSON. Origin of the F^{19} hyperfine structure in transition element fluorides 343
——— (see Watson, R. E.) 277; 388(E)
FRENCH, J. B. (see Alford, W. P.) 119
FUBINI, S. (see Bergia, S.) 367
FUKUI, KATSURA (see Filz, Robert) 626
FULTON, T. (see Wali, K. C.) 644

GALLAGHER, J. J. (see Derr, V. E.) 572(E)
GALLET, R. M. and W. F. UTLAUT. Evidence on the laminar nature of the exosphere obtained by means of guided high-frequency wave propagation 591
GALT, J. K., F. R. MERRITT, and P. H. SCHMIDT. Cyclotron resonance observations in cadmium 458
GARWIN, R. L. (see Charpak, G.) 128
GATTI, G., P. HILLMAN, W. C. MIDDELKOOP, T. YAMAGATA, and E. ZAVATTINI. Inverse photoproduction reaction $\pi^- + p \rightarrow \gamma + n$ in flight 706
GEBALLE, T. H., B. T. MATTHIAS, G. W. HULL, JR., and E. CORENZWIT. Absence of an isotope effect in superconducting ruthenium 275
GELL-MANN, MURRAY. The reaction $\gamma + \gamma \rightarrow \nu + \bar{\nu}$ 70
GERHOLM, T. R. (see Pettersson, B. -G.) 14
GHIORSO, ALBERT, TORBJØRN SIKKELAND, ALMON E. LARSH, and ROBERT M. LATIMER. New element, lawrencium, atomic number 103 473
GLASHOW, SHELDON LEE. Direct Ξ decay and muonium-antimuonium transitions 196
——— (see Coleman, Sidney) 423
GOLDSCHMIDT-CLERMONT, Y. (see Bartke, J.) 303
GOOD, MYRON L. (see Alston, Margaret H.) 300; 698
——— (see Fowler, William B.) 134
GOODMAN, B. B. Simple model for the magnetic behavior of superconductors of negative surface energy 597
GORDON, E. I. (see LeCraw, R. C.) 620
GRAHAM, T. P. (see Barnes, R. G.) 221; 506(E)
GRANATO, A. V. and T. G. NILAN. Stored energy release below 80°K in deuteron-irradiated copper 171
GRARD, F. (see Bartke, J.) 303
GRAZIANO, WILLIAM (see Alston, Margaret H.) 300; 698
GREENBERGER, DANIEL M. and B. MARGOLIS. Two-parameter approximation to S-wave scattering 310; 428(E)
GSCHNEIDNER, K. A., JR., R. R. McDONALD, and R. O. ELLIOTT. Influence of spin on electronic transformations 218
GUSS, D. E. (see Davis, L. R.) 492
——— (see Fichtel, C. E.) 495
GUTOWSKY, H. S., I. J. LAWRENSON, and K. SHIMOMURA. Nuclear magnetic spin-lattice relaxation by spin-rotational interactions 349

HAAS, F. A. (see Vaughan-Williams, R. W.) 165
HAERING, R. R. and P. B. MILLER. Oscillations in the longitudinal tunnel current of tunnel diodes 269
HAKE, R. R. (see Berlincourt, T. G.) 671
HALL, D. J. Electromagnetic meson mass differences 31
HAND, L. and C. SCHAERF. Pion photoproduction at backward angles near the second nucleon-pion resonance 229
HANSEN, LUISA F. (see Albert, Richard D.) 13
HANSEN, RICHARD T. Cosmic-ray flare of November 20, 1960 260
HANSON, H. (see Pomerantz, M. A.) 362
HARA, OSAMU. Possible effect of collective correlation between vacuum nucleons in pion physics 425
HARTWICK, T. S., E. R. PERESSINI, and M. T. WEISS. Suppression of subsidiary absorption in ferrites by modulation techniques 176
HARVEY, GLADYS A. (see Covington, Arthur E.) 51
HASTE, G. R. (see Barnett, C. F.) 589
HATCH, ALBERT J. High-frequency potential well for dense plasmas 53
HAYWARD, R. W. (see Hoppes, D. D.) 115
HELLAND, JEROME A. (see Wood, Calvin D.) 481
HELLWARTH, R. W. Theory of the pulsa-

tion of fluorescent light from ruby 9
HERMAN, ROBERT (see Hofstadter, Robert) 290; 293
HERRIOTT, D. R. (see Javan, A.) 106
HERSIL, J., I. ESCOBAR, D. SCOTT, G. CLARK, and S. OLBERT. Observations of extensive air showers near the maximum of their longitudinal development 22
HILL, R. D. (see Davis, D. H.) 132
HILLMAN, P. (see Gatti, G.) 706
HINDS, S., R. MIDDLETON, A. E. LITHERLAND, and D. J. PULLEN. New isotope of carbon: C^{16} 113
HINNOV, E. (see Kuckes, A. F.) 337
HIRSCHBERG, J. G. (see Kuckes, A. F.) 337
HODGSON, P. E. Radii of optical-model potentials in proton scattering at 183 Mev 358
HOFSTADTER, ROBERT, C. de VRIES, and ROBERT HERMAN. Dirac and Pauli form factors of the neutron 290
—— and ROBERT HERMAN. Electric and magnetic structure of the proton and neutron 293
HOLMBERG, S. (see Bergström, J.) 525
HOPPES, D. D., E. AMBLER, R. W. HAYWARD, and R. S. KAESER. Matrix elements in the forbidden beta decay of Ce^{141} 115
HORWITZ, NAHMIN (see Dahl, Orin I.) 142
HSU, F. S. L. (see Kunzler, J. E.) 89
HUDIS, J. (see Cumming, J. B.) 484; 646(E)
HUGHES, V. W. (see Prepost, R.) 19
HULL, G. W., JR. (see Geballe, T. H.) 275
HULL, M. H., JR. (see Breit, G.) 138
HUMMER, D. G. and M. J. SEATON. Excitation of H 2 s by electron impact 471
HUMPHREY, WILLIAM E., J. KIRZ, ARTHUR H. ROSENFELD, J. LEITNER, and Y. I. RHEE. Evidence for low rates for β decay of Σ^- and Λ hyperons 478
HYAMS, B. D. (see Backenstoss, G.) 415

ILAKOVAC, K., L. G. KUO, M. PETRAVIĆ, I. ŠLAUS, and P. TOMAŠ. Proton spectra from $D(n,p)2n$ reaction at 14.4 Mev 356
INGALLS, R. (see DeBenedetti, S.) 60

JACCARINO, V. (see Walker, L. R.) 98
JACKSON, H. E., L. M. BOLLINGER, and R. E. COTÉ. Capture of slow neutrons by nuclei bound in crystals 187
JACOBSOHN, B. A. and R. M. RYNDIN. Test for K^--hyperon relative parity 27
JAVAN, A., W. R. BENNETT, JR., and D. R. HERRIOTT. Population inversion and continuous optical maser oscillation in a gas discharge containing a He-Ne mixture 106
JOHNSON, C. E., M. S. RIDOUT, T. E. CRANSHAW, and P. E. MADSEN. Hyperfine field and atomic moment of iron in ferromagnetic alloys 450
JOHNSON, R. E. (see Derr, V. E.) 572(E)
JONES, B. D. (see Davis, D. H.) 132
JONES, W. H., JR. (see Barnes, R. G.) 221; 506(E)
JOSEPHSON, VERNAL, M. H. DAZEY, and R. F. WUERKER. Instability mechanisms in transverse pinches 33(E)
JOSHI, G. H. Energy conversion mechanism in a bounded magnetized current-carrying plasma 339

KAESER, R. S. (see Hoppes, D. D.) 115
KAHALAS, S. L. and R. K. NESBET. Quadrupole moment of Li^7 and quadrupole coupling constant of Li_2 549
KAISER, W., S. SUGANO, and D. L. WOOD. Splitting of the emission lines of ruby by an external electric field 605
KAMINOW, I. P. Microwave modulation of the electro-optic effect in KH_2PO_4 528
KANE, WALTER M. (see Spratt, James P.) 341
KAPLAN, MORTON and D. A. SHIRLEY. Nuclear orientation of paramagnetic impurity ions 361
KAPLAN, R. (see Kim, Y. W.) 4
KASUYA, T. and R. C. LeCRAW. Relaxation mechanisms in ferromagnetic resonance 223
KATUL, J. and A. B. ZAHLAN. Evidence for the existence of surface excitons in tetracene microcrystals 101
KAZES, E. Consequence of the crossing symmetry for a class of π-π scattering diagrams 374
KHALATNIKOV, I. M., E. M. LIFSHITZ, and V. V. SUDAKOV. Singularities of the cosmological solutions of gravitational equations 311
KIM, Y. S. Dispersion relations for produc-

tion amplitudes 313
KIM, Y. W., R. KAPLAN, and P. J. BRAY. Resolved hyperfine spectra of electron-spin paramagnetic resonance in irradiated LiF 4
KING, R. C., R. E. LANOU, JR., and S. F. TUAN. Low-energy $\bar{K}$-nucleon interaction 500
KINO, G. S. (see Allen, M. A.) 163
KIRZ, J. (see Berge, J. P.) 557
——— (see Humphrey, William E.) 479
KITTEL, C. Phonon masers and the phonon bottleneck 449
KLAUDER, J. R. and J. E. KUNZLER. Transverse-even voltage: A high-field galvanomagnetic effect associated with open orbits in metals 179
KNECHTLI, R. C. and J. Y. WADA. Generation and measurement of highly ionized quiescent plasmas in steady state 215
KNEIP, G. D. (see Betterton, J. O., Jr.) 532
KNOP, G. (see Backenstoss, G.) 415
KRAYBILL, H. (see Stonehill, D.) 624
KROMMINGA, A. J. and I. E. McCARTHY. Determination of the parity change in inelastic scattering from the angular distribution 62
KROPSCHOT, R. H. (see Arp, V. D.) 452
KUCKES, A. F., R. W. MOTLEY, E. HINNOV, and J. G. HIRSCHBERG. Recombination in a helium plasma 337
KUGLIN, C. D., M. R. ELLETT, and K. F. CUFF. Oscillatory magnetoresistance in n-type PbTe 177
KUNZLER, J. E., E. BUEHLER, F. S. L. HSU, and J. H. WERNICK. Superconductivity in Nb_3Sn at high current density in a magnetic field of 88 kgauss 89
——— (see Klauder, J. R.) 179
KUO, L. G. (see Ilakovac, K.) 356
KURZ, RICHARD J. (see Barish, Barry C.) 297

La FORCE, RICHARD CONLEY, S. FREDERICK RAVITZ, and GENE F. DAY. Effect of dilute solid solutions of iron and of nickel on the nuclear resonance of Co^{59} 226
LAGNAUX, J. P. (see Davis, D. H.) 132
LANG, G. (see DeBenedetti, S.) 60
LANGENBERG, D. N. (see Burstein, E.) 92
——— (see Stiles, P. J.) 667
LANOU, R. E., JR. (see King, R. C.) 500
LARSH, ALMON E. (see Ghiorso, Albert) 473
LARY, E. C. (see Salz, F.) 523
LASSILA, K. E. (see Breit, G.) 138
LATIMER, ROBERT M. (see Ghiorso, Albert) 473
LAWRENSON, I. J. (see Gutowsky, H. S.) 349
LAX, BENJAMIN and YUICHIRO NISHINA. Theory of interband Faraday rotation in semiconductors 464
LeCRAW, R. C., E. G. SPENCER, and E. I. GORDON. Extremely low loss acoustic resonance in single-crystal garnet spheres 620
——— (see Kasuya, T.) 223
LEHNERT, B. (see Bergström, J.) 525
LEIPUNER, L. B. (see Martin, H. J.) 283
LEITNER, J. (see Humphrey, William E.) 478
LESLIE, D. H. (see Berlincourt, T. G.) 671
LICHTEN, WILLIAM. Angular distribution of Lyman-α radiation emitted by H ($2S$) atoms in weak electric fields 12; 197(E)
LIFSHITZ, E. M. (see Khalatnikov, I. M.) 311
LILLETHUN, E. (see Cocconi, G.) 231
LINDENFELD, PETER. Thermal conductivity of normal and superconducting lead alloys 613
LINSLEY, JOHN, LIVIO SCARSI, and BRUNO ROSSI. Extremely energetic cosmic-ray event 485
LITHERLAND, A. E. (see Hinds, S.) 113
LITTLE, W. A. (see Parks, R. D.) 539
LIU, L. Valence spin-orbit splitting and conduction g tensor in Si 683
LOMON, E. (see Feshbach, H.) 635
LONGO, MICHAEL J. (see Wood, Calvin D.) 481
LORY, M. L. (see Blamont, J. E.) 403
LOVE, W. F. (see Arp, V. D.) 452

MacDOWELL, S. W. Coupled integral equations of the Omnés-Muskhelishvili type 385
MacLEOD, G. R. (see Bartke, J.) 303
MADSEN, P. E. (see Johnson, C. E.) 450
MAIER, E. J., B. L. BLOCH, R. M. EDELSTEIN, and R. T. SIEGEL. Measurement of the rate $\mu^- + C^{12} \rightarrow B^{12} + \nu$ 417
MANELLI, I. (see Bartke, J.) 303
MANUS, CLAUDE (see Bonnal, Jean-François) 665

MARCH, R. (see Erwin, A. R.) 628
MARCUS, PAUL M. (see Seraphim, D. P.) 680
MARGOLIS, B. (see Greenberger, Daniel M.) 310; 428(E)
MARIN, P. C. (see Backenstoss, G.) 415
MARINOV, A. (see Bauminger, R.) 467
MARTIN, D. W. (see Barnes, W. S.) 110
MARTIN, H. J., L. B. LEIPUNER, W. CHINOWSKY, F. T. SHIVELY, and R. K. ADAIR. Properties of the Y^* as observed in the interaction $K_2^0+p \rightarrow \Lambda^0+\pi^++\pi^0$ 283
MASLEY, A. J. (see Winckler, J. R.) 488
MATTHIAS, B. T. (see Geballe, T. H.) 275
MAY, T. C. (see Winckler, J. R.) 488
McAVOY, B. R., D. W. FELDMAN, J. G. CASTLE, JR., and R. W. WARREN. Optical saturation of F-center spin resonance 618
McCARTHY, I. E. (see Kromminga, A. J.) 62
McDANIEL, E. W. (see Barnes, W. S.) 110
McDONALD, R. R. (see Gschneidner, K. A., Jr.) 218
McEWEN, J. G. (see Connolly, P. L.) 554
McMANIGAL, PAUL G. (see Barish, Barry C.) 297
MEAD, C. A. Anomalous capacitance of thin dielectric structures 545
MERRITT, F. R. (see Galt, J. K.) 458
MEYER, PETER and ROCHUS VOGT. Electrons in the primary cosmic radiation 193
MEYERAND, R. G., JR. (see Salz, F.) 523
MIDDELKOOP, W. C. (see Gatti, G.) 706
MIDDLETON, R. (see Hinds, S.) 113
MILES, JOHN L. (see Smith, Paul H.) 686
MILLER, DONALD H. (see Berge, J. P.) 557
—— (see Dahl, Orin I.) 142
—— (see Dalitz, R. H.) 562
MILLER, P. B. (see Haering, R. R.) 269
MILLS, R. L. and A. F. SCHUCH. Crystal structure of the β form of He^4 263
—— (see Schuch, A. F.) 596
MINGUZZI-RANZI, A. (see Bartke, J.) 303
MIYAMOTO, SHIGEKO (see Mizuno, Hiroyuki) 410
MIZUNO, HIROYUKI and SHIGEKO MIYAMOTO. Influence of dislocation of diffusion rate of F centers in KCl 410
MOFFAT, J. W. (see Bransden, B. H.) 708
MONTANET, L. (see Bartke, J.) 303
MOORHEAD, W. G. (see Bartke, J.) 303
MORRIS, D. E. and M. TINKHAM. Effect of magnetic field on thermal conductivity and energy gap of superconducting films 600
MORRISON, D. R. O. (see Bartke, J.) 303
MORRISON, S. ROY (see Palmer, D. R.) 170
MOTLEY, R. W. (see Kuckes, A. F.) 337
MOYER, BURTON J. (see Wood, Calvin D.) 481
MULLER, T. (see Charpak, G.) 128
MUNIR, B. A., E. PICKUP, D. K. ROBINSON, and E. O. SALANT. Pion production branching ratios through the 900-Mev resonance 192
MURRAY, JOSEPH J. (see Berge, J. P.) 557
—— (see Dahl, Orin I.) 142
MUSTARD, D. (see Derrick, G.) 69

NAGASHIMA, K. (see Pomerantz, M. A.) 123
NAMBU, Y. and J. J. SAKURAI. Odd $\Lambda\Sigma$ parity and the nature of the $\pi\Lambda\Sigma$ coupling 377; 506(E)
NEAGU, D., E. O. OKONOV, N. I. PETROV, A. M. ROSANOVA, and V. A. RUSAKOV. Decay properties of K_2^0 mesons 552
NESBET, R. K. (see Kahalas, S. L.) 549
NEURINGER, L. J. and W. BERNARD. Generation-recombination noise in p-type gold-doped germanium 455
NICOL, JAMES (see Smith, Paul H.) 686
NILAN, T. G. (see Granato, A. V.) 171
NILSSON, S. (see Bartke, J.) 303
NISHINA, YUICHIRO (see Lax, Benjamin) 464
NOSANOW, L. H. and R. VASUDEVAN. Nuclear paramagnetic susceptibility of the possible low-temperature phase of liquid He^3 1

OEHME, REINHARD (see Bernstein, Jeremy) 639
OFER, S. (see Bauminger, R.) 467
OGILVIE, K. W. (see Davis, L. R.) 492
OKONOV, E. O. (see Neagu, D.) 552
OLBERT, S. (see Hersil, J.) 22
OLIPHANT, T. A. (see Bendt, P. J.) 213
OLSEN, J. L. (see Daunt, J. G.) 267
OLSON, D. N., H. F. SCHOPPER, and R. R. WILSON. Electromagnetic properties of the proton and neutron 286
ONEDA, S., J. C. PATI, and B. SAKITA. Asymmetry parameter of Λ decay and

the intermediate boson of weak interactions 24
OREAR, J. (see Connolly, P. L.) 554

PACK, J. L. (see Phelps, A. V.) 111
PALMER, D. R., S. ROY MORRISON, and C. E. DAUENBAUGH. Surface states on cleaved silicon 170
PARKS, R. D. and W. A. LITTLE. Magnetic cooling with paramagnetic metals 539
PATI, J. C. (see Oneda, S.) 24
PEIERLS, RONALD F. Possible mechanism for the pion-nucleon second resonance 641
PENDLETON, H., III (see Barshay, S.) 421
PERESSINI, E. R. (see Hartwick, T. S.) 176
PEREZ-MENDEZ, VICTOR (see Barish, Barry C.) 297
——— (see Wood, Calvin D.) 481
PERKINS, WALTON A. (see Post, Richard F.) 85
PETERSON, S. W. and H. G. SMITH. Anomalous neutron diffraction in α cadmium sulfide 7
PETRAVIĆ, M. (see Ilakovac, K.) 356
PETROV, N. I. (see Neagu, D.) 552
PETTERSSON, B. -G., T. R. GERHOLM, J. THUN, and K. SIEGBAHN. Decoupling of a time-dependent perturbation caused by aftereffects of hole formation 14
PEYROU, C. (see Bartke, J.) 303
PHELAN, R. (see Arp, V. D.) 452
PHELPS, A. V. and J. L. PACK. Collisional detachment in molecular oxygen 111
PICKUP, E. (see Munir, B. A.) 192
PIKUS, G. E. and G. L. BIR. Cyclotron and paramagnetic resonance in strained crystals 103
PINSKI, G. Test for pion-pion resonance 136
POMERANTZ, M. A., S. P. AGARWAL, P. SCHWED, and H. HANSON. Satellite determination of heavy primary cosmic-ray spectrum 362
———, S. P. DUGGAL, and K. NAGASHIMA. Solar-produced cosmic rays near the north and south poles 123
POSKANZER, A. M. (see Cumming, J. B.) 484; 646(E)
POST, RICHARD F. and WALTON A. PERKINS. Velocity-space plasma instabilities observed in a mirror machine 85
POSTMA, H. (see Barnett, C. F.) 589
POWELL, B. W. (see Bartke, J.) 303
POWELL, WILSON M. (see Fowler, William B.) 134
PREPOST, R., V. W. HUGHES, and K. ZIOCK. Observation of the hyperfine structure splitting of muonium by use of a static magnetic field 19
PRICE, P. B. Direct observations of ion damage in cadmium 615
PULLEN, D. J. (see Hinds, S.) 113

RADO, GEORGE T. Mechanism of the magnetoelectric effect in an antiferromagnet 609
——— (see Folen, V. J.) 607
RAVITZ, S. FREDERICK (see La Force, Richard Conley) 226
RAY, D. (see Caspari, M. E.) 345
RAY, J. A. (see Barnett, C. F.) 589
RAYNE, J. A. (see Castle, J. G., Jr.) 409
——— (see Chandrasekhar, B. S.) 3
REALE, A. (see Berkelman, K.) 234
REINHARDT, R. G. (see Barnett, C. F.) 589
RHEE, Y. I. (see Humphrey, William E.) 479
RHODES, R. S., J. H. BURGESS, and A. S. EDELSTEIN. Exchange-ordering and observation of forbidden spin resonance transitions in crystalline organic radicals 462
RIBE, F. L. (see Bearden, A. J.) 257
RIDOUT, M. S. (see Johnson, C. E.) 450
ROBERTS, B. W. Ultrasonic cyclotron resonance in gallium 453
ROBINSON, D. K. (see Munir, B. A.) 192
ROBSON, B. A. (see Bradford, E.) 550; 711(E)
ROCKMORE, RONALD M. Nuclear paramagnetic susceptibility of low-temperature He^3 and the flow properties of superfluid systems of fermions 166
ROOS, C. E. (see Betterton, J. O., Jr.) 532
ROSANOVA, A. M. (see Neagu, D.) 552
ROSE, D. C. (see Carmichael, H.) 49
ROSEN, S. P. $\Delta I = 1/2$ rule in Σ decay: a problem of sign 504
ROSENFELD, ARTHUR H. (see Bastien, Pierre) 702
——— (see Berge, J. P.) 557
——— (see Humphrey, William E.) 478
ROSSI, BRUNO (see Linsley, John) 485
RUEDL, E., P. DELAVIGNETTE, and S. AMELINCKX. Evidence for focusing collisions in irradiated platinum 530
RUPPEL, H. M. (see Breit, G.) 138
RUSAKOV, V. A. (see Neagu, D.) 552

RYDE, HANS, PEDRO THIEBERGER, and TORSTEN ALVÄGER. Two-photon de-excitation of the 0+ level in Zr^{90} 475
RYNDIN, R. M. (see Jacobsohn, B. A.) 27

SACHS, R. G. and B. SAKITA. Existence of the ω^0 particle 306
SAKITA, B. (see Oneda, S.) 24
——— (see Sachs, R. G.) 306
SAKURAI, J. J. (see Nambu, Y.) 377; 506(E)
SALANT, E. O. (see Munir, B. A.) 192
SALINGER, G. L. (see Anderson, A. C.) 331; 443
SALZ, F., R. G. MEYERAND, JR., E. C. LARY, and A. P. WALCH. Electrostatic potential gradients in a Penning discharge 523
SANDWEISS, J. (see Stonehill, D.) 624
SANFORD, J. (see Stonehill, D.) 624
SANJEEVAIAH, B. (see Davis, D. H.) 132
SARLES, LYNN R. (see Wieder, Irwin) 95
SAWYER, G. A. (see Bearden, A. J.) 257
SCARSI, LIVIO (see Linsley, John) 485
SCHAERF, C. (see Hand, L.) 229
SCHAWLOW, A. L. and G. E. DEVLIN. Simultaneous optical maser action in two ruby satellite lines 96
SCHILL, W. J. (see Barnett, C. F.) 589
SCHMIDT, P. H. (see Galt, J. K.) 458
SCHMITZ, NORBERT (see Anderson, Jerry A.) 365
SCHOPPER, H. F. (see Olson, D. N.) 286
SCHUCH, A. F. and R. L. MILLS. New allotropic form of He^3 596
——— (see Mills, R. L.) 263
SCHULTZ, J. (see Chambers, R. H.) 273
SCHWARTZ, M. Proposed method of measuring the spin of the K' meson 556
SCHWARZ, RUTH F. (see Spratt, James P.) 341
SCHWED, P. (see Pomerantz, M. A.) 362
SCOTT, D. (see Hersil, J.) 22
SEATON, M. J. (see Hummer, D. G.) 471
SELLERI, FRANCO. Role of the peripheral interaction in proton-proton collisions 64
SENS, J. C. (see Charpak, G.) 128
SERAPHIM, D. P. and PAUL M. MARCUS. First and second order stress effects on superconducting transitions in Ta and Sn 680
SHAPIRO, SIDNEY (see Smith, Paul H.) 686
SHELINE, RAYMOND K. Core reconstitution in heavy deformed nuclei 691
SHEPPARD, A. P. (see Derr, V. E.) 572(E)
SHERRILL, M. D. and H. H. EDWARDS. Superconducting tunneling on bulk niobium 460
SHIMOMURA, K. (see Gutowsky, H. S.) 349
SHIREN, N. S. Phonon-photon double-quantum transitions as a detector of microwave ultrasonics 168
——— and E. B. TUCKER. Selection rule for the interaction of microwave ultrasonics with spins 105
SHIRLEY, D. A. (see Kaplan, Morton) 361
SHIVELY, F. T. (see Martin, H. J.) 283
SIEGBAHN, K. (see Pettersson, B. -G.) 14
SIEGEL, R. T. (see Maier, E. J.) 417
SIKKELAND, TORBJØRN (see Ghiorso, Albert) 473
SILVESTRINI, V. (see Bartke, J.) 303
SINGER, J. R. and S. WANG. General analysis of optical, infrared, and microwave maser oscillator emission 351
ŠLAUS, I. (see Ilakovac, K.) 356
SMITH, H. G. (see Peterson, S. W.) 7
SMITH, PAUL H., SIDNEY SHAPIRO, JOHN L. MILES, and JAMES NICOL. Superconducting characteristics of superimposed metal films 686
SOLOMON, JULIUS (see Barish, Barry C.) 297
SPECTOR, HAROLD N. Mapping of the Fermi surface by a combination of geometric resonance and tilt effect 407
SPENCER, E. G. (see LeCraw, R. C.) 620
SPRATT, JAMES P., RUTH F. SCHWARZ, and WALTER M. KANE. Hot electrons in metal films: injection and collection 341
STALDER, E. W. (see Folen, V. J.) 607
STANGHELLINI, A. (see Bergia, S.) 367
STEINBERGER, JACK (see Franzini, Paolo) 281
STELJES, J. F. (see Carmichael, H.) 49
STERN, FRANK. Aspherical $3d$ electron distribution in body-centered cubic metals 675
STERNHEIMER, R. M. Antishielding of nuclear electric hexadecapole moments 190
STEYERT, W. A. (see Anderson, A. C.) 331
STIERLIN, U. (see Backenstoss, G.) 415
STILES, P. J., E. BURSTEIN, and D. N. LANGENBERG. Observations of de Haas–van Alphen oscillations in p-type PbTe 667
STONEHILL, D., C. BALTAY, H. COURANT, W. FICKINGER, E. C. FOWLER, H. KRAYBILL, J. SANDWEISS, J. SAN-

FORD, and H. TAFT. Pion-pion interaction in pion production by π^+-p collisions 624
STRATTON, T. F. (see Bearden, A. J.) 257
STRONGIN, MYRON, GEORGE O. ZIMMERMAN, and HENRY A. FAIRBANK. Specific heat of liquid He^3 down to 0.054°K 404
SUDAKOV, V. V. (see Khalatnikov, I. M.) 311
SUGANO, S. (see Kaiser, W.) 605
SUGIURA, MASAHISA. Some evidence of hydromagnetic waves in the earth's magnetic field 255
SUHL, H. Restoration of stability in ferromagnetic resonance 174

TAFT, H. (see Stonehill, D.) 624
TANG, Y. C. (see Wildermuth, K.) 17
TANGHERLINI, FRANK R. Nonclassical structure of the energy-momentum tensor of a point mass source for the Schwarzschild field 147
TAYLOR, B. N. (see Burstein, E.) 92
TAYLOR, J. B. Diffusion of plasma across a magnetic field 262
TAYLOR, J. G. Pion-pion interaction and high-energy $p+d$ collisions 237
TAYLOR, MICHAEL ALAN (see Burger, Jean-Paul) 185
TELEGDI, V. L. (see Charpak, G.) 128
TEMKIN, A. Polarization and the triplet electron-hydrogen scattering length 354
THIEBERGER, PEDRO (see Ryde, Hans) 475
THORSEN, A. C. and T. G. BERLINCOURT. de Haas–van Alphen effect in potassium 617
THUN, J. (see Pettersson, B. -G.) 14
TICHO, HAROLD K. (see Alston, Margaret H.) 300; 698
——— (see Fowler, William B.) 134
TINKHAM, M. (see Morris, D. E.) 600
TIOMNO, J., A. L. L. VIDEIRA, and N. ZAGURY. Possible existence of a new K' meson 120
TOMAŠ, P. (see Ilakovac, K.) 356
TREMBLEY, J. (see Bartke, J.) 303
TRIPP, R. D. (see Berge, J. P.) 557
TRUONG, TRAN NGUYEN. Analysis of the anomaly in double meson production in $p+d$ collisions and the S-wave pion-pion interaction 308
TUAN, S. F. (see King, R. C.) 500
TUBIS, A. (see Feshbach, H.) 635
TUCKER, E. B. Amplification of 9.3-kMc/sec ultrasonic pulses by maser action in ruby 547
——— Attenuation of longitudinal ultrasonic vibrations by spin-phonon coupling in ruby 183
——— (see Shiren, N. S.) 105

UTLAUT, W. F. (see Gallet, R. M.) 591

VAN VLECK, J. H. (see White, J. A.) 412
VASUDEVAN, R. (see Nosanow, L. H.) 1
VAUGHAN-WILLIAMS, R. W. and F. A. HAAS. An error in the thermal conductivity for a fully ionized gas 165
VERGANELAKIS, A. (see De Tollis, B.) 371
VETTE, J. I. and F. G. CASAL. High-energy x rays during solar flares 334
VIDEIRA, A. L. L. (see Tiomno, J.) 120
VIGNOS, JAMES H. and HENRY A. FAIRBANK. New solid phase in He^4 265; 646(E)
VILLI, C. (see Bergia, S.) 367
VOGT, ROCHUS (see Meyer, Peter) 193

WADA, J. Y. (see Knechtli, R. C.) 215
WAKABAYASHI, J. (see Wanlass, L. Kent) 271
WALCH, A. P. (see Salz, F.) 523
WALDORF, D. L. (see Alers, G. A.) 677
WALI, K. C., T. FULTON, and G. FELDMAN. Scattering matrix approach to the Λ-π resonance 644
WALKER, L. R., G. K. WERTHEIM, and V. JACCARINO. Interpretation of the Fe^{57} isomer shift 98
WALKER, W. D. (see Erwin, A. R.) 628
WANG, S. (see Singer, J. R.) 351
WANLASS, L. KENT and J. WAKABAYASHI. Stimulated spin-echo measurement of cross-relaxation in neutron-irradiated calcite 271
WARNER, R. M. (see Barnett, C. F.) 589
WARREN, R. W. (see McAvoy, B. R.) 618
WATSON, M. B. (see Berge, J. P.) 557
WATSON, R. E. and A. J. FREEMAN. Exchange polarization and the magnetic interactions of rare earth ions 277; 388(E)
——— (see Freeman, A. J.) 343
WEBB, ROBERT H. Dynamic polarization anomalies in organic free radicals 611
WEINBERG, S. (see Feinberg, G.) 381

WEISS, M. T. (see Hartwick, T. S.) 176
WELLS, E. R. (see Barnett, C. F.) 589
WERNICK, J. H. (see Kunzler, J. E.) 89
WERTHEIM, G. K. (see Walker, L. R.) 98
WEST, E. (see Erwin, A. R.) 628
WETHERELL, A. M. (see Cocconi, G.) 231
WHEATLEY, J. C. (see Anderson, A. C.) 331; 443
WHITE, J. A. and J. H. VAN VLECK. Sign of Knight shift in samarium intermetallic compounds 412
WHITE, PAUL G. (see Dahl, Orin I.) 142
WIEDER, IRWIN and LYNN R. SARLES. Stimulated optical emission from exchange-coupled ions of Cr^{+++} in Al_2O_3 95
WILDERMUTH, K. and Y. C. TANG. Study of nuclear structure from Coulomb energy differences of mirror levels 17
WILLIAMS, W. L. (see Doyle, W. T.) 537
WILSON, B. G. (see Carmichael, H.) 49
WILSON, J. H. (see Arp, V. D.) 452
WILSON, R. R. (see Olson, D. N.) 286
WINCKLER, J. R., P. D. BHAVSAR, A. J. MASLEY, and T. C. MAY. Delayed propagation of solar cosmic rays on September 3, 1960 488
WINGERSON, RICHARD C. "Corkscrew"—a device for changing the magnetic moment of charged particles in a magnetic field 446
WISKOTT, D. (see Bartke, J.) 303
WOJCICKI, STANLEY G. (see Alston, Margaret H.) 300; 698
WONG, DAVID Y. (see Ball, James S.) 29
WOOD, CALVIN D., THOMAS J. DEVLIN, JEROME A. HELLAND, MICHAEL J. LONGO, BURTON J. MOYER, and VICTOR PEREZ-MENDEZ. π^--p elastic scattering at 550, 600, 720, 900, and 1020 Mev 481
WOOD, D. L. (see Kaiser, W.) 605
WOOD, G. T. (see Caspari, M. E.) 345
WORSHAM, R. E. (see Betterton, J. O., Jr.) 532
WUERKER, R. F. (see Josephson, Vernal) 33(E)

YAGODA, HERMAN, ROBERT FILZ, and KATSURA FUKUI. Emission of carbon group heavy nuclei from a 3+ solar flare 626
YAMAGATA, T. (see Gatti, G.) 706

ZAGURY, N. (see Tiomno, J.) 120
ZAHLAN, A. B. (see Katul, J.) 101
ZAKRZEWSKI, J. (see Davis, D. H.) 132
ZAVATTINI, E. (see Gatti, G.) 706
ZELENY, W. B. I-space parity connection in nonleptonic weak interactions 570
ZICHICHI, A. (see Charpak, G.) 128
ZIMMERMAN, GEORGE O. (see Strongin, Myron) 404
ZIOCK, K. (see Prepost, R.) 19